Chem Soc Rev

Multiphotochromic Molecular Systems

Journal:	*Chemical Society Reviews*
Manuscript ID:	CS-REV-02-2015-000137.R1
Article Type:	Review Article
Date Submitted by the Author:	31-Mar-2015
Complete List of Authors:	Fihey, Arnaud; Université de Nantes, CEISAM - UMR 6230 Perrier, Aurélie; Université Paris Diderot-Paris VII, ITODYS Browne, Wesley; University of Groningen, Organic and Molecular Inorganic Chemistry Jacquemin, Denis; Université de Nantes, CEISAM - UMR 6230

Multiphotochromic Molecular Systems

Arnaud Fihey[a], Aurélie Perrier[b,c], Wesley R. Browne[d] and Denis Jacquemin*[,a,e]

Received Xth XXXXXXXXXX 2015, Accepted Xth XXXXXXXXX 2015
First published on the web Xth XXXXXXXXXX 2015
DOI: 10.1039/b000000x

Molecular systems encompassing more than one photochromic entity can be used to build highly functional materials, thanks to their potential multi-addressability and/or multi-response properties. Over the last decade, the synthesis, spectroscopic and kinetic characterisations as well as the modeling of a wide range of multiphotochromes have been achieved in a field that is emerging as a distinct branch of photochemistry. In this review, we provide an overview of the available multiphotochromic compounds which use variety of photoactive building blocks, *e.g.*, diarylethene, azobenzene, spiropyran, naphtopyran or fulgimide derivatives. Their efficiency in terms of multi-responsiveness is discussed and several strategies to circumvent the most common limitation (*i.e.*, the loss of photochromism of one part) are described.

1 Introduction

Photochromic compounds undergo isomerisation between at least two forms, with the reactions induced by external stimuli of which light triggers at least one of the isomerisations. Molecular based photochromic reactions have been observed in a wide variety of organic compounds,[1–3] and photochromes have been used as molecular switches, providing key building blocks in data storage materials and optoelectronic devices. Indeed, optical data storage with organic photochromic compounds has been a field of active research for over 25 years.[4–7]

The main families of photochromic compounds discussed in this review are shown in Figure 1. Among the many photochromes, those in which the switching process involves reversible electrocyclisation of a π-system or *E*/ *Z* isomerisation have received most attention. Dithienylethene (DTE) derivatives stand out as a highly efficient class of reversible photochromes, as the light induced isomerisations are normally thermally irreversible and can often be carried out over many cycles (strong fatigue-resistance).[8–11] DTEs can be switched, by inducing an electrocyclisation, from a colourless open form featuring a hexatriene core to a closed coloured form characterised by an extended π-system with a cyclohexadiene core. So called "inverse" and "normal" DTEs, which differ in the binding position of the thiophene rings with respect to the bridging alkene have been reported[12–14] (see Figure 1). DTEs are promising candidates for optical data storage as this application requires, on the one hand that the two isomers are thermally stable, and on the other hand that the write-erase process can be achieved over a large number of cycles without loss in photochromic performance.[15,16] Spiropyrans (SPs) constitute a quite different class of electrocyclisation based photochromic compounds compared to DTEs. The stable spiropyran form absorbs in the UV only, due to an sp^3 spiro centre between the indoline and the chromene moieties. Upon UV (or two photon excitation with NIR light)[17,18] spiropyrans can undergo a ring opening reaction leading to a more conjugated merocyanine (MC) zwitterionic form that absorbs in the visible.[19,20] Their UV-induced opening and thermal back reaction processes have allowed applications at the industrial level in ophthalmic and solar-protection lenses, smart windows, as well as in decorative objects.[21] The related photochromes, the fulgimides (FGs), have been studied widely also,[22,23] and as for DTEs the generally thermally stable open and closed forms of FGs absorb in the UV and visible, respectively. In FGs, the open form can be present in both *cis* and *trans* configurations, providing further possibilities in modifying optical properties.[24,25] In contrast to photochromism based on electrocyclisation, azobenzene (AZB) derivatives undergo a *E*-*Z* (*trans*-*cis*) isomerisation about their azo-double bond (see Figure 1). The *E* form is normally the most stable with the *Z* form accessed by irradiation with UV light.[26,27] For most AZBs, the reverse *Z*-*E* isomerisation can occur thermally, and hence the *Z* form is generally unstable at room temperature, albeit with notable recent exceptions.[28,29] The large change in geometry that accompanies the *Z*-*E* isomerisation is often used in optomechanics to produce shape-changing molecular based devices

[a] *Laboratoire CEISAM, UMR CNRS 6230, Université de Nantes, 2 Rue de la Houssinière, BP 92208, 44322 Nantes Cedex 3, France. Fax: +33 251 125567; Tel: +33 251 125743; E-mail: Denis.Jacquemin@univ-nantes.fr*
[b] *Université Paris Diderot, Sorbonne Paris Cité, ITODYS, UMR CNRS 7086, 15 rue Jean Antoine de Baif, 75205 Paris Cedex 13, France*
[c] *Institut de Recherche de Chimie Paris, PSL Research University, CNRS - Chimie Paris Tech, 11 Rue Pierre et Marie Curie, 75231 Paris Cedex 05, France*
[d] *Center for Systems Chemistry, Stratingh Institute for Chemistry, Faculty of Mathematics and Natural Sciences, University of Groningen, Nijenborgh 4, 9747AG Groningen, The Netherlands*
[e] *Institut Universitaire de France, 103 bd St. Michel, 75005 Paris Cedex 5, France*

that can be applied to induce movements in polymers[30–32] or to control biological environments.[33,34] Beyond these especially popular families of organic photochromic compounds, photochromic systems based on dihydroazulene (DHA),[35] indoline,[36] naphtopyran (NP),[37] dihydropyrene (DHP)[38] and phenoxynaphthacenequinone (PNQ) cores,[39] that switch following ring-opening and ring-closing reactions for the four former families and a *trans* to *ana* interconversion for the latter, have attracted widespread interest. Their photochromic behaviour is summarised in Figure 2.

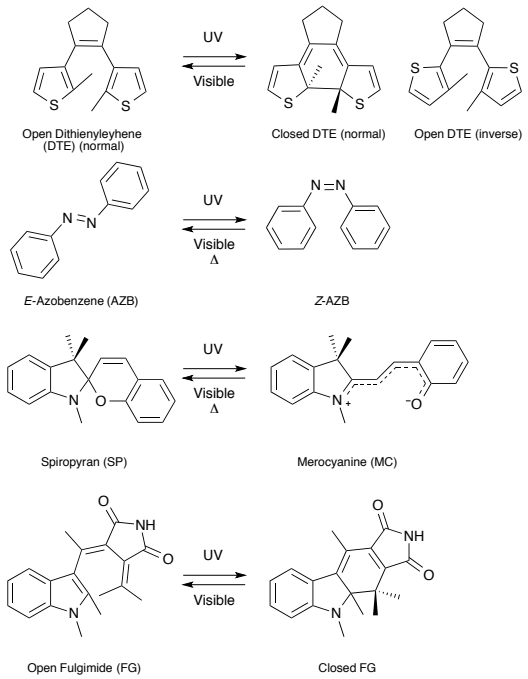

Fig. 1 Main families of organic photochromic compounds and their isomerisation reactions.

All of these classes of organic photochromic compounds have seen application in wide range of chemical environments, including coordinated to metal ions in coordination complexes,[40–42] immobilised onto metallic supports,[43–45] into polymer matrices[46] and in biological systems.[47,48] Photochromism in organic compounds has been applied successfully in optoelectronic devices,[49,50] to control nonlinear properties,[51–55] and to capture metal ions.[56] Photochromism can also be combined with fluorescence[57–59] and other types of *chromisms*, *e.g.*, electrochromism,[60–63] solvatochromism,[61,64,65] and acidochromism[66–69] to widen the range of possible applications.

Integrating more than one photochromic unit within a single compound has the potential to increase the amount of information that it can store, as well as provide access to more complex phenomena. This approach, however, requires a multiaddressable behaviour; that is to say an efficient use of different inputs yielding a panel of distinguishable responses. Indeed, while a photochromic compound is expected to provide two states, that can be viewed as "on/off" states or as a binary "0/1" information, multiphotochromic compounds go beyond this dual functionality and potentially provide a maximum of 2^n distinct states (with n the number of photochromes). Thus far the design of multiphotochromic compounds has been a challenging task.[70,71] The main difficulty this field faces is in achieving the delicate equilibrium between obtaining emergent properties resulting from the active coupling of the photochromes, and yet at the same time ensuring that the final system retains the intrinsic switching properties of its components. As shown in this review, fulfilling the latter condition is highly challenging, most notably due to energy transfer (ET) between the different subunits. The chemical connection between the sub-units is thus a critical consideration in the design of multiphotochromic compounds because the linker determines the through bond, and to some extent the through space, communication between the components. Either each unit can be "aware" of the photochromic state(s) of

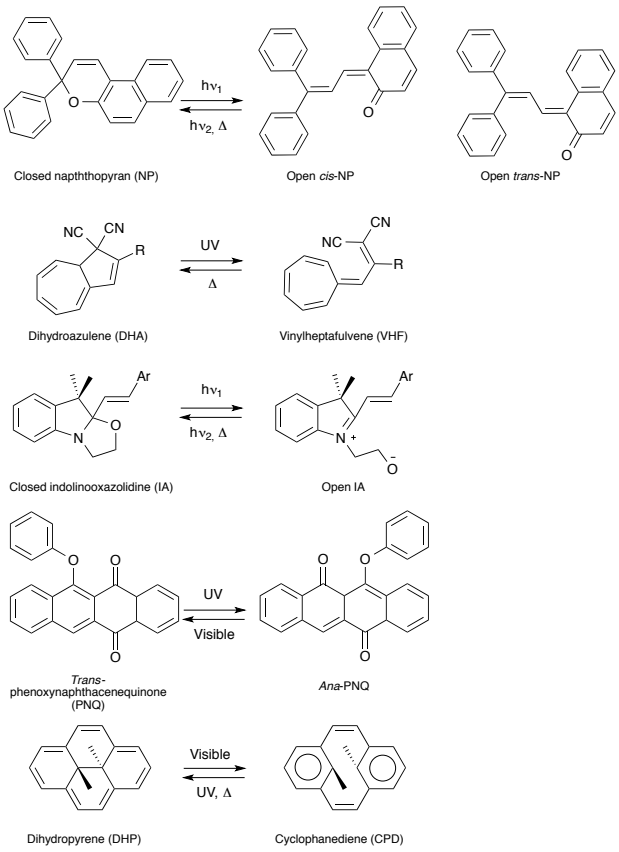

Fig. 2 Alternative families of organic photochromic compounds and their isomerisation reaction.

its neighbour(s), providing more "intelligent" systems, or the photochromes are electronically distant, with the supramolecular system consequently acting as the sum of independent and isolated switches. In this framework, theoretical studies, notably based on the Density Functional Theory (DFT) and Time-Dependent (TD-DFT) formalisms[72–74] have proven to be valuable tools not only to rationalise the optical properties of multiphotochromes,[70] but also to provide insights into the key features determining the efficiency of photoactivity in these complex systems.

In this review we will discuss several organic multiphotochromic compounds reported in the recent literature, considering only molecular systems encompassing at least two photoactive units, belonging to any of the families of photochromes mentioned above. We stress that our intention is to review compounds presenting several photochromic units and consequently multifunctional compounds associating one photochromic function with other types of switching functionalities (*e.g.*, acidochromism or electrochromism) are outside the review's scope and the interested reader is referred to several reviews relevant to those topics.[56,75–80] The same holds for polymers incorporating photoswiching units,[11,81–83] or for details of the synthetic procedures used in the preparation of the multiphotochromes discussed here. This review will describe several families of multiphotochromic systems. In Section 2, the most simple coupled systems, that is to say homo-dimers of photochromic compounds in which the two photochromic units belong to the same family, are reviewed, followed by a discussion of the various photochromic homo-multimers (Section 3). In Section 4 multi-photochromic compounds that utilise coordination chemistry will be reviewed followed by a discussion of the "hybrid' multiphotochromic systems in which different types of photochromes are incorporated within a single compound (Section 5). The state of the art in theoretical analysis methods used so far to rationalise the behaviour of multiphotochromic compounds is discussed in Section 6.

2 Dimers of photochromic compounds

Full photochromism in photochromic dimers implies that all the possible combination of states can be accessed, *e.g.*, if two different photoactive units **a** and **b** (possessing each two forms **1** and **2**) are present, four distinct isomers, namely **a1b1**, **a2b1**, **a1b2** and **a2b2**, can be generated. However, for symmetric dimers, where the two units are identical, one cannot distinguish the two singly switched systems, which are therefore degenerate, so that only three structures are relevant, namely **a1a1**, **a2a1**, and **a2a2**. In contrast, when the two subunits are inequivalent, for example when they bear additional substituents, the symmetry is broken and a four state molecular system can in principle be achieved. In the following Sections, various dimers and the larger multimers are discussed with an emphasis on: i) whether or not a system is photoactive and provides additional performances above that achieved by a simple mixture of the corresponding monomers, ii) the number of addressable functions that arise from the coupling of the photochromic units.

2.1 DTE dyads

DTE dimers are already non-trivial systems, as the achievement of a full photochromic system (where the two DTE units can close) is far from guaranteed. This can be illustrated by comparing Figures 3 and 4, in which, dimers that undergo partial photochromism and full photochromism, respectively, are shown. In the following discussion the notations **oo**, **co**, and **cc** refer respectively to the fully open, mixed closed/open and fully closed isomers of the DTE dimer. In the following, stepwise photochromism means that the intermediate isomers, *e.g.*, **co**, can be isolated and studied experimentally.

2.1.1 DTE dimers exhibiting partial ring-closure

To the best of our knowledge, the first dimer of DTEs, **1** in Figure 3, was reported by Uchida *et al.* fifteen years ago.[84] In this system the two DTEs are bridged through a tetrathiafulvalene unit, in which the two rings constitute the bridges of the DTE units, thus the two photochromes can be seen as being separated by only a double bond. The dimer with R=Me showed photochromic activity, whereas the compound with R=H remained colourless upon irradiation, which was ascribed to conformational effects, *i.e.*, planarity and hence delocalization in the open form interfered with ring closing. For the active compound, only the mono-closed system could be accessed, presumably due to intramolecular energy transfer quenching.

In the DTE dimer **2**, the two photochromic units are linked directly via a single α-α bond between the thiophene rings, *i.e.* without an additional spacer.[85] In this case also only the **co** isomer was obtained upon irradiation of the **oo** isomer. In fact prolonged irradiation of the mixed **co** form resulted in the formation of a non-photochromic side-product, originating from a diatropic rearrangement of the closed DTE unit. This reaction is quantitative within 30 minutes of irradiation. This side product is also formed with several DTE monomers,[86,87] but with a quantum yield that is several orders of magnitude lower than for **2**, illustrating that DTE dimers, such as these, are not simple extensions of their individual components. The mixed **co** isomer is thermally stable (for more than three months at room temperature). The introduction of chlorine substituents or change in solvent did not significantly affect the observed photochromic behaviour of the dimer. Interestingly, a similar dimer incorporated within a polymer showed efficient pho-

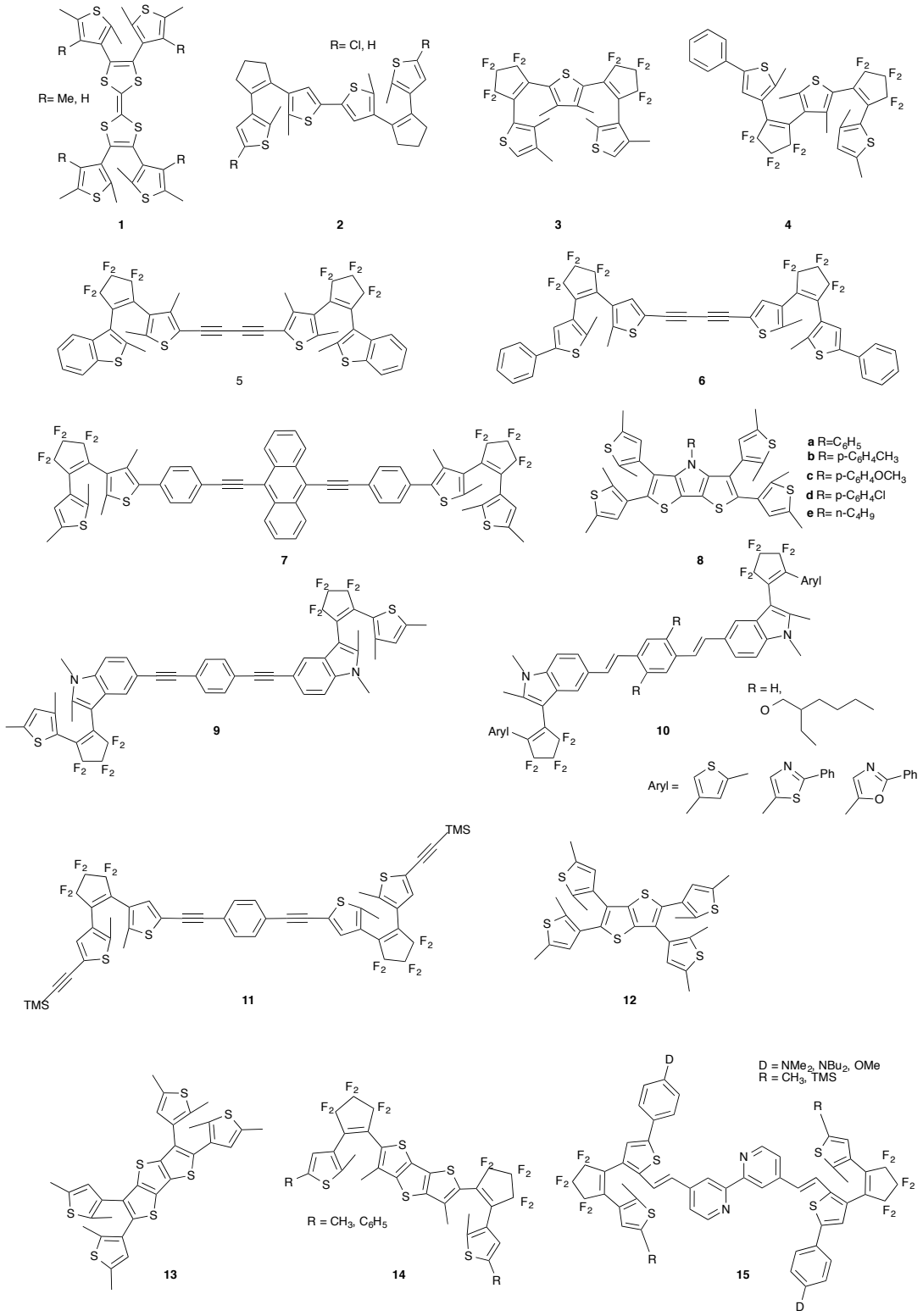

Fig. 3 DTE dimers showing partial photochromism.

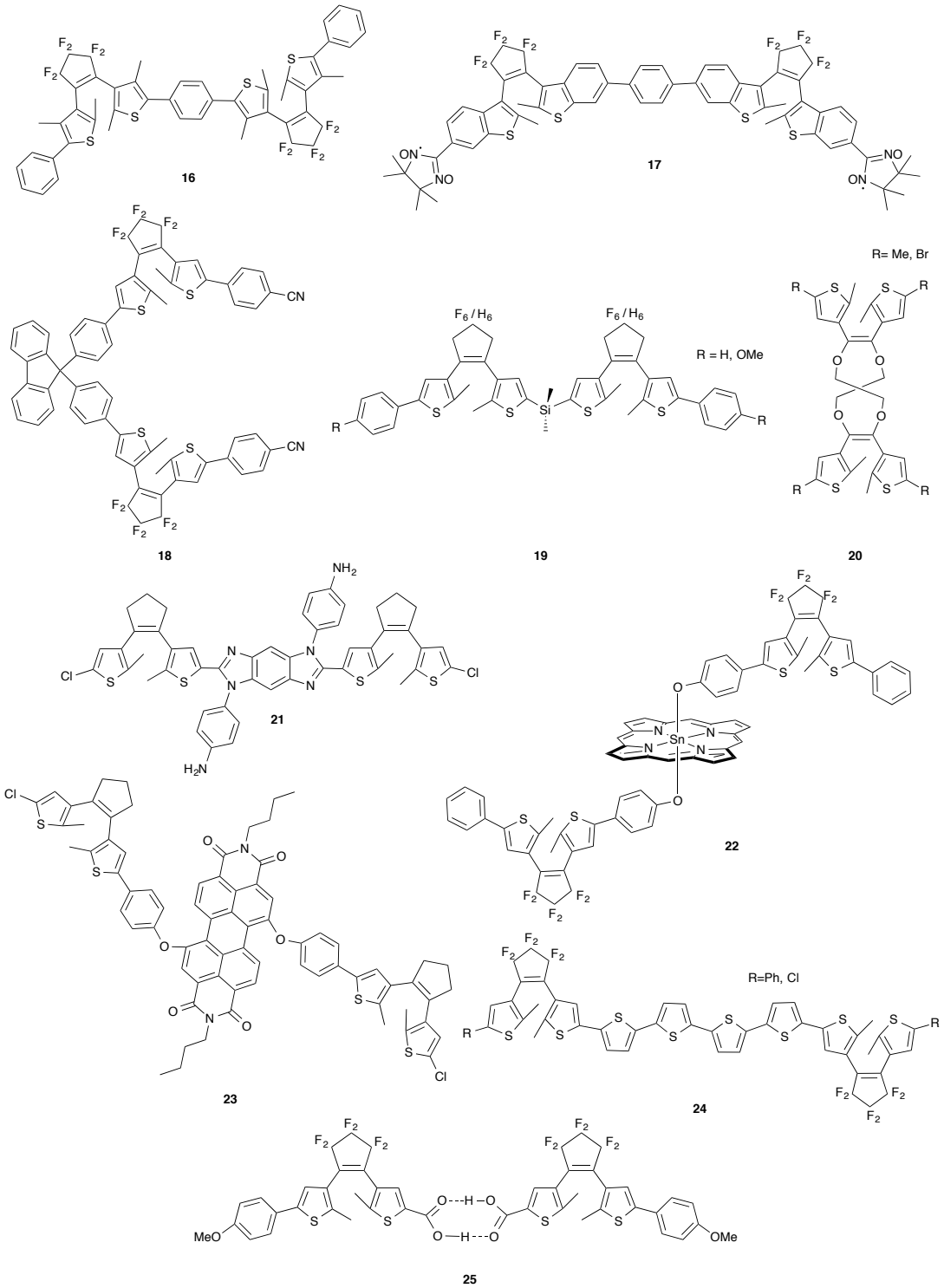

Fig. 4 DTE dimers showing full photochromism.

tochromism, with no byproduct formed,[88] a difference with respect to the dimer that remains unexplained.

Dimer **3** was reported by Higashiguchi *et al.* by "fusing" two units through a shared thiophene ring,[89] and therefore constituting a highly compact dyad. The fully closed isomer has not been observed, which was rationalized, on the basis of DFT calculations, as a consequence of the high degree of steric stress imposed on the second unit upon ring closing of the first unit: forming the **cc** isomer would lead to a thermodynamically unstable product.[90] Indeed, as illustrated in Figure 5, forming this isomer would result in a separation between the methyl groups of less than 2.0 Å, and would also require elongated bonds between the reactive carbon atoms, which is known to be detrimental to the (thermal) stability of the product.[91] Nevertheless, thanks to the lack of symmetry (inverse *versus* hybrid normal/inverse DTE), both possible singly-closed systems, **co** and **oc**, could be distinguished in solution, allowing the development of one of the first three-state photochromic system. The photocyclisation quantum yields are not equivalent for the two possible open-closed forms, with values of 0.20 for the closing of the inverse DTE (creating a new absorption band at 456 nm) and only 0.034 for the closing of the normal DTE within hybrid unit (resulting in a band at 475 nm). The former isomer is produced in the crystalline phase only.[89]

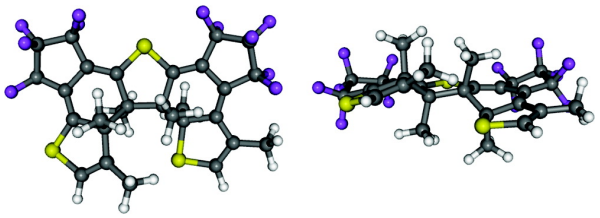

Fig. 5 Top (left) and side (right) views of the putative **3(cc)** product obtained by DFT calculations. Reprinted with permission from Ref. 89, Copyright 2011 American Chemical Society.

In the same vein, in **4**, a normal and an inverse DTEs are linked through a thiophene unit.[92] The three isomers that were characterized, **oo**, **co** and **oc** can provide five colours as using a combination of different irradiation wavelengths (313 nm, 365 nm and 436 nm) yields specific blends of the three isomers (see Figure 6). The quantum yields for the closing of each of the two DTE units were different, 0.14 for the inverse and 0.032 for the normal DTE.

The dyad **5** with a diyne linker was reported by Yagi *et al.*[93] Under irradiation at 350 nm, the dark blue mixed **co** isomer is formed, manifested in the appearance of an absorption band at 574 nm, but the fully closed form is absent. The intensity of fluorescence from **5** is also controlled by the photochromism, as the **co** isomer emits at 720 nm, whereas the **oo** isomer does not fluoresce. Similarly, for **6**, Li and coworkers have shown that the fully closed isomers cannot be obtained in solution, in contrasts to its gold complex,[94] for which the **cc** isomer could be isolated (see Section 4).

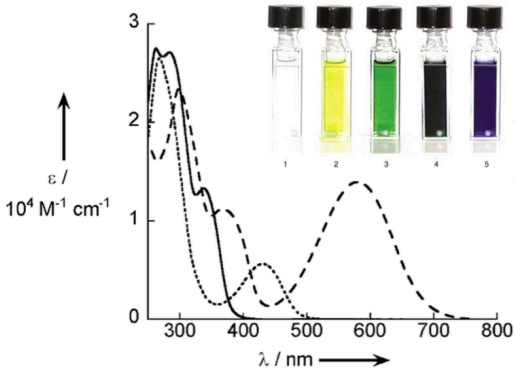

Fig. 6 UV/vis absorption spectra of **4** in its **oo** (full line), **oc** (dotted line) and **co** (dashed line) forms in n-hexane. Inset: colour before irradiation (1), after irradiation at 365 nm (2 and 3), after irradiation at313 and 365 nm (4) and after irradiation at 313 and 436 nm (5). Adapted with permission from Ref. 92, Copyright 2003 Wiley-VCH Verlag GmbH & Co. KGaA, Weinheim.

Several other DTE dimers have been reported using an extended aromatic linker, as this strategy allows the observation of fluorescence from the linker. For example, in **7**, which bears an anthracene bridge,[95] only the mixed **co** form is obtained, with the closing of the second unit being quenched by an ET from the excited open DTE moiety to the already closed DTE moiety. The fluorescence of the anthracene unit is quenched by ET to the closed DTE also, which illustrates that the emission in this type of system can be dependent on the state of the DTE. In a dimer formed by two DTE units linked through a highly-conjugated bridge (**8**),[96] Wong *et al.* observed two isosbestic points when monitoring the evolution of the UV/vis absorption spectrum during irradiation with UV light, and concluded that only one of the DTE units can undergo cyclisation. As in **7**, the DTE unit that undergoes photocyclisation first quenches the fluorescence of the aromatic linker unit, as well as the excited state of the remaining open DTE unit, precluding cyclisation.

A series of DTE derivatives have been reported by Saita *et al.* (**9** and **10**) incorporating a 1,4-bis(ethenyl)benzene or a 1,4-bis(ethynyl)benzene bridge.[97] As for the previous examples, ET impedes the formation of the **cc** isomer, and the same holds for the structurally similar **11**.[98] For **10**, several substitution patterns were compared in order to pinpoint a compound possessing the maximum photochromic activity and a **co** form that absorbs in the visible/NIR region (around 800 nm). The two-photon absorption (TPA) properties of these compounds were also measured to assess their potential as candidates for optical data storage materials. Based on these investigations,

the dyad of the series possessing oxazole rings as aryl groups was found to exhibit the best overall performance, with a TPA cross-section of 43 GM. In **12** and **13**, thienothiophene moieties were used as central connectors.[99] NMR spectroscopic studies highlighted that prolonged irradiation leads to the closing of one photochromic unit. Both the cyclisation and cycloreversion quantum yields are higher in **12** (0.36 and 0.06), than in **13** (0.24 and 0.04). **14** also incorporates a thienothiophene bridge,[100] that is used to replace one of the active thiophene rings in each DTE. Only the **co** system is formed, in 90% yield, with two well-defined isosbestic points present in the absorption spectra recorded during irradiation

15 constitutes the first example in which the two DTE units are linked, via a bipyridyl moiety, at their reactive carbon atoms.[101] The **co** isomer of this dimer was obtained in 80% yield in cyclohexane, but the photoactivity is strongly solvent dependent. Indeed in a polar environment, low-lying charge transfer excited states prevent electrocyclisation, whereas in apolar solvents, fluorescence competes with the photoreaction, which leads to much poorer quantum yields (0.081 for cyclisation and 0.016 for the cycloreversion). The photoreactivity of this dimer has also been studied in a more recent study by the Guerchais' group,[102] who investigated the influence of changes in the substituents on the optical properties. They concluded that the photochromism of the dimer is due to the appearance of the mixed form when the donor, D in Figure 3, is an amino group, while the **cc** form can be obtained with methoxy substituents. At the photostationary state the **oo**:**co**:**cc** ratio are 30:70:00 and 11:58:31 for D=NMe_2 and D=OMe, respectively.

2.1.2 Fully active DTE dimers

The DTE dimer **16**, in which the two DTE units are connected via a phenyl linker at the α position of the two thiophene rings, was reported in 2003 by Kobatake *et al.*[103] The photochromism of this system is total and stepwise: both the mono and doubly closed isomers are formed (the colour changes from purple to blue under prolonged irradiation). The absorption spectra of the three forms are shown in Figure 7. The overall photocyclisation quantum yield is found to be 0.50. The cycloreversion quantum yields are respectively 0.0026 and 0.0096 for the first and second cycloreversion.[103] Similarly, a dimer of DTE with a phenyl bridge and nitronyl nitroxide substituents on the periphery has been reported by Matsuda and Irie (**17**).[104] The side groups were introduced to generate magnetic properties that could be modulated by switching the DTE units. As shown by electron spin resonance (ESR) spectroscopy, the interaction between the two nitronyl nitroxide groups is low in both **oo** and **co** but is greatly enhanced for **cc** where the two extremities can communicate with each other through a conjugated pathway. The photochromic reaction in **17** is essentially complete and stepwise upon irradiation at 313 nm, each of the isomers can be isolated and the **oo**:**co**:**cc** ratio is 0:23:77 at the photostationary state. By studying the kinetics of this ratio upon irradiation, it was found that the first ring closing is the critical step, the second cyclisation only happening when a sufficient amount of **co** form is present. For the cycloreversion, which is also efficient, the critical step is the opening of the first ring as accumulation of **co** was not observed.

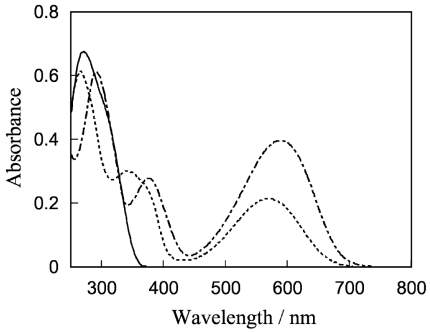

Fig. 7 Absorption spectra of the **oo** (solide line), **co** (regular dotted line) and **cc** (mixed dashed line) of **16**. Reprinted from Ref. 103, Copyright 2003, with permission from Elsevier.

18 is a dyad where the two photochromes are linked at the 9-9' position of a fluorene core.[105] Both DTE units can be closed by irradiation at 313 nm, the absorption of **cc** corresponds to a simple increase in the absorption of the **co** form, indicating that the two photochromes are almost independent, an expected outcome resulting from the presence of an sp^3 carbon atom between the two DTE units. The quantum yields for cyclisation are 0.46 and 0.29 for the first and second steps, respectively whereas the reported cycloreversion quantum yield is 0.0058 (for both processes). The lower value obtained for the second ring-closure may be rationalized by considering a weak but significant ET between the two subunits. Photochromism is observed both in solution and in single crystals where the orientation of the two units enables selective closure of one of the two DTE with polarized light. When two DTE units are linked through a bimethyl-silyl group (**19**), the photochromism is total and stepwise.[106] As in the previous case, the lack of conjugation mediated by the linker precludes electronic interaction between the two DTE units. Indeed, the absorption spectrum of the **co** isomer is a superposition of the absorption spectrum of the **o** and **c** DTE, indicating minimal electronic communication. The different forms of **19** (**oo**, **oc**, **cc**) were isolated by chromatography. The first cyclisation reaction is found to be more efficient than in the monomer, but the second ring closure is much less efficient, presumably because an ET from the excited open DTE to the closed DTE occurs demonstrating that "through space" interactions are still

possible even if "through bond" interactions are limited.

In **20**, the two photochromes are linked through their bridging double bond to a spiro structure, the lateral thiophenes being either -H or -Br capped.[107] In solution the three isomers **oo**, **oc** and **cc** have been isolated using HPLC. As expected, the absorption at 465 nm for **cc** is twice that of the **co** isomer (the same holds for both **18** and **19**), the photoconversion being 16% and 0.6% for the first and second steps respectively. The authors noted that it is possible that reabsorption by the closed DTE unit in the **co** isomer could explain, even in solution, the decrease in the quantum yield when irradiated with UV light. In this case, ET quenching was not invoked, but instead it was ascribed to inner filter effects.

21 constitutes the first photochromic dimer that is pH-sensitive due to its benzobis(imidazole) bridging unit.[108] The two DTEs units are found to close at the same time (the **co** form could not be isolated), for both the non-protonated and protonated forms of the imidazole. However, the photoconversion was estimated from ^{1}H NMR spectroscopy to be as low as 10%. Protonation leads to a bathochromic shift of the absorption of both isomers but does not significantly influence the photochromism. There are thus 4 states in this system if both chemical and light stimuli are considered. **21** can therefore be viewed as the basic building block for a half-adder circuit (see Figure 8). In a further study, the authors noted that the four available nitrogen atoms (two on the benzimidazole, two on the aniline) show acid base chemistry over a specific pH interval (-1.5 to 4.5) and that the tetraprotonated species could not be fully closed, a fact rationalized by theoretical studies.[109] Indeed, TD-DFT demonstrates that both the LUMO and LUMO+1 present an anti-bonding character (between the two carbon atoms implied in the σ-bond formation) in the **co** form of the fully-protonated structure.

Use of an inherently fluorescent linker does not necessarily imply the loss of full photochromism. For example in **22** where the two DTEs are attached to a Sn porphyrin, both photochromes close independently to reach 63% of closed isomers at the photostationary state. The fluorescence of the porphyrin is decreased when switching the DTE from the open (fluorescent) to the closed (quenched) states.[110] In another report by Tan *et al.*,[111] two DTEs units were attached to a perylene diimide (PDI) derivative (**23**). As the PDI absorbs strongly in the visible and is red coloured, the photochromism of the DTE units is not easily observed but a detailed examination of the evolution of the absorption bands allows one to detect the isomerisation. The quantum yield for photocyclisation is slightly less than for the monomer (resp. 0.18 and 0.28), the same holding for the cycloreversion quantum yield (resp. 0.35 and 0.26). The fluorescence of the PDI, surprisingly, increases after the cyclisation of the DTE, and this was interpreted as the result of the cessation of the electron transfer from the open DTE to the PDI that previously quenched the emission. In

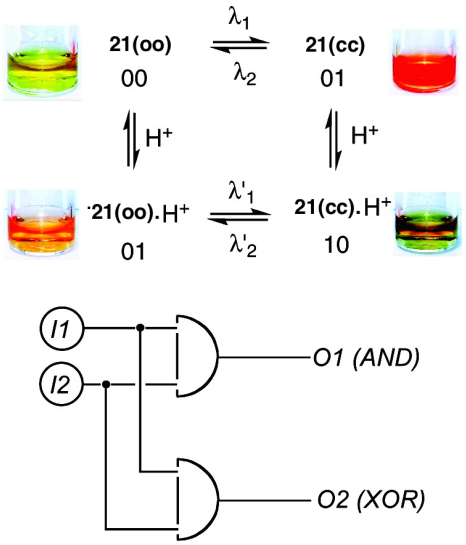

Fig. 8 Illustration of the four states (photochromic+acidochromic) that can be obtained for **21** together with the corresponding logical half-adder. Adapted with permission from Ref. 108, Copyright 2010 American Chemical Society.

Figure 9, the energy levels computed with DFT methods for the **oo** and **cc** forms of **23** are compared. Tan *et al.*,[111] proposed that the presence of an intermediate **co** compound is the reason why the fluorescence does not recover the intensity of the isolated PDI after the switching of the photochromes.

Several studies have been conducted on dyads where two hexafluoro-DTE units are located at both extremities of a sexithiophene molecular wire (**24**).[112–116] Full photochromism is observed for this dimer however both **co** and **cc** forms showed moderate thermal stability, which precluded their isolation by preparative HPLC. Nevertheless, more than 90 % of conversion to the **cc** form could be achieved. DFT calculations showed that the frontier orbitals are localised on the central sexithiophene fragment for the **oo** form explaining the minor influence of the external substitutions on the absorption spectrum (in contrast to the closed form). This also rationalizes the lack of electrochemically driven cyclisation. The properties of the open form are closer to those of a sexithiophene substituted with ethylene-thiophene and **oo** therefore exhibits intense fluorescence. In those systems, the properties of the closed form are essentially the same as in a DTE substituted by thiophenes.

Dimer **25** is the only example of a DTE dimer formed through hydrogen bonding.[117] In this case, the two DTE units interact weakly and only the **cc** isomer could be detected. Its absorption spectrum resembles the spectrum of the closed monomer except for a small red shift of the visible absorption band (5 nm), and the photocyclisation quantum yield is also unaffected by dimerisation (0.38 *versus* 0.36 for the

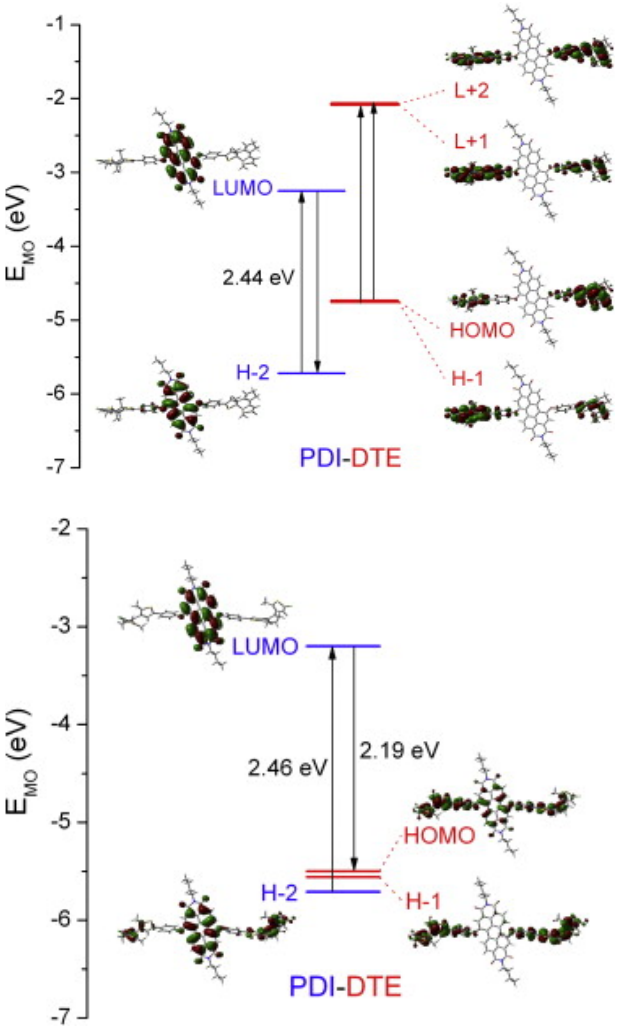

Fig. 9 Energy levels of the open (bottom) and closed (top) **23** together with the key frontier orbitals. Reprinted from Ref 111, Copyright 2011, with permission from Elsevier.

monomer), indicating that there is no significant ET between the units. The OH stretching band was followed by infrared spectroscopy to prove that the **oo** dimer was formed prior to switching. Longer H-bonded chains of carboxylic substituted-DTE have also been studied.[118]

The dimers of DTE are a remarkable illustration of the difficulties encountered in the design of efficient multiphotochromic compounds. On the one hand, dimers with weakly interacting DTEs do not exhibit any other optical properties than a simple addition of those of their components (*e.g.*, **18**, **19** and **20**). On the other hand, strong communication between the two units tends to modify the characteristics of the DTE to a point where the photochromism is limited, if not lost (*e.g.*, **1**, **2** and **5**). When full photochromism is not observed, energy transfer from the excited state of the open form to the closed form is often concluded. This quenching has been observed with several families of relatively short and highly conjugated linkers (*e.g.*, ethynyl, diyne, etc.). On contrast, in dyads where the two DTEs share a common thiophene ring (*e.g.*, **3** and **4**) a steric effect was highlighted as the factor preventing further cyclisation. These conclusions are quite specific to DTE derivatives where the LUMO of the closed isomer is stabilised, which creates an energetic trap, and can therefore be quite different for other families of photochromes. For example, Mitchell *et al.* have discussed the differences between DTE and dihydropyrene dimers linked with the same dyene[119] and showed that unlike the DTE dyad, the dihydropyrene dyad is able to close in a stepwise fashion up to the fully closed system.

2.2 Azobenzene dimers

Two main types of AZB dimers have been reported in the literature: either the two units are linearly attached, or they are connected at both ends to form a supramolecular ring. The linear azobenzene dimers and supramolecular rings reported to date are depicted in Figures 10 and 11, respectively.

2.2.1 Linear compounds

A straightforward strategy is to build an AZB dyad where the two photochromes share a central phenyl ring. **26** and **27**, both capped by oxo groups are *meta* and *para* examples of this scheme.[120] **26** and **27** differ in the degrees of electronic coupling between the two photochromic units, the interaction being greater in the latter compound. As a consequence of this difference, in the *meta* compound, the *ZZ* isomer is formed readily, while the intermediate *EZ* isomer is barely detectable. In contrast, for the *para* compound, a small amount of *EZ* is formed and the *ZZ* isomer is completely absent. This difference has been rationalized through DFT calculations, which indicate that the degree of delocalisation of the π^* molecular orbitals involved in the absorption differs.

Robertus *et al.*[121] reported a more complex AZB dimer where the two units share a benzene ring in the *meta* position (**28**). This compound showed stepwise photochemically and thermally reversible photochromism. In **28**, an asymmetry arises due to the two possible orientations of the carboxyl groups in the *EZ* isomer, and both isomers can be isolated. As for **26**, the coupling between the two units is found to be relatively weak, explaining the relative efficiency of the photochromism. Peters *et al.* have shown that the photochromism in this type of linear AZB dyad is not only affected by the interactions between the two subunits but also by the presence of non-innocent neighbours. For a system where the AZB dimer is linked to a zinc porphyrin (**29**), the photoactivity is lost,

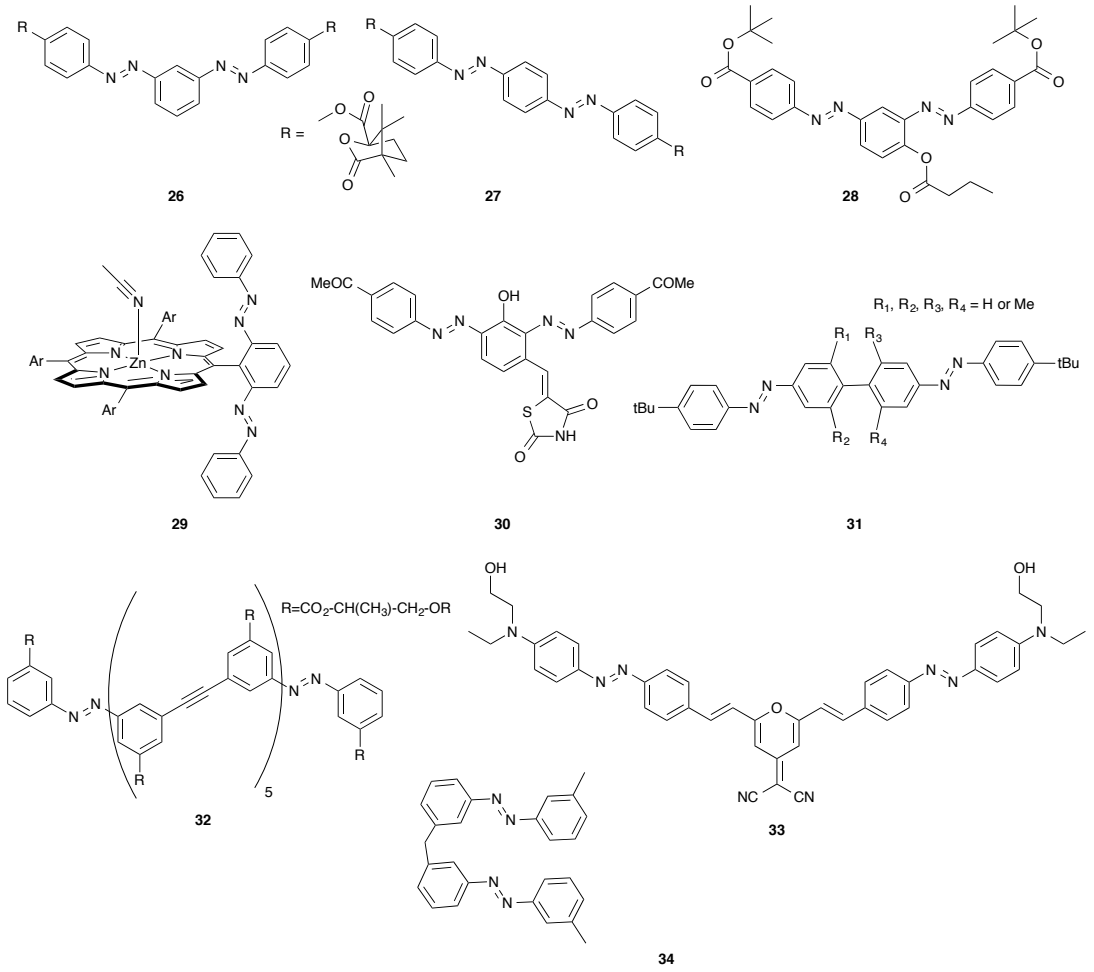

Fig. 10 Non-cyclic azobenzene dimers.

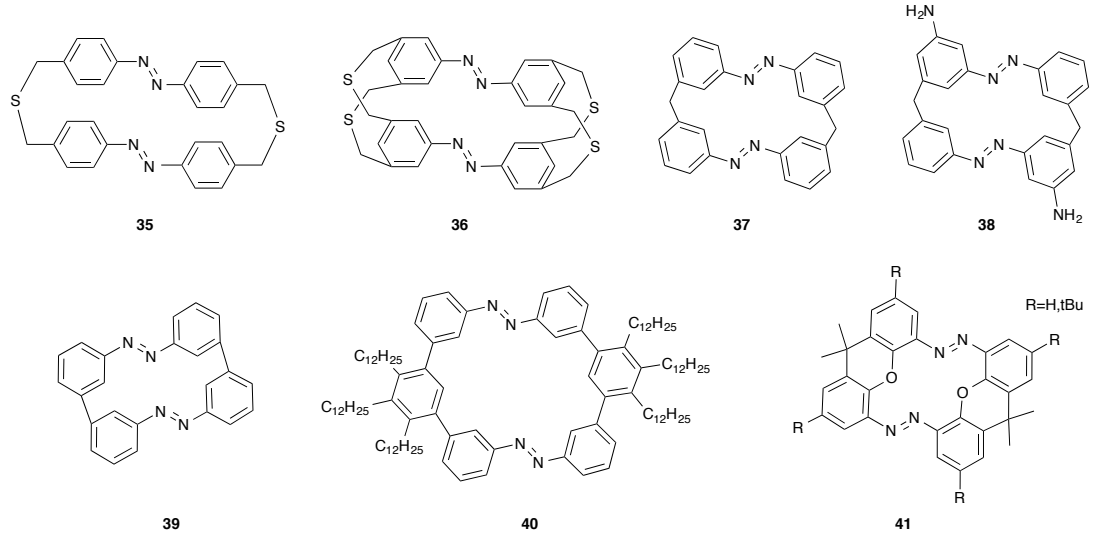

Fig. 11 Azobenzenophanes based on AZB units.

likely due to ET between the two moieties.[122] Mohammadi *et al.* have shown that *meta*-AZB dimers can be modulated by a tautomerisation also when the bridging phenyl is substituted with a hydroxyl group *ortho* to the diazo groups (**30**).[123] The tautomerisation was studied in solvents over a range of polarities and pH but the details of the photochromism of the dimer were not reported. A linear *meta*/*para* AZB dimer sharing a phenyl ring has been studied as part of a polymeric system also.[124] As in the previous examples, the differences in coupling between the two positions are obvious. Indeed, the isomerisation quantum yields are greater in the *meta* case, the photochromism being multi-addressable: different isomeric mixtures can be generated depending on the wavelength of irradiation (*e.g.*, at 365 and 405 nm). The authors concluded that the highly conjugated polymer of *para* dimers may be useful in inducing photo-orientation effects whereas the multi-adressable polymer of *meta* dimers is promising for controlling movement in materials.[124]

Bléger *et al.* have set up a protocol to decrease the extent of electronic interactions when two AZB moieties are tethered to each other at the *para* position of their phenyl rings (**31**).[125] They decoupled the two units by increasing the dihedral angle between the two phenyl rings, through addition of methyl groups at the *ortho* position of the biphenyl linker connecting the two AZB units. The dihedral angle of the biphenyl linker increased from 36° (without methyl groups) to 90° (with four methyl groups). The *ZZ* ratio at the photostationary state composition increased steadily to 95% with this approach while only 3% of *ZZ* was observed for the methyl-free derivative This increase is logically reached at the price of a decrease in the proportion of the *EZ* intermediate obtainable. Similar AZB dimers corresponding to the substitution of a bipyridine unit at the 4,4' positions have also been obtained by Le Bozec and coworkers,[126–128] though they were primarily designed to be used as ligands in a coordination complex, and are thus discussed in Section 4.

Azobenzene dimers have also been prepared using larger and more complex linkers. Two AZBs have for example been incorporated into a conjugated oligomer of phenyl-ethyne groups to photo-induce a bending motion.[129] The resulting helicoid-shaped compound shows a Cotton effect, which correlates directly to the state of the two switches (stepwise photochromism). Compared to the isolated AZB, the isomerisation of the second unit is found to be facilitated by the folding of the oligomer induced by the first isomerisation, albeit that the quantum yield does not exceed 16%. Various arrangements of the photochromes have been assessed and the highest quantum yields have been obtained with **32** when the AZB are placed at the extremities of the oligomer. The presumed bending motions are illustrated in Figure 12.

Additionally, a series of compounds composed of two AZBs connected with a bridge encompassing two stilbenes

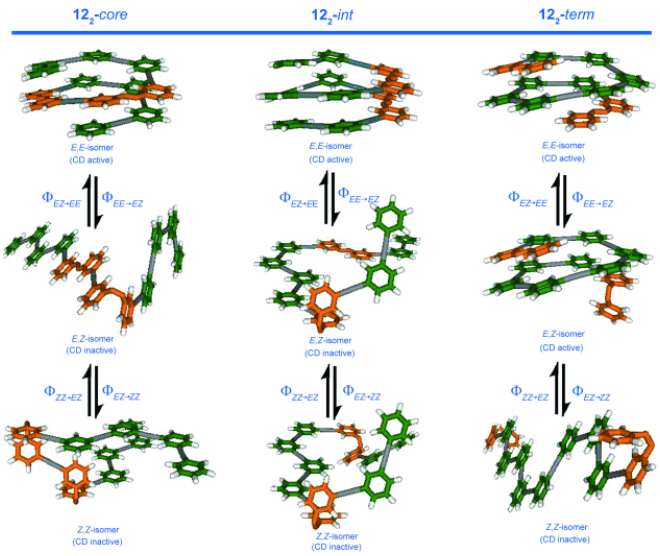

Fig. 12 Proposed bending motion in the foldamer as a function of the position of the two AZB units. The various conformations obtained have different CD signals The 12-2 notation indicates 2 AZBs within a 12 unit (phenylene) oligomer backbone. Reprinted with permission from Ref. 129, Copyright 2012 Wiley-VCH Verlag GmbH & Co. KGaA, Weinheim.

and a central aromatic ring appeared recently.[130] The photochromism of **33** was monitored by measuring the change in the absorbance with and without irradiation at 505 nm, and the conversion was estimated to reach 40%. The thermal retro-isomerisation was similarly appraised, as well as TPA behaviour to estimate the potential use of these compounds in photoactive polymers. Indeed this class of large π architectures are known to give high TPA cross sections, and the incorporation of the AZB units in **33** presents the possibility to modulate the TPA. **34** is discussed further below, together with its cyclic counterpart.

2.2.2 Azobenzenophanes

A widely studied group of AZB dimers is the azobenzenophane class, where the supramolecular ring is formed by two switches connected to each other at both ends. Azobenzenophanes can be obtained with a straightforward two-step synthesis, initially described by Kang *et al.*[131] As illustrated in Figure 11, several azobenzenophanes have been obtained, using a variety of linkers.

The first azobenzenophanes were reported more than 30 years ago by Rau *et al.*[132] **35** and **36** were prepared to gain insight into mechanism of the *E* to *Z* isomerisation. Indeed, the isomerisation in AZBs can proceed via either of two mechanisms: a rotation around the axis of the N=N bond or a direct inversion of the orientation of one of the phenyl rings The in-

version mechanism is known to be induced by a $n \rightarrow \pi^*$ excitation (S_1) whereas the rotation corresponds to a $\pi \rightarrow \pi^*$ excitation (S_2).[133,134] The constraints experienced by a macrocycle serve to enforce one mechanism over the other in the AZB. An inversion mechanism has been suggested in the azobenzenophane,[132] contrasting with the isolated AZB which favours the rotation pathway. This difference is expected since a rotation in the supramolecular architecture requires breakage of a covalent bond, which is energetically unfavourable. Both **35** and **36** isomerise when irradiated at 366 nm. For the former, the quantum yield of the first isomerisation is 0.21 (the second isomerisation does not occur), in line with isolated AZBs whereas for the latter the photochromism becomes very inefficient, because the strain imposed on the ring increases the efficiency of the thermal back-reaction that takes place before the potential *Z* isomer could be detected.

Norikane *et al.* have proposed dyad **37** in which two AZBs are connected at both ends with a simple methylene group.[135] All three possible isomers, *EE*, *ZE* and *ZZ* were observed and could be addressed by applying specific wavelengths, though the *EZ*-*ZZ* isomerisation quantum yield was found to be significantly lower than its *EE*-*EZ* counterpart. Semi-empirical AM1 calculations indicated that the *EZ* isomer experiences the greatest amount of ring strain of the three isomers. In a similar compound, **38**, each of the two AZBs bore an amino group.[136] The *EE* to *EZ* isomerisation (no *ZZ* was obtained) was found to be efficient, though the coupling between the two photochromes is non-negligible, as it significantly affects the shape of the lowest π^* molecular orbitals. The NH_2 groups are responsible for the fast back reaction, and the macrocyclic strain lowers the photoreactivity (50% photoconversion) compared to the monomer (80%). In a further study, Norikane *et al.* compared the absorption spectra and thermodynamic properties of **37** with the corresponding acyclic dimer **34**.[137] Both compounds can isomerise fully through a stepwise process. In the majority of the isomerisation steps the quantum yield is higher for the cyclic compound: although the activation barrier was found to be larger in **37**, the ring strain prevents any other conformational process besides isomerisation. More recently, the same group reported an azobenzenophane which omitted the spacer entirely.[138] Indeed, in **39** the phenyl rings of the AZB units are connected directly at both ends. The steric hindrance generated by this configuration is able to promote unusual thermal *EE* to *ZZ* and photochemical *ZZ* to *EE* isomerisation processes (intermediates were not observed), with good fatigue resistance.

Müri *et al.*[139] obtained four types of azobenzenophane encompassing two AZB and presenting a phenyl linker substituted with long and/or bulky alkyl chains between the two photochromes (*e.g.*, see **40** in Figure 11). For all members of this family an efficient but not stepwise photoreactivity between the *EE* and the *ZZ* form was observed, the intermediate remaining undetected, probably due to the high distortion of the supramolecular cycle in the *ZE* conformation. The rigidity of the *ZZ* compound results in a high thermal stability.

A supramolecular system able to undergo a hinge motion induced by the isomerisation was achieved by Norikane *et al.* by linking two AZB units side by side (**41**).[140,141] The hinge motion, illustrated in Figure 13 is guided by the strain of the supamolecular cycle and its rigidity. The *EZ* intermediate could be observed but its lifetime is extremely short (28 s). On the other hand, this ring strain also results in a remarkable thermal stability for the *ZZ* isomer (more than two weeks) and thus a potential use of this type of dimer in memory storage devices was foreseen.

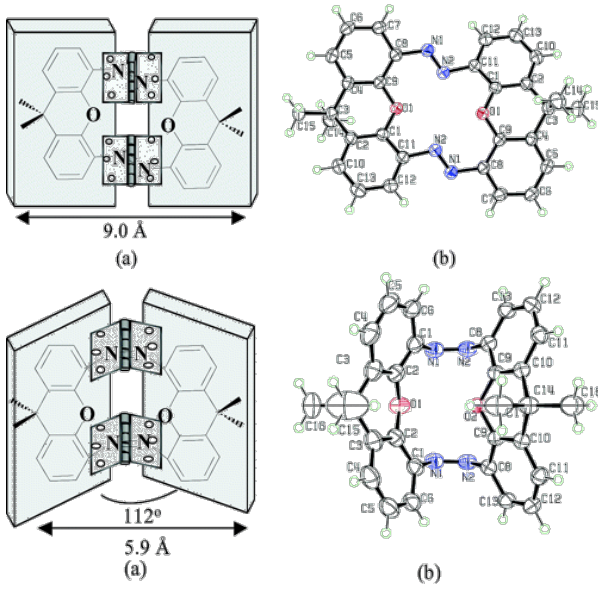

Fig. 13 Representation (left) of the *EE* (top) and *ZZ* structures of a parent of **41** together with the X-ray structures (right), illustrating the possible hinge motion. Reprinted with permission from Ref. 141, Copyright 2005 American Chemical Society.

2.3 Dyads of fulgimides, spiropyrans & dihydropyrenes

A series of FG, SP and DHP dimers are shown in Figure 14. Fulgimide derivatives have only scarcely been used in dimers. To the best of our knowledge, only one series has been reported by Luyksaar *et al.*[142] who have synthesized bisfulgimides, connected through various types of aromatic bridges (**42**). In the case of the FG open form, a *Z*/*E* isomerisation also occurs (and thus provides a third photoactive state). In **42**, the intermediate open/closed forms are not detected, and all of the compounds are found to be *Z*. Though the position of the absorption bands are essentially unaltered

by the linker, the longest linker shows the lowest ratio between the colouration and decolouration rates.

Dimers of SPs have been studied by several groups with attachment of two photochromes through either the indoline or chromene moieties. For example, Fukushima *et al.* used click chemistry to link two units through a phenol spacer.[143] After 3 min of irradiation, the colour of a solution of **43** changes from pale orange to blue-green (absorption band centered at 590 nm), the original colour being rapidly restored at room temperature. Under a prolonged irradiation (more than 10 min.), the accumulation of the zwitterionic MC isomers results in aggregates that undergo a much slower thermal back isomerisation (a week is necessary to bleach the precipitate). These changes are shown in Figure 15 for toluene solution. Incorporation of the dimer into a polymer matrix through the phenol linker results in a slower photochromism.

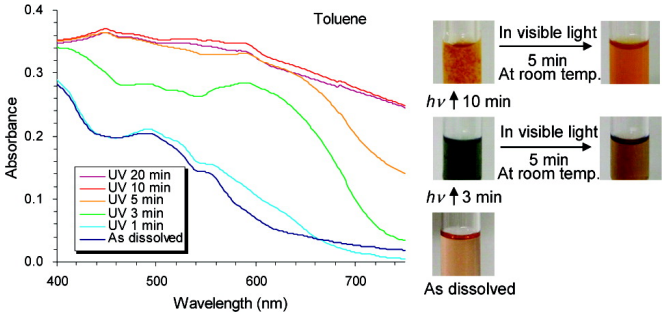

Fig. 15 UV-vis absorption spectra and typical color changes of **43** before and after UV irradiation. Reprinted with permission from Ref. 143, Copyright 2007 American Chemical Society.

The dyad **44** where the two units are directly connected through their indoline moieties, has been studied by Ivashenko *et al.*[144,145] The mechanism of electrochemical dimerisation of the SPs was investigated along with the corresponding optical properties.[144] The appearance of an absorption band at 589 nm demonstrated that the photochemical isomerisation was retained to some extent with the compound returning to its closed form at room temperature. The same dimerisation process has been conducted on a gold surface where the spiropyrans are anchored as a self-assembled monolayer (see Figure 16).[145] The photochromism of the dyad formed on the surface is similar to the one of the anchored monomer: the photoconversion to the MC isomer is achieved up to 31 % in the dyad form. Natali *et al.* have also studied the interaction of SP derivatives with copper(II) and their spontaneous oxidative dimerisation to yield a compound similar to **44** which also retained its colouration.[146] A probable mechanism for the dimerisation is through coupling of radical cationic SPs generated by the oxidation by Cu(II). The related dyads **45** and **46** reported by Lee *et al.*[147] show a new absorption band in the visible domain upon irradiation at 254 nm, though only two (non fully characterised) states are obtained in these dimers. The two compounds differ by the position of their nitro substituent and the point of attachment of the two SPs. In **45**, the zwitterionic MC form is significantly stabilised and this yields a more effective photochromism and a greater optical density.

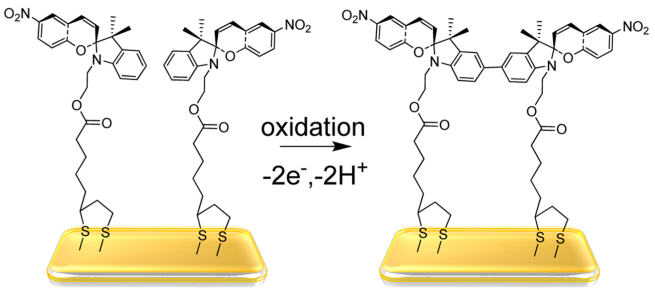

Fig. 16 Dimerisation of spiropyran upon a gold surface to form **44**. Reprinted with permission from Ref. 145, Copyright 2013 American Chemical Society.

Two types of SP dimers, synthesized by Shao *et al.*[148] with a piperazine (**47**) and a binaphtol linker (not shown), have been used as binding receptors for glutathione by taking advantage of the charge complementarity between the MC zwitterionic form and the target, **47** staying in the fully closed form when not complexed with the glutathione. A bidentate SP dimer (**48**) has also been anchored onto lanthanide-doped nanoparticles.[149] The switching from SP to MC can be triggered by energy transfer from the nanoparticle which has been excited in the near IR. The light stimuli for the photoreaction is thus interestingly in the IR region for the opening of the SP and in the visible one for the closure of the MC once the dimer is anchored onto the nanoparticle, which is of potential use for biological applications.

In two studies, Watkins and coworkers synthesized spironaphtho-oxazine dyads.[150,151] The two photoswitches were connected to a central phenyl ring via alkyne spacers (**49**, **50** and **51**). Upon irradiation at 340 nm, the colour changed from pale yellow to dark blue with a new absorption band appearing at ca. 600 nm. The back reaction was spontaneous at room temperature. The dependence of both the position of the visible absorption band and the rate constant for thermal relaxation on the solvent nature indicate that the MC isomer presents a non polar quinoid form rather than its usual zwitterionic form. The compounds retain their photochromic properties when attached at the end of polyethylene glycol (PEG) (but the colouration be- comes less intense). Comparison of **49**, **50** and **51**, indicates that the greater the extent of conjugation (**51**), the more facile the isomerisation in both directions is.

Symmetric SP and NP dyads **52** and **53** were reported by Samat and coworkers by linking the photochromic units

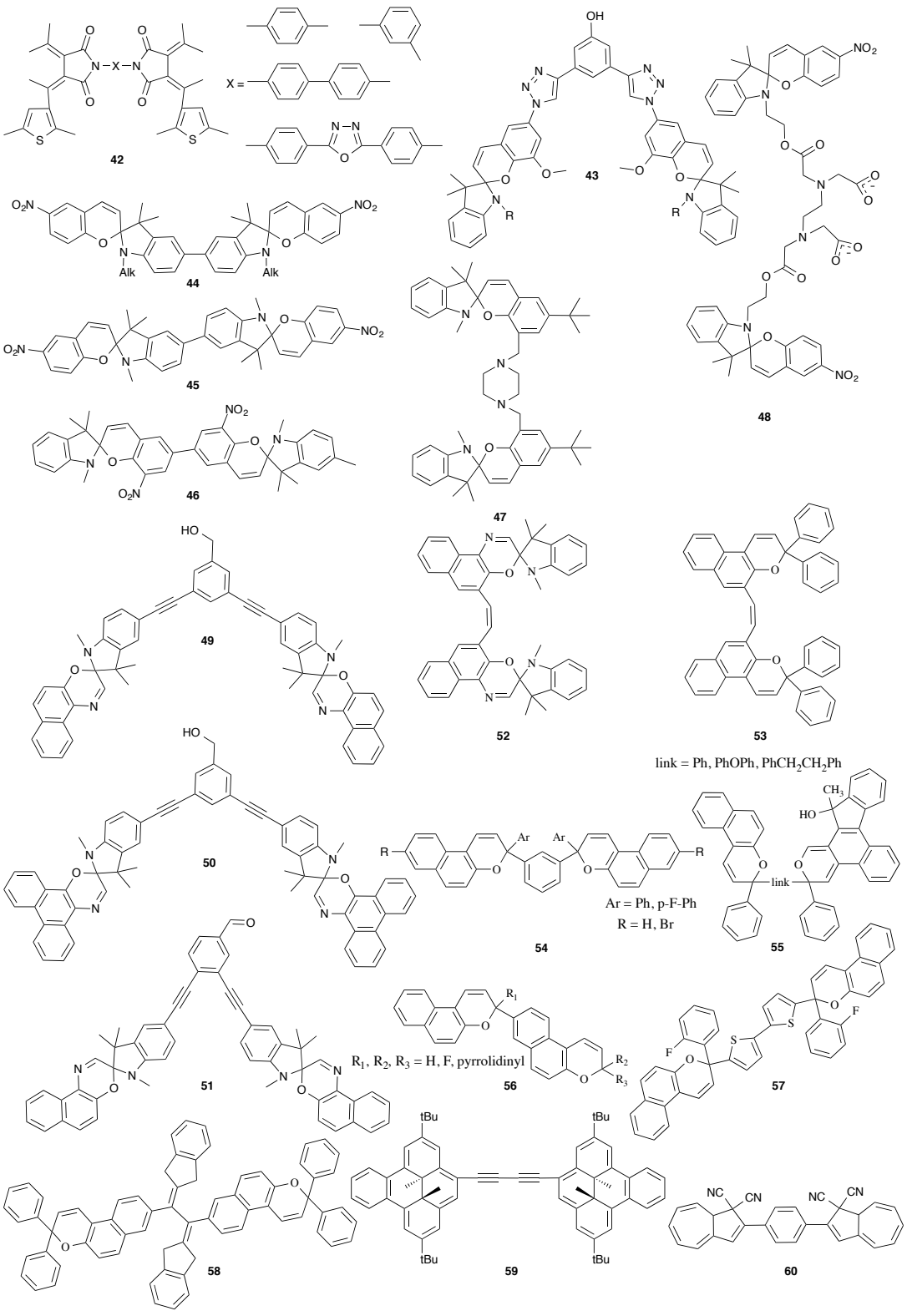

Fig. 14 Selected FG, SP, NP and DHP dimers.

with an ethylenic bridge.[152] In both cases, a coloured form was obtained upon UV irradiation, and these conjugated isomers were thermally stable, in contrast to their respective monomers. The bleaching of the solution was achieved upon irradiation with visible light. The presence of mixed isomers (SP-MC and open/closed NP for **52** and **53**, respectively) was not mentioned. For **53**, it was shown that creating a dissymmetric dyad by changing only the point of linkage on the naphthalene ring of one of the fragments can cause both the loss of thermal stability and the failure of the opening of the second NP.

Concerning NP derivatives, an important synthetic effort has been directed towards obtaining NP dyads with various linkers and substitution patterns.[153–161] Compounds **54**,[160] **55**,[161] **56**,[157] **57**,[154] and **58**[159] are representative of this family, with different bridges, though additional homologous dimers can be found also.[155,156,158]

The photochromic properties of the NP dyad **54**,[160] where the two units are connected to a central phenyl ring at the *meta* position, were compared to those of the same compound with a *para* orientation. An interesting temperature-dependent photochromism was observed: for those two types of dimer only the mixed **oc** isomer is obtained at room temperature but the **oo** isomer can be formed at low temperature (-20 ^{o}C). Additionally, changing from the *meta* to the *para* configuration increases the efficiency of the photochromism of the dimer (both coloration rate and and thermal stability), which was ascribed to the steric interactions generated upon conversion of the *meta* closed to the open form.

NP dimers were reported by Coelho *et al.* with different connectors separating the two photochromes,[161] *e.g.*, **55** and similar but symmetric derivatives. The nature of the phenyl-based bridge is found to have a negligible influence on the photochromic properties. The bathochromic shift in the dimers compared to the corresponding monomers indicated that the **oo**-NP can be formed by irradiation, and detailed analysis of the absorption spectra prooved that the optical properties of the dyads are the sum of those of their individual components. However, the potential multi-addressability of **55** was not discussed in this series as the same irradiation wavelength was applied systematically to induce ring opening.

Derivatives of **56** where the two NP are covalently linked have been obtained.[157] In these compounds, a thermally reversible photochromism is observed, by the appearance of a new band in the visible between 450 and 550 nm, depending on the R substituents (see Figure 14). As for **54** this series exhibited a temperature-dependent photochromism with a stronger coloration at low temperature (10^{o}C), attributed to the increased persistence of the open form. Two thiophene rings link the NP moieties in **57** and a significant electronic communication is observed in this dimer.[154] Consequently, the absorption spectrum of the doubly closed isomer is similar to that of the corresponding monomer but the absorption spectrum of the fully conjugated colored form is more complex and two bands appear in the visible (at 517 nm and 580 nm), suggesting stepwise opening of both NPs.

58 has been electrosynthesised through a dimerisation of the corresponding monomers.[159] As the redox groups remain active in the bridge of the dyad **58**, electrochemical switching between a neutral and a dicationic closed-ring isomer is possible. The neutral form showed however a nearly vanishing coloration upon UV irradiation (the photochromism of the cationic form was not investigated) presumably due to the steric hindrance brought about by the linker.

Mitchell *et al.* reported a series of DHP dyads.[119,162] In these so-called "negative" DHP-based photochromic systems, the stable form is the coloured one, which is bleached upon visible irradiation. In **59**, the two DHP units are connected via a diyne unit.[119] In contrast to the corresponding DTE dimer with the same bridge, both DHP units remain active. Under irradiation at 490 nm, a solution of **59** is bleached from brown to pale yellow, and ultimately colourless. Nevertheless, the presence of the intermediate isomers, **co**, could not be confirmed by ^{1}H NMR spectroscopy, and detailed analysis of the absorption bands and its evolution under visible irradiation pinpointed only the **cc** and **oo** isomers. Alternative DHP dimers combining two moieties through different conjugated spacers have also been reported.[162] It has been found that a quite long spacer (chrysene) allows the two DHPs to open but the intermediate isomer was not detected. In contrast with a much shorter link (phenyl) the intermediate form is observed but the fully closed isomer is thermally unstable and opens quickly to give this intermediate, highlighting the difficulty faced in obtaining three-state photochromism with DHP dimers. It is also notable that all of the various DHP dyads with fused conjugated spacers were found to lack stability.

The only example of a DHA dyad (**60**) has been reported recently, in which the two photochromes are linked through a phenyl ring, in a *para* or *meta* configuration.[163] As for dimers of AZBs,[120,124] these two binding positions lead to different degrees of electronic communication between the photoactive units, and the global efficiency of the DHA to VHF ring opening reaction is lower in the former case (strong interactions) than in the latter (weak interactions). Stepwise photochromism could only be reached in the *meta* structure, providing a three state system. More precisely, the first ring opening quantum yield was found to be 0.65, and an ET from the DHA to the VHF acceptor in the intermediate DHA-VHF isomer explains the lower efficiency for the second isomerisation step.

2.4 Summary

The homo-photochromic dimers reviewed in this Section illustrate the challenge of creating efficiently coupled photoactive systems. On the one hand, to reach emergent properties, different from a simple sum of the properties of the respective monomers, the two subunits should communicate either electronically or sterically. On the other hand, if the electronic interactions between the components of the system are too strong, the characteristic features of the photochromes may be lost, notably the ability to switch one or several units might disappear. The most striking examples of this duality are the DTE dimers, for which numerous systems have been reported, connecting the two units with a wide variety of linkers and strategies: full photochromism is rarely achieved except when the two units are uncoupled. In most cases, limited photochromism is ascribed to energy transfer from the excited state of the open form to the closed form. Comparison of DTE and DHP dimers with a diyne linker showed that, when full isomerisation is attained (in a DHP dyad), it is at the cost of the loss of the presence of intermediate isomers that are present in the DTE dyad. AZB dimers are found to be more robust in this regard, the most prominent decrease in the photoreactivity being found for linear dimers sharing a phenyl ring with *para* substitution. Nevertheless, in most AZB dyads, only the full *E* and full *Z* isomers could be isolated, the *EZ* intermediate being too unstable, so that multiaddressability remains the exception rather than the rule. Photochromism in dimers of FG, NP, DHA and SP derivatives has not been investigated with the same intensity and hence it remains difficult to reach definitive conclusions at this stage for those compounds.

3 Multimeric of photochromic compounds

3.1 DTE multimers

Systems that contain more than two DTE units linked through an organic bridge include trimers,[65,94,164–168] tetramers[98,165,169] and hexamers[170,171] (see Figures 17 and 18). In the following section the notations **o** and **c** are used for the two possible states of each DTE unit.

As for DTE dimers, multimers can be obtained by "fusing" the respective units together through shared thiophene rings and this strategy was applied successfully by Higashiguchi *et al.* to reach **61**.[164] In this compound the isomerisation of the DTE can be achieved for up to two non-consecutive units. Consequently, apart from the colourless fully open isomer, four distinct colours can be observed (blue, red, yellow and black, see Figure 19 for the three former colors) making the compound a five state switch thanks to the asymmetry of the DTE units. The colours are assigned to the possible isomers, **oco**, **coo**, **ooc** and **coc**, respectively and can be obtained selectively by a judicious choice of the irradiation wavelength(s). Irradiation at 313 nm induces the closure of either of the two terminal DTE units, to lead to a yellow and ultimately orange solution, while a prolonged irradiation leads the black **coc** isomer. The cyclisation of the central DTE is possible but the associated quantum yield is minuscule (0.0023), which was rationalised by examination of X-ray crystallographic data. Indeed, this DTE presents a highly distorted conformation,[164] a fact in line with theoretical simulations.[90] Irradiation at several wavelengths (460, 578 and 633 nm) enables selective opening of the DTE units and the isolation of the blue **oco** form from the mixture of the other isomers, as this isomer shows a relatively low quantum yield for cycloreversion.

In a work by Liu *et al.*, two DTEs are attached to a third central photochrome via an imidazole bridging ring at the α position of the thiophenes (**62**).[65] The three DTEs can close and two different partially/fully closed forms, namely **oco** or **ccc** can be formed selectively as the chemical structure of the two types of DTE in **62** are distinct from each other. Indeed, irradiation at 254 nm allows both the terminal and the central DTEs to be closed, generating a new absorption band at 520 nm, whereas irradiation at 365 nm is only able to induce photocyclisation of the central DTE unit, yielding a coloured isomer absorbing at 562 nm. The quantum yields of these two cyclisation processes are 0.43 and 0.35, respectively. All of the closed isomers return to the fully open state upon irradiation at 450 nm.

Multimers of two, three and four DTE units organised in arrays have been obtained by linking the photochromic centres through ethynyl bridges (**63**).[165] As the length of the array increases, the total photocyclisation quantum yield increases as well, from 0.21 for the monomer to 0.40 for the tetramer. For the dimer, as expected (see Section 2) only the system containing one closed unit has been detected by HPLC and NMR spectroscopy. For the trimer, three types of partially closed systems are observed, **ooc**, **oco**, and **coc** with a photostationary state ratio of 54:39:3 at 320 nm. For the tetramer array, the irradiation in the UV leads to four distinct isomers : the two singly closed **oooc** and **ocoo** isomers, formed with a respective quantum yield of 0.10 and 0.30, and the two doubly closed **ococ** and **cooc** isomers (for which the quantum yields have not been determined). In other words, in **63**, it is impossible to close two adjacent switches. Efficient intramolecular ET is assumed to be responsible for both the partial photochromism (energy transfer from the excited open to the vicinal closed DTE being more efficient than the photocyclisation) and for the improved quantum yields (energy transfer from the inactive open parallel conformation to the active anti-parallel conformation). The dimer and trimer **63** have been investigated with TD-DFT also (see Section 6).[71,172] Li *et al.* have linked three DTE units using ethynyl bridges (**64**),[94] but could only detect the **coc** form, further cyclisation was not observed in

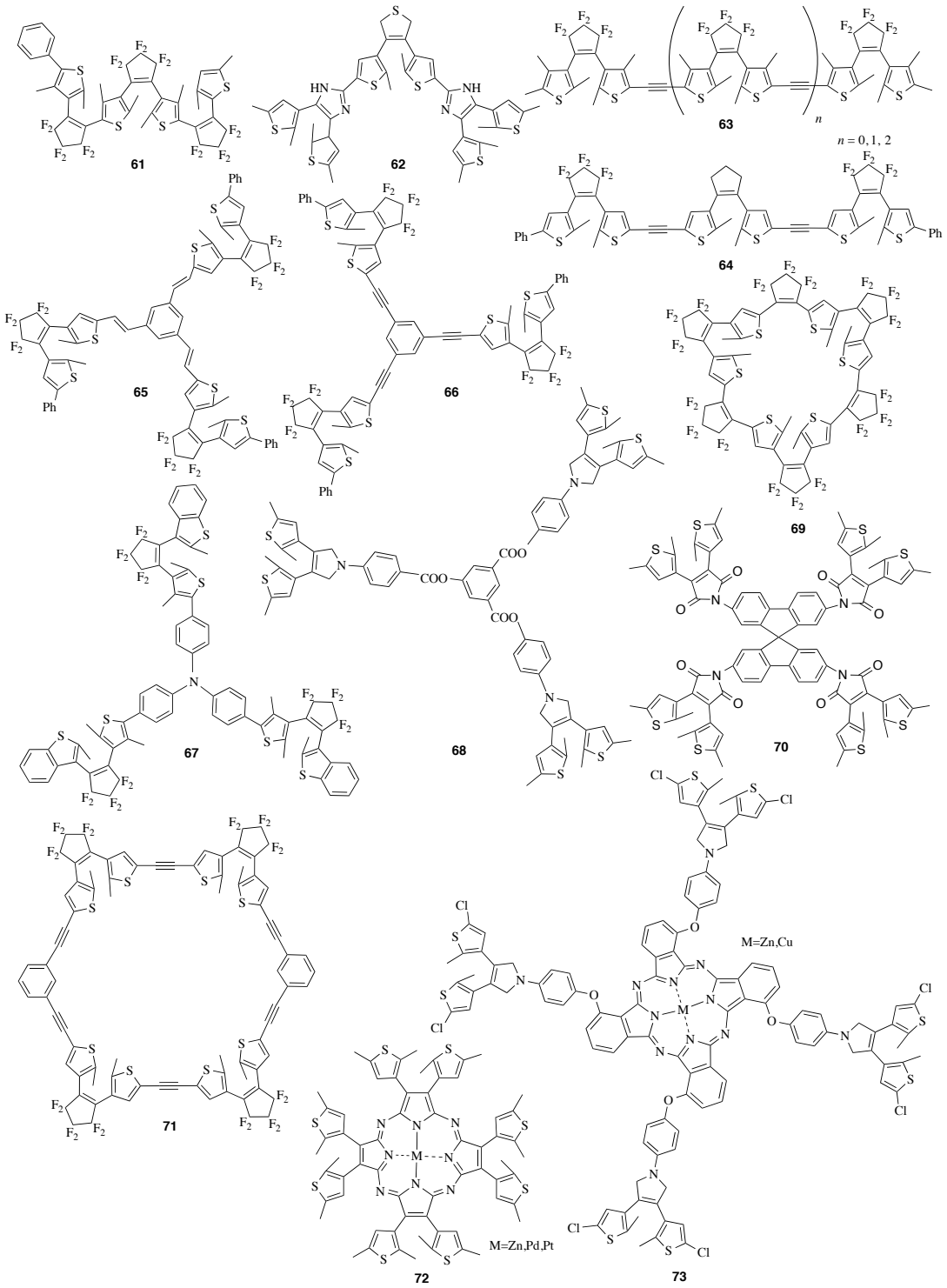

Fig. 17 DTE trimers and tetramers.

contrast to a similar trimer in which gold atoms are inserted between the DTE units (see Section 4).

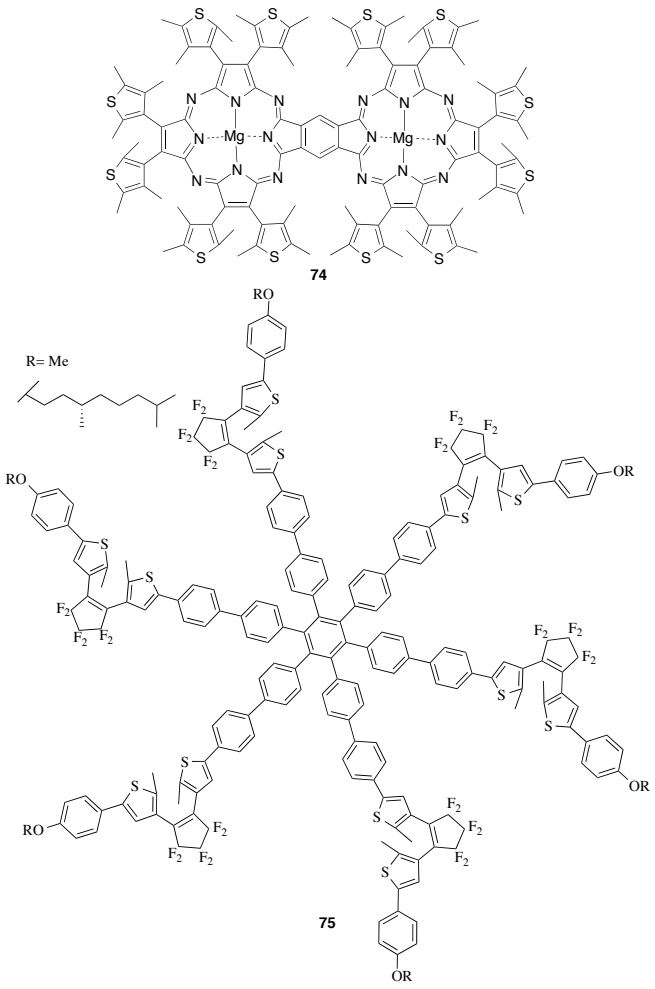

Fig. 18 DTE hexamers.

Fig. 19 Colour changes in **61** when closing one of the three DTE units. The black **coc** (not shown) form can been obtained also. Adapted with permission from Ref. 164, Copyright 2005 American Chemical Society.

In several studies, star-shaped trimers have been obtained by connecting three DTE units to a central linker.[166–168] Trimers of DTEs linked to a phenyl core, **65** and **66**, were obtained by Choi *et al.*[166] using either ethenyl or ethynyl linkers. In the former, one, two or three DTE units can be closed consecutively under prolonged irradiation at 365 nm, resulting in a tripling of the intensity and a slight redshift of the hallmark DTE absorption band at ca. 600 nm. Each of the partially closed systems were stable and were isolated. The respective quantum yields for the three cyclisations are 0.23, 0.18 and 0.11, making an overall yield of 0.52, greater than in the corresponding linear array.[165] For the latter derivative with ethynyl bridges, the **ccc** isomer could not be formed, a surprising outcome that was latter rationalised by theoretical studies (see Section 6).[173] In the similar trimer **67**, the DTE units are attached to a central triphenylamine.[167] Under irradiation at 334 nm, a mixture of all possible closed isomers is obtained at the photostationary state: **coo** (54%), **cco** (41%), **ccc** (5%). All of the isomers of **67** present the same absorption maxima in the visible (centered at 559 nm), and the successive reactions only induce an increase in intensity of this visible band, indicating weak communication between the π systems of the three closed DTEs. The photocyclisation quantum yields decrease steadily as the mixed open-closed isomers are formed: 0.47 (close to the monomer, 0.52), 0.029 and 0.015, for the first, second and third ring-closure respectively. In contrast, the ring- opening quantum yields are within the same order of magnitude for all steps: 0.092, 0.075 and 0.060, respectively. In the bulk amorphous phase, the photochromism is still observed, but only the **coo** and the **cco** isomers are formed upon irradiation. A DTE star-shaped triad built around a central phenyl ring has also been studied by Zeng *et al.*[168] (**68**). In **68**, the photochromes are obviously electronically decoupled and only an increase in the total intensity is observed upon formation of the closed isomers. The efficiency of the photocyclisation was demonstrated both in solution and in a PMMA polymer film. A macrocyclic trimer, **69**, consisting of three DTEs has also been described, together with the corresponding dimer.[174] While the dimer did not undergo ring closure upon irradiation with UV light in dichloromethane, due to excessive ring strain, **69** (see XRD structure in Figure 20) can switch reversibly between the colourless open structure to a yellow-green closed form. The number of closed DTE units in the macrocycle was not determined.

Organic dyes encompassing four DTE units have been studied such as that by Tian *et al.*, who reported a tetramer of DTEs with a spiro bifluorene bridge, **70**.[169] As with its parent dimer, **18**, the DTE units interact only weakly. For this first tetramer, only the **oooo** and the **cccc** forms were observed, suggesting that, in contrast to **64**, energy transfer between the different units did not take place to a significant extend. In **71**, the four DTEs are arranged to form a macrocycle with two ethynylene and two phenylethynylene connectors.[98] In addition to the fully open isomer, only the isomers containing one or two closed DTE units have been found, the geometrical

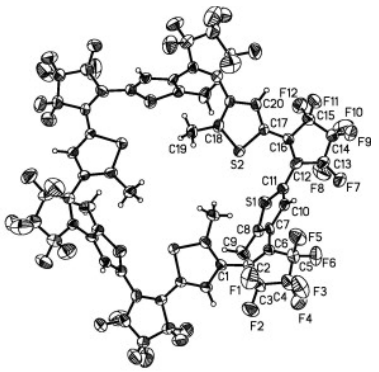

Fig. 20 XRD molecular structure of **69**. Reprinted from Ref 174, Copyright 2008, with permission from Elsevier.

constraints imposed on the cycle probably impede the movements necessary for ring closure. In addition, ET quenching could not be excluded on the basis of the fluorescence and absorption spectra of the open and closed DTE units, respectively. The respective cyclisation yields from the fully open to the singly and doubly closed isomers are 0.33 and 0.25, which are greater than the yields observed for a simple array of four DTE units,[165] presumably due to the larger proportion of the antiparallel conformers in the macrocycle. Phthalocyanine-based multimers of DTE, containing between one to four photochromes (**72**) have also been reported.[175,176] In these compounds, the same photochromic pattern appears systematically: the ring closure of two opposite DTEs is achievable while the simultaneous isomerisation of two neighbour photochromes is impossible, even with prolonged irradiation. In another investigation, Zn-**72** was shown to form J-aggregates when the DTEs are closed.[177] In this study, up to three DTEs were reported to close, leading to a new absorption band at ca. 700 nm, though the system exhibited a poor fatigue resistance due to photodegradation. To reach full isomerisation, one can decouple the DTEs from the central macrocycle by using phenoxy spacers (**73**),[178] but in this case mixed closed-open isomers were not reported.

To date, the largest molecular multimers reported in the literature contain six DTEs. Luo *et al.* incorporated six DTE units at the periphery of a biporphyrazine.[171] Only two states of this supramolecular compound, **74** (see Figure 18), fully opened and partially closed were detected, the luminescence quantum yield of the macrocycles being controlled by the state of the photochromes. NMR studies indicate that in the partially closed system the two most opposite DTE units close, while the four other units remain open. A snowflake-shaped hexamer (**75**) was synthesised[170] by substituting all branches of a hexaphenylbenzene core with DTEs. **75** exhibits the same absorption and electrochemical features as the separated units, and all DTEs are photoactive. Indeed, in **75**, the photochromes are electronically decoupled due to the presence of biphenyl linkers,[179] and only a six-fold photochromic signal is measured following the simultaneous isomerisation of all switches. The reversibility of the system is preserved in the supramolecular arrangement, and the conversion rate is found to be very high (90% for the ring closure and 100% for the ring opening).[170]

Beyond molecular systems, at least a brief mention of oligomers and polymers of DTEs that have been synthesised is warranted.[11,81–83,180] Cho *et al.* reported for example oligomers in which the DTEs were separated by phenylenlvinylene groups.[180] The photochromic properties of these oligomers are similar to those of the isolated DTEs. Besides the expected increase in absorbance, a redshift of the absorption bands of both the open and closed isomers was observed. States other than **o** and **c** were not identified and the ratio of closed DTE in the full oligomer was not determined. More generally, it has been shown that designing DTE-heteropolymers is also a valid strategy to achieve a multi-addressable materials[181–183] but, as stated in the Introduction, this is beyond the scope of the present review.

3.2 Azobenzenes multimers

Supramolecular assemblies of AZBs have received considerable attention in recent years, and representative systems are reported in Figure 21.

Linear molecular wires of AZB derivatives have been reported by Humphrey *et al.*, whom linked increasing numbers of photochromic units via ethynyl bridges (**76**).[184] This study aimed primarily at investigating dependence of both linear and non-linear optical (NLO) properties on chain lengths, the AZB units being viewed as chromophores rather than photochromes. Short oligomers of AZBs containing from 3 to 5 units, with substitutions at the *ortho* positions have also been studied (**77**).[185] The switching of these chains was found to be impossible irrespective of the oligomer length, in contrast to the monomer. By contrast for the corresponding *meta* and *para* derivatives, the photoactivity was preserved. Two hypotheses have been proposed to explain the peculiar behaviour of the *ortho* linked chains: i) the back *Z* to *E* isomerisation is faster than the time needed to monitor absorption; ii) the *ortho* position favours strong electronic communication preventing switching. Moneo *et al.* studied the delocalisation of the charge in the radical anion **78** built with three AZBs.[186] In that study, the coupling between the sites bearing a localized charge was quantified by electron paramagnetic resonance (EPR) spectroscopy, but the mechanism of photochromism of this derivative remained unexplored.

As for DTE multimers, star-shaped supramolecular assemblies have been built with AZB photochromes. **79** was obtained by linking three identical azobenzenes derivatives to

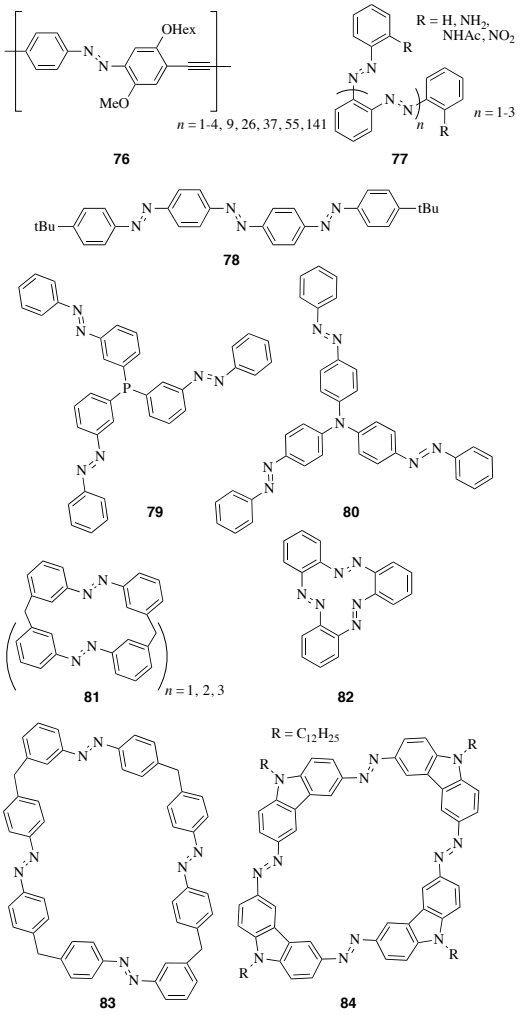

Fig. 21 Representation of selected AZB multimers.

a triphenylphosphine core.[187] Starting from the *EEE* isomer, only two new isomers were observed by ^{1}H NMR spectroscopy, albeit that the structures were not determined. This phosphine derivative was used as a ligand in a Pt complex, without impacting its photoreactivity. A similar AZB dendrimer, **85** (see Figure 22), has been reported with bulky substituents added at its periphery[188] to take advantage of the change in the geometry between the possible states. Upon isomerisation of the three photochromes, a contraction of ca. 30% of the molecular volume was observed. Three unsubstituted AZBs were connected to a central nitrogen atom,[189] to form **80**, which can undergo *E/Z* isomerisation to a point that all three AZBs are switched (the all-*Z* isomer representing 12% of the blend at the photostationary state). Interestingly, it was observed that the lifetime of the *Z*-isomer is longer in the trimer than in the corresponding dimer.[189] When going from the monomer to the dimer and next to the trimer, the increase

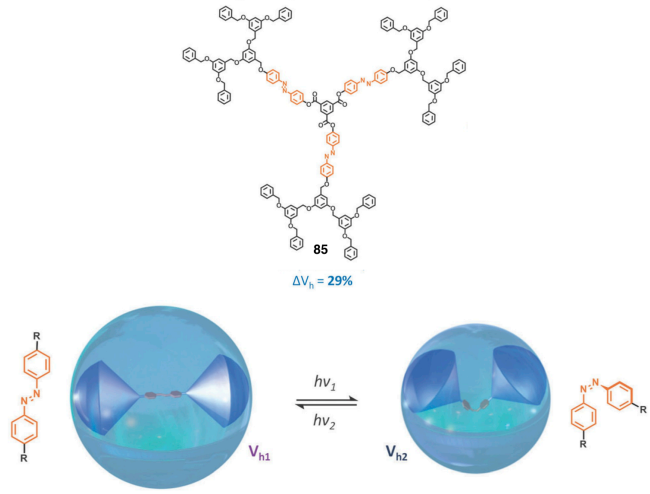

Fig. 22 AZB dendrimer **85**, and volume reduction following the isomerisation. Reproduced from Ref. 188 with permission from The Royal Society of Chemistry

in the effective π-conjugated length induces successive red-shifts in the absorption (of 51 nm and 20 nm, respectively for the all-*E* form).

As for the dimers, a large number of the AZB multimers that have been reported are azobenzenophanes. For instance, three or four AZB units have been connected through a methylene unit, to form supramolecular rings.[135] Those azobenzenophanes, **81**, showed stepwise photochromism and all of the possible isomers were isolated using HPLC. For both trimers and tetramers, the full *Z* isomers can be obtained efficiently, with a ratio exceeding 60%, indicating that the constraints imposed on the ring are less than in the corresponding dimer. In contrast, the highly compact cyclotrisazobenzene **82** in which AZBs share their phenyl ring is photo-inactive.[190] Indeed, irradiation at various wavelengths do not trigger isomerisation, due to the extreme ring strain. Four AZBs can also be linked to form azobenzenophanes.[191,192] In the work of Shen *et al.*[191] several partially isomerised forms of **83** have been obtained, each presenting various conformations. As illustrated in Figure 23, these isomers can be distinguished readily by scanning tunneling microscopy (STM). In the same vein, four AZBs have been connected through intermediate carbazole groups to yield **84**.[192] The goal of that recent investigation was to obtain a multi-adressable system in which the distortions of the supramolecular ring can be controlled by switching only one or several specific AZBs (rather than activating all of them as in most azobenophanes). The proportion of each isomer was quantified by ^{1}H NMR spectroscopy and it was concluded that the symmetry of the arrangement dictates the stability of the photoproduct, *e.g.*, the *EEZZ* and *EZEZ* isomers show different rates of thermal fading although they both encompass two

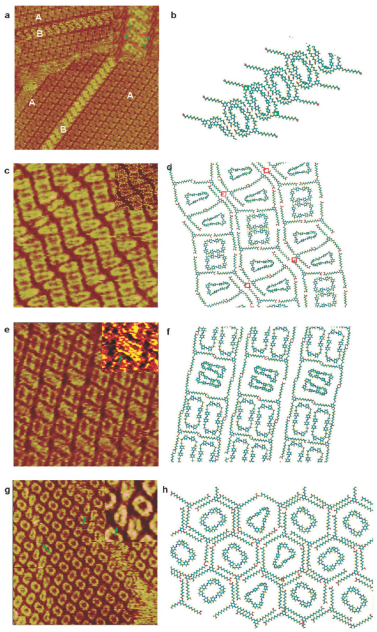

Fig. 23 STM images of the different isomers of **83**. Reprinted with permission from Ref. 191, Copyright 2009 American Chemical Society.

Z and *E* units.

3.3 Spiropyran dendrimers

Aside from multimers of DTEs and AZBs, a few studies have been devoted to other families of photochromic compounds. For instance, SPs have been incorporated in dendrimers (see Figure 24). A point of interest with such architectures, typically encompassing three or six SP switches,[193] is to improve the stability of the coloured MC form with respect to the corresponding polymers based on the same photochrome. In **86**, the photocyclisable chalcone linker was found to enhance the stability of the MC form. Likewise, the performances of the photochromic dendrimer **87** based on the same SP units, were found to be greatly enhanced compared to the monomer, with both an increase in absorbance and greater stability of open MC isomers.[194]

3.4 Summary

The potential of multimers of photochromic compounds is clearly high in terms of number of distinct responses to light stimulus. However most multimers are highly symmetric, and present electronically uncoupled units, leading to an increased intensity of the photochromic response compared to the monomer, but to a number of distinguishable states limited to two even in hexamers. Some asymmetric systems have been

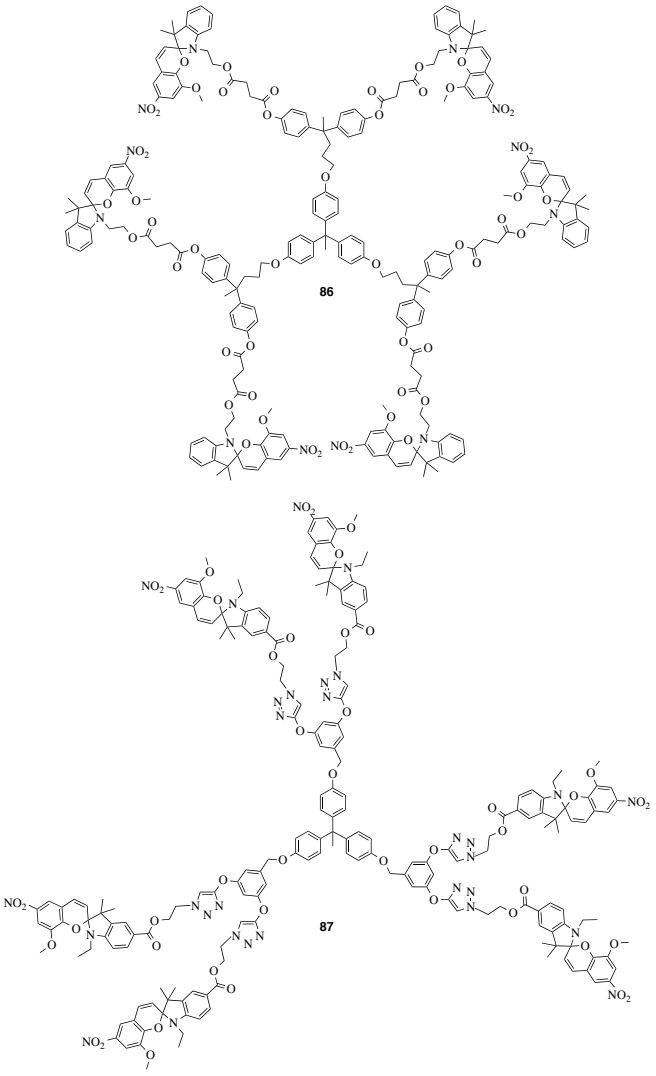

Fig. 24 SP dendrimers

developed successfully, especially for DTEs that are probably the best candidates for multi-addressability: at least one trimer displaying five distinguishable states (five colours controllable by selection of wavelength(s) of irradiation) was reported.[164] Overall, it also appears that star-shaped architectures tend to be more successful, as they are less prone to the ET that generally impedes photochromism of some units in linear or square supramolecules.

4 Metallic multiphotochromic complexes

There are many benefits of using coordination complexes to couple several photochromic units: i) it is much easier to control the supramolecular shape that is guided by the coordination geometry of the metal. In this regard, the attachment to

the metal is often achieved using pyridine ligands,[102,195–201] or carbenes with ethynyl linkers;[94,202–205] ii) stepwise photochromism is often observed as the metal can act as a barrier between the different photochromic centres and prevent excessive perturbation of the intrinsic electronic structure of individual photoswitches; and iii) electrochemical stimuli may, in some cases, be an alternative mode to trigger the photoisomerisation by augmenting the electrochromic properties of the switching units.[41,42] Transition metal complexes involving various photochromes are described below, provided that they possess at least two photochromic units.

4.1 Dithienylethene-based compounds

Multimers of DTE have been synthesised using several metal centres: Fe,[197–199,201] Ru,[199,204,205] Cu,[195,206] Pd,[207,208] Au,[94,208] Pt,[98,202,203,209] Zn,[102,196,197,200] Co[198,199] and Re[102] (see Figures 25 and 26). The appearance of both emergent properties and stepwise photochromism (that is, the presence of mixed closed-open isomers) depends on the nature of the metal and of the ligands bearing the DTE.

Guerchais, Le Bozec and coworkers have proposed a wide range of complexes using bi-pyridine ligands bearing two DTEs with a focus on second-order NLO properties. They considered two families of ligands with the photochromes linked to the bi-pyridine either by their thiophene rings (**88**, **89** and **90**) or their reactive carbon atoms (**91**).[210] In the Cu(I) complex **88**, the presence of two ligands, that is of four DTEs, gives birth to an octupolar T_d compound.[195] The second-order NLO properties of **88** have been investigated both experimentally and theoretically, and the response was found to increase by one order of magnitude when going from **o** to **c** DTEs. The photostationary state contains 90% of closed DTE but the isomers have not been separated. *Ab initio* calculations nevertheless indicated that the fully closed system is reachable in terms of steric hindrance and stability of the **cccc** isomer.[195] The same type of bidentate DTE dimer has been coordinated to a Zn(II) ion by Ordronneau *et al.*[196] DFT and TD-DFT calculations predicted full photochromism for **89**, which matches experiment, though the UV/vis absorption spectroscopy and kinetics indicate that the quantum yield of ring-closure is drastically reduced for the second cyclisation. The quantum yields are nevertheless identical for both cycloreversion processes. The ring closure is also more efficient for the isolated photochromic ligand than within the Zn(II) complex, while adding donor (NMe_2, NBu_2, OMe) or acceptor (OAc, Cl) groups to the DTE induces a decrease of the cyclisation quantum yield. Using the same ligand associated to Zn(II) and Fe(II), octahedral complexes containing six photochromes have also prepared (**90**).[197] It should be noted that **90** presents a D_3 point group (which contrasts with the organic hexamer **75**,[170] that belongs to the C_6 point group). For the Fe(II)-**90** complex, full reversible photochromism was assumed as none of the possible intermediates could be detected by ^{1}H NMR spectroscopy. As in **88**, the NLO properties have been investigated in a combined theoretical and experimental study. The enhancement factor of the second-order response was determined as being 8.0 and estimated by TD-DFT as being 6.9 at the photostationary state of the R=$NAlk_2$ derivative (60% of **c** isomers). For the Zn(II)-**90** complex, partial dissociation was detected by ^{1}H NMR spectroscopy, and NLO have not been reported. The DTE dimer **15** with a bidentate bypriridine link at the reactive carbon atoms has been used to tether Zn(II) and Re(I) complex (**91**).[102] While the Re(I) complex is photochemically inactive, the Zn(II) complex exhibits the same photoactivity as the free dimer, though the photoreactivity is less compared to the "normal" ligands. In **92**, four DTEs complex an Fe(II) center via monodentate pyridine rings, the coordination being completed by two isothiocyanate groups.[201] This complex exhibited reversible photochromism, with an absorption spectrum similar to the isolated ligand, both in solution and in the solid state, *i.e.* the crystal going from orange to indigo (and *vice-versa*) under irradiation at 365 nm and 650 nm, respectively. The magnetic susceptibility of the crystal increases after switching the DTEs, indicating spin cross over to a high spin state.

Another approach has been to bind two DTE presenting cycles bearing lone pairs to two metals, and this strategy is illustrated by **93** and **94** in Figure 25. The bi-metallic Cu(I) complex **93** in which each DTE binds two metal atoms through peripheral oxazoline rings is, to our knowledge, the first metal-DTE dimer reported in the literature.[206] Full cyclisation was observed and the chirality of the various diastereoisomers arising from this arrangement has been analysed. The recording of the change in the CD spectrum provided the possibility of non-destructive readout at a wavelength (450 nm) outside the photoactive regions (see Figure 27). In **94** two DTEs complexe a Zn atom and the photochromism is found to be enhanced compared to the isolated ligands.[200] Indeed, the cyclisation yield goes from 0.15 up to 0.40, and the change of fluorescence of the pyridine-DTE upon ring-closure allows nearly non-destructive readout: the emission of the Zn cation at 463 nm is stopped after ring-closure.

Two DTEs possessing a terpyridine unit have been connected via a complexation with Fe(II) or Co(III) (**95**).[198] With Fe(II), the cyclisation reaction is found to be blocked and allowed when the DTEs are capped by chlorine and phenyl groups, respectively. With Co(III), a more interesting photochromic behaviour was noted: the chlorine substituted system exhibited 40% photoconversion, whereas the phenyl-substituted **95** achieved a quantitative isomerisation. The authors did not specify whether or not the "closed" form corresponds to the **co** or **cc** isomer. The same group has also linked three bidentate pyridine-terminated DTE ligands to three metallic centres (Fe(II), Co(III), Ru(II) in **96**).[199] In case

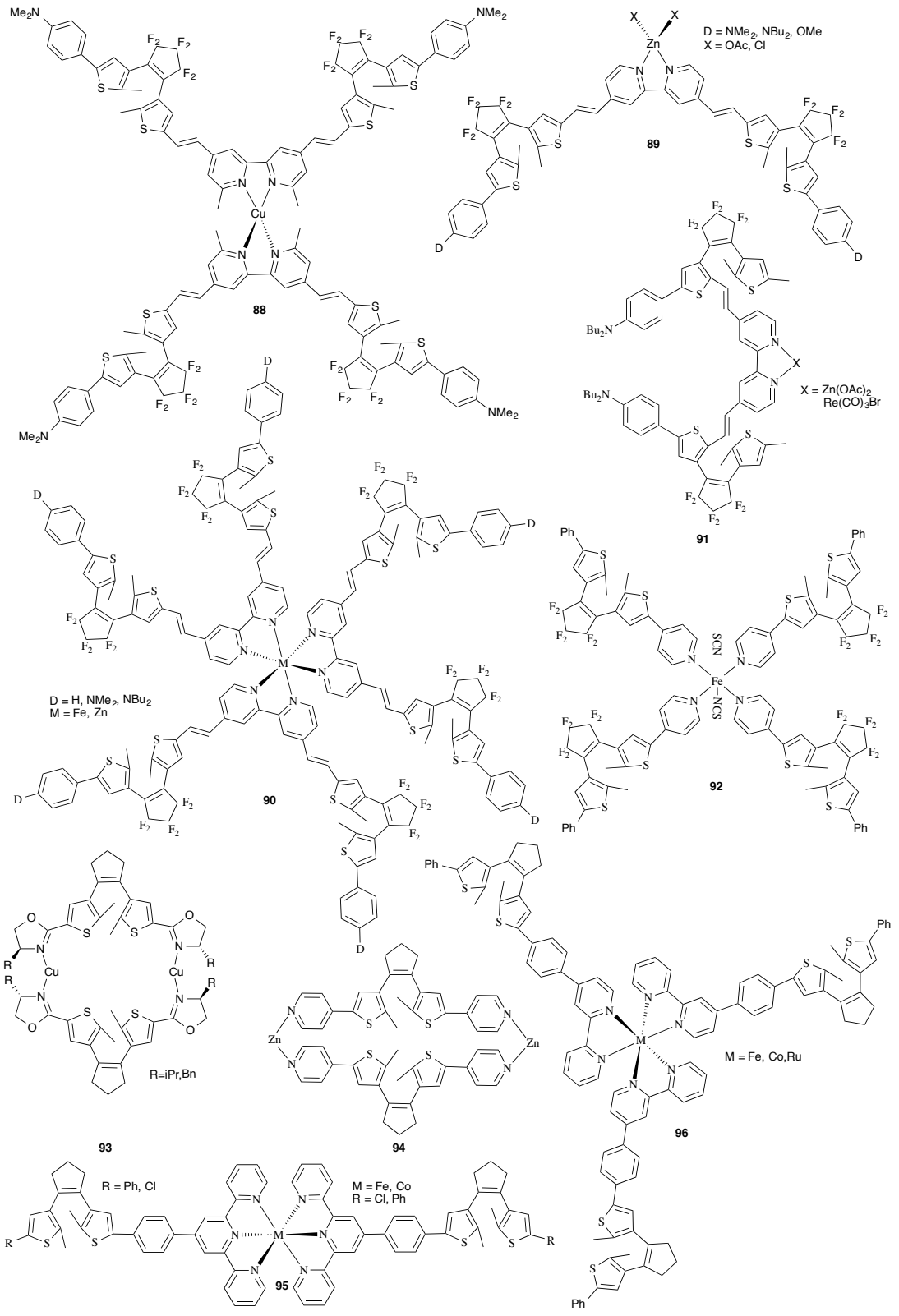

Fig. 25 Multi-DTE complexes built with mono-, bi- or ter-pyridine ligands. The charges and counter-ions have been omitted for clarity.

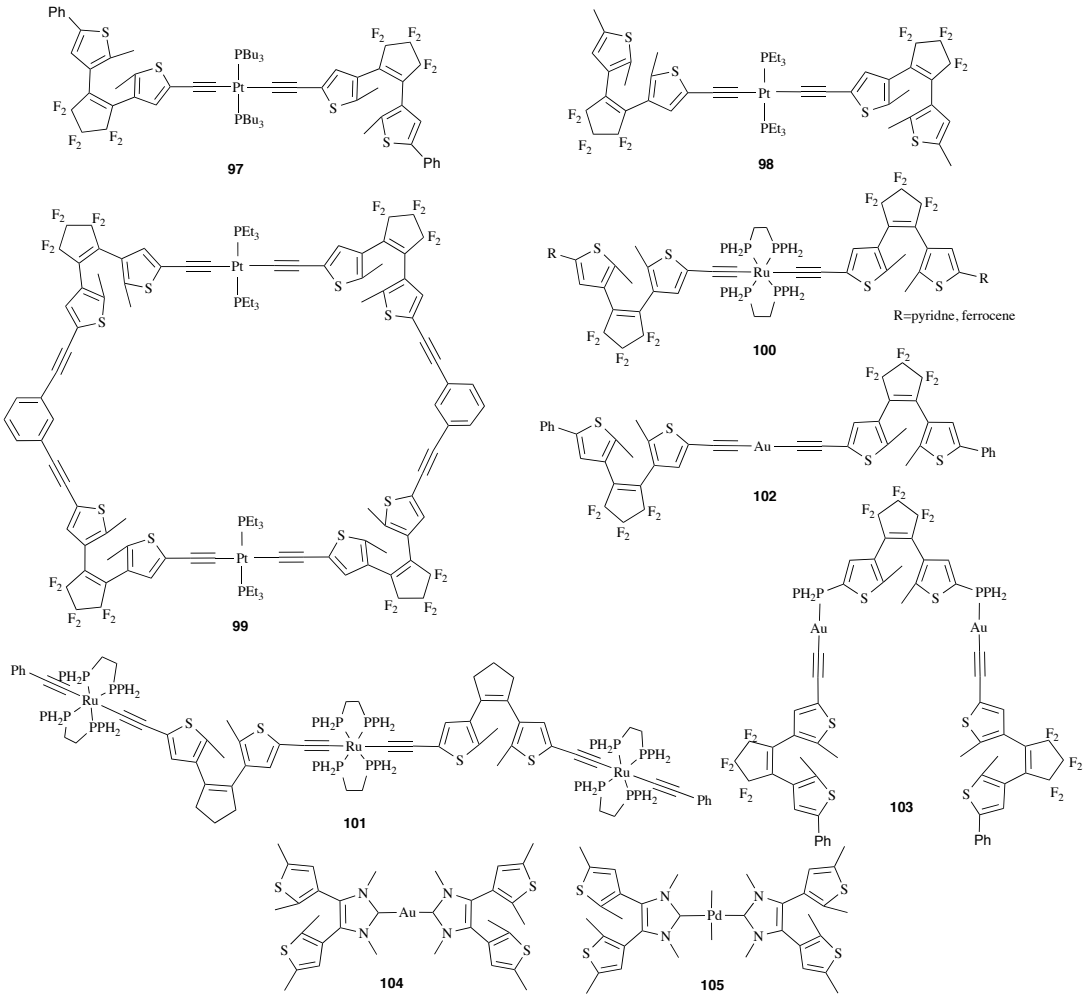

Fig. 26 Multi-DTE complexes built with a cyclometallated strategy.

of Fe(II) only two out of three DTEs can be closed, whereas in the Co(III) case, all three DTEs are photoactive. The lower efficiency of the isomerisation in the Fe complex is attributed to a ligand-to-metal charge transfer transition. For the Co(III) complex, the ring closure reaction can be triggered by an irradiation at 350 nm and at 470 nm thanks to a metal-to-ligand charge transfer (MLCT) electronic transition.

Pt(II)-based complexes of DTE are abundant in the literature and they are typically formed by linking the DTE to Pt through an ethynyl bridge added at the α position of the thiophene rings.[202] In the dimer **97**, photochromism is observed and the intermediate **co** isomer was isolated. The photoactivity of the two DTEs is attributed to the localised character of the excitation due to the presence of the metal ion, but a triplet cyclisation pathway was also suggested.[202,211] It is of note that irradiation at 415 nm is sufficient to ring close **97** while irradiation at 340 nm is necessary for the isolated DTE. In a related study, Li *et al.* proposed very similar structures but with normal, mixed and hybrid DTE centers (*e.g.*, **98**).[203] The transformation of **co** to **cc** is enhanced from 0 to 67% when using normal DTEs instead of mixed or inverse photochromes, as well as by adding peripheral pyridine rings to the normal structures (100%). The improved yields are accompanied by bathochromic shifts. TD-DFT calculations have been performed to rationalise the difference in the photocyclisation efficiency between the compounds. The macrocycle **71** synthesised by Jung and coworkers[98] discussed in Section 3 has also been used to prepare Pt-connected systems. In **99**, as in **71**, only one or two DTEs can be simultaneously closed, the addition of metal ions in the bridge having only a minor influence on the photochromic behaviour.

Ru(II)-based multimers have been developed[204,205,212] In **100** with pyridine caps, the stepwise photochromism was demonstrated to be very pronounced.[205] In addition, the pho-

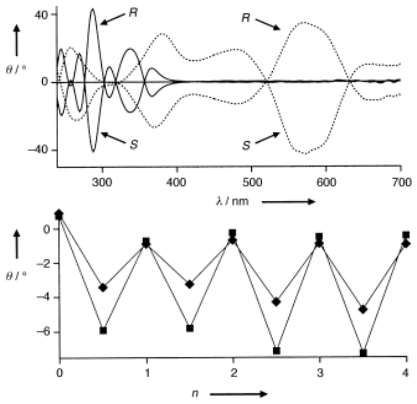

Fig. 27 Top: CD spectra of **93** in dichloromethane considering both R and S structures. Bottom: modulated optical rotation at 450 nm (diamonds) and 475 nm (squares) during alternating irradiation at 313 nm at wavelengths greater than 458 nm (*n*=number of cycles). Reprinted with permission from Ref. 206, Copyright 2001 Wiley-VCH Verlag GmbH & Co. KGaA, Weinheim.

toreactivity of the oxidised species is less efficient than in the neutral form, a property rationalised by the reduced electronic density in the LUMO that is intimately linked to the photochromic process. A derivative of **100** has been proposed recently where ferrocene groups replace the pyridines, providing additional active redox sites.[212] The photochromic process is still stepwise, leading to the **co** and ultimately **cc** forms (with a respective quantum yield of 0.32 and 0.02) and the electrochemical studies highlighted an increase in the extent of communications between the three metal centers as these isomerisation steps occur. Hervault *et al.*, reported a structure with an alternation of (two) DTEs and (three) ruthenium coordination complexes (**101**).[204] Light and electrochemical stimuli offer control of the cyclisation: irradiation with UV light induces the closing of both DTEs, while stepwise electrochemical oxidations allow the progressive closing of one then two photochromes.

Finally a few systems involving gold and palladium complex are available.[94,208] Li *et al.* undertook a comparison of dimers (**102**) and trimers (**103**) of DTEs linked through either a triple bond or a gold complex and showed that the presence of the metal ion provides access to stepwise photoreactions up to a full closing of all photochromes, while the organic linker (**64**) prevents the formation of the fully closed form (see previous Section).[94] Yam *et al.*, reported two DTEs that are bridged via their cyclopentene ring, through a gold or a palladium ion (**104** and **105**).[208] The cyclisation quantum yield of the DTEs was found to be improved once linked to the gold ion compared to the isolated ligand, but only one of the two photochromes is active.

If more than one metal centres is used, more complex

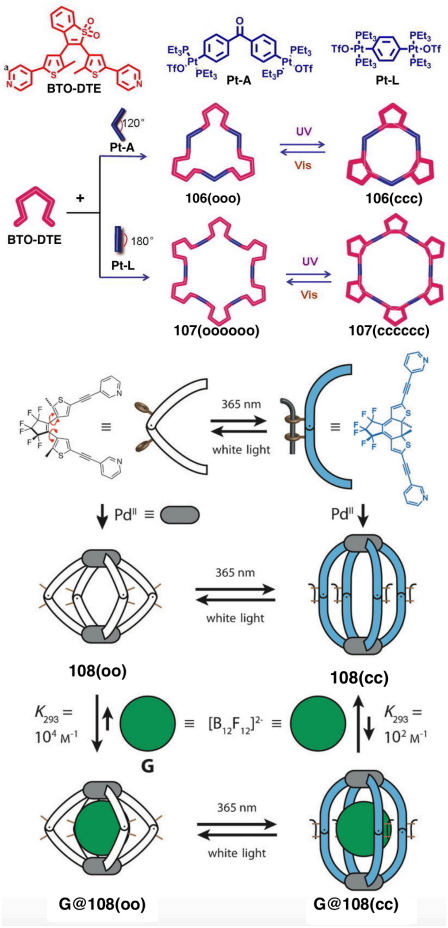

Fig. 28 Examples of DTE supramolecular cycles (top) and cages (bottom) built by coupling switchable DTEs and coordination complexes. Adapted with permission Ref. 209, Copyright 2012 American Chemical Society and reprinted with permission from Ref. 207, Copyright 2013 Wiley-VCH Verlag GmbH & Co. KGaA, Weinheim., respectively.

shapes than in **93**, **94** or **103** can also be attained. For example, the construction of Pt based metallacycles containing three or six photochromic (DTE) units has been reported by Chen *et al.*[209] (**106** and **107**, see Figure 28). In these compounds, the photoreactivity is fully retained, but only two states (open or closed) can be observed. The very high quantum yield of photocyclisation (99%, *i.e.* better than in the corresponding DTE ligand) is attributed to the predominance of the anti-parallel conformation of the DTE units incorporated in the macrocycle. In the same vein, supramolecular cages have also been built with pyridine-functionalised DTE as ligands in two Pd(II) complexes (**108**).[207] The control over the shape of the cage enables the encapsulation and the release of boron anions, with a working principle depicted in Figure 28.

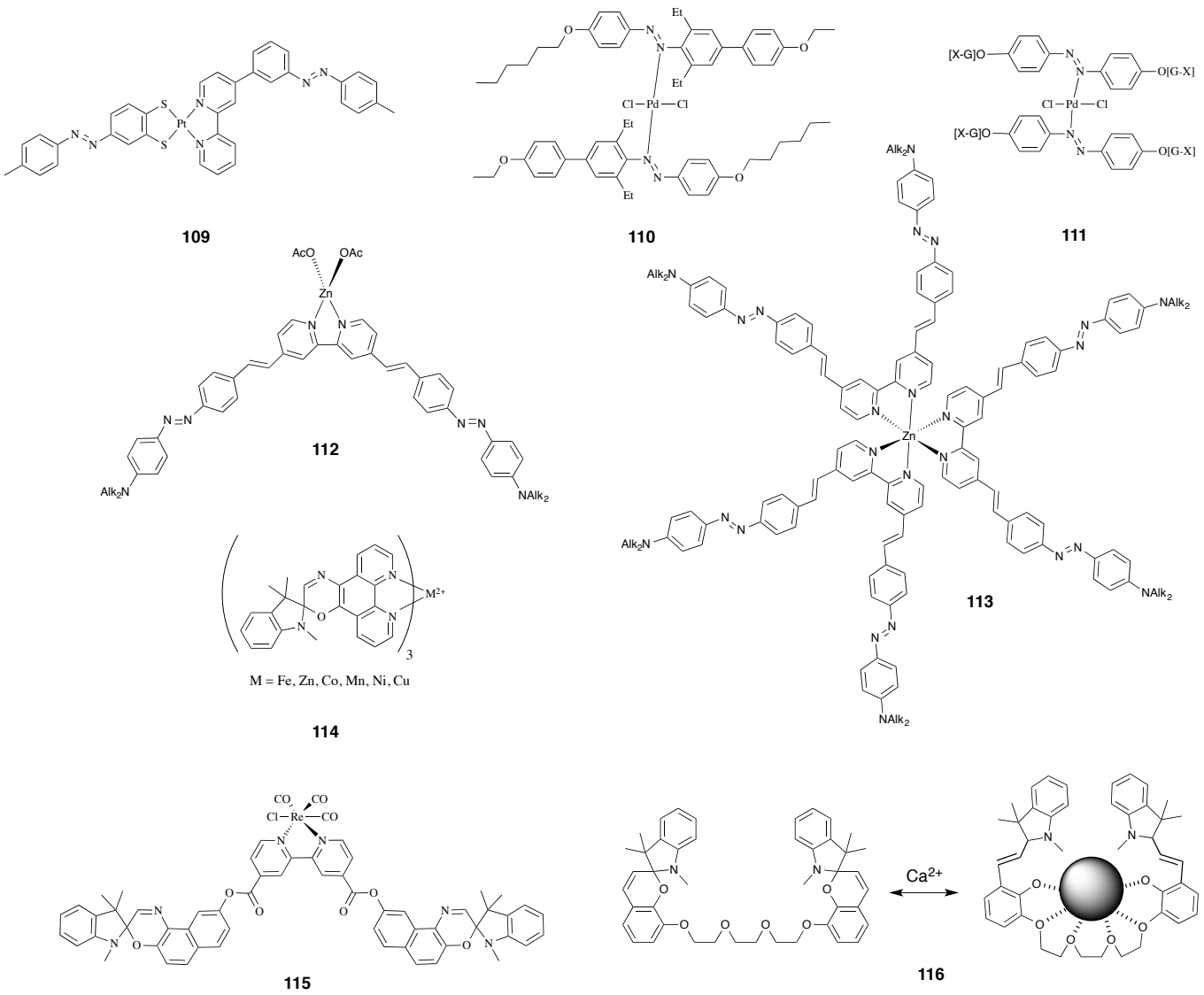

Fig. 29 AZB and SP coordination complexes. For **111** G-X stands for a dendrimer based on 1 to 7 benzyl ether units.

4.2 Other derivatives

Coordination complexes based on other photochromes are shown in Figure 29. In **109**, two AZBs are linked to a Pd(II) centre, the two switches present distinct chemical structures allowing the differentiation of the properties of all isomers.[213] In practice, **109** is a three state system (see Figure 30), one of the possible isomer, *ZZ*, remaining unobserved. Interestingly, the MLCT transition at long wavelength can induce a low-energy *trans*-isomerisation of the photochrome.

Pd(II) complexes bearing two AZB ligands bound to the metal through one of their nitrogen atoms have been synthesised (**110** and **111**).[214,215] **110** is stable and the photocyclisation is reversible. Under UV irradiation the *Z*:*E* ratio lies in favour of the *Z* isomer but is inverted to ca. 2:3 under visible irradiation. The thermal *Z* to *E* isomerisation is slow in **110** (2 days instead of 2–3 h in dendritic AZBs), probably due to the steric hindrance brought about by the ethyl chains of the AZBs. In **111**, the two AZBs bear dendritic substituents on all phenyl rings[215] and the isomerisation reaction is again reversible. However, the ratio of active photochromes deduced from changes in the UV/Vis absorption and ^{1}H NMR spectra is limited to a few percent, while the thermal stability is in the range of 2–3 h.

Zn(II) complexes **112** and **113** possess respectively one and three 2,2-bipyridines ligands substituted at the 4,4-positions by two AZBs units.[126–128] With the aim to obtain NLO switch-

able materials, these compounds have been designed to be implemented in a PMMA matrix through an atom transfer radical polymerization (ATRP) of their terminal alkyl chains. In solution **113** complex exhibited an isomerisation qualitatively similar to the metal-free AZB dyad ligand, though this isomerisation is quantitatively less efficient: the total photoconversion reaches 53 % for the ligand but 25% for **113**.[126] Considering the overall relatively low photoconversion percentage of the ligand, the authors suggested that the three possible forms (*ZZ*, *EZ* and *EE*) of the ligand coexist. Polymer films made of **112** and **113** are interestingly still photo-efficient, with roughly the same conversion percentage, making them useful for NLO applications.

Several compounds use SP or spirooxazine (SO) as ligands (see Figure 29), but their photochromic properties have been only rarely addressed. Indeed, the multi-addressability of the complexes are infrequently evoked, as the main target is the change of charge distribution between the neutral SP form and the zwitterionic MC form that induces the emergence of new complexation sites in the latter form.[216] Kopelman *et al.* have incorporated three phenanthroline-capped SOs into a series of metallic complexes (**114**).[217] The photoactivity is preserved and is reversible after complexation, though it is tuned by the nature of the metal. Indeed, the complexation stabilises the MC isomer and the thermal relaxation of this form is slowed after complexation. Some data indicated that a third state (beyond fully closed and fully open) exists but it was not characterised.[217] The emission of the rhenium(I) complex **115**, where one of the ligands is an SP dimer linked to a bipyridine, is switched from a MLCT based emission at ca. 650 nm to a ligand-centered (LC) phosphorescence at ca. 710 nm when opening the SP.[218] The quantum yield of photoconversion (measured at 365 nm), which lies in the range 0.40–0.60 for the ligands, is decreased to 0.15–0.20 by complexation, most likely due to the presence of low-lying MLCT excited states. In SP complexes, the presence of a metal ion can also induce the SP to MC isomerisation, or alternatively the light-induced isomerisation controls the capture of the metal. For instance, with **116**, Yagi *et al.* were able to complex alkaline metal ions.[219] Optical monitoring of the photochromism functioned as an indirect detection method for the ion complexation.

4.3 Summary

Many photochromic complexes encompassing at least two photoactive units have been obtained and they cover a wide variety of shapes, linkers and central metal ions. DTE complexes are by far the most used in the experimental studies, with most showing full photochromism, and stepwise photocyclisation was obtained in several cases apparently more easily than in conjugated organic structures. Therefore, coordination of metal ions may be considered as an efficient approach to link photochromes and to build multiphotochromic architectures, as they also enable better control of the supramolecular shape to be formed, often provide access to electrochemical stimuli and, in several cases, also offer low-energy transitions (ligand-to-metal) that can be used to activate a series of photochromes.

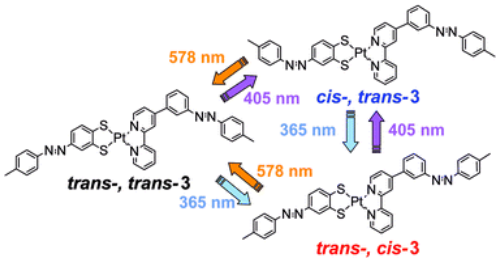

Fig. 30 Three possible isomers of **109** together with the activation wavelengths. Reproduced from Ref. 213 with permission from The Royal Society of Chemistry.

5 Hybrid photochromic compounds

In parallel to dimers and multimers built with a single family of photoactive species, an efficient way to design multiphotochromic systems in which the addressability of the different subunits is preserved, is to connect photochromic compounds belonging to different classes. Such "hybrid" multiphotochromes (see Figure 31) have appeared in the literature since the early 2000s, and most of them involve at least one DTE unit. Their properties are generally complex and numerous theoretical studies have been devoted to rationalise their behaviour (see Section 6).

5.1 Dithienylethene-based compounds

The first example of a hybrid multiphotochromic derivative is the strongly coupled **117** constituted of a DTE and a DHA unit sharing a double bond (see Figure 32).[220,221] Both the ring opening of the DHA and the ring closure of the DTE can be achieved by irradiation in the 254–366 nm range starting with the most stable open DTE/DHA isomers. The ring opening of the DHA to provide VHF (see Figure 2) is thermally reversible while the ring closure of the DTE is not. The composition of the photostationary state is thus related to the irradiation wavelength, to the quantum yields of the DHA/VHF opening and DTE closure (which are comparable, ca. 0.1, and compete with each other), and also to the duration of irradiation with respect to the thermal VHF/DHA relaxation process. The less stable closed DTE/VHF zwitterionic form was not observed.

In compound **118** a DTE is linked to a phenoxynaphthacenequinone (PNQ) unit through a phenyl linker.[222] In this

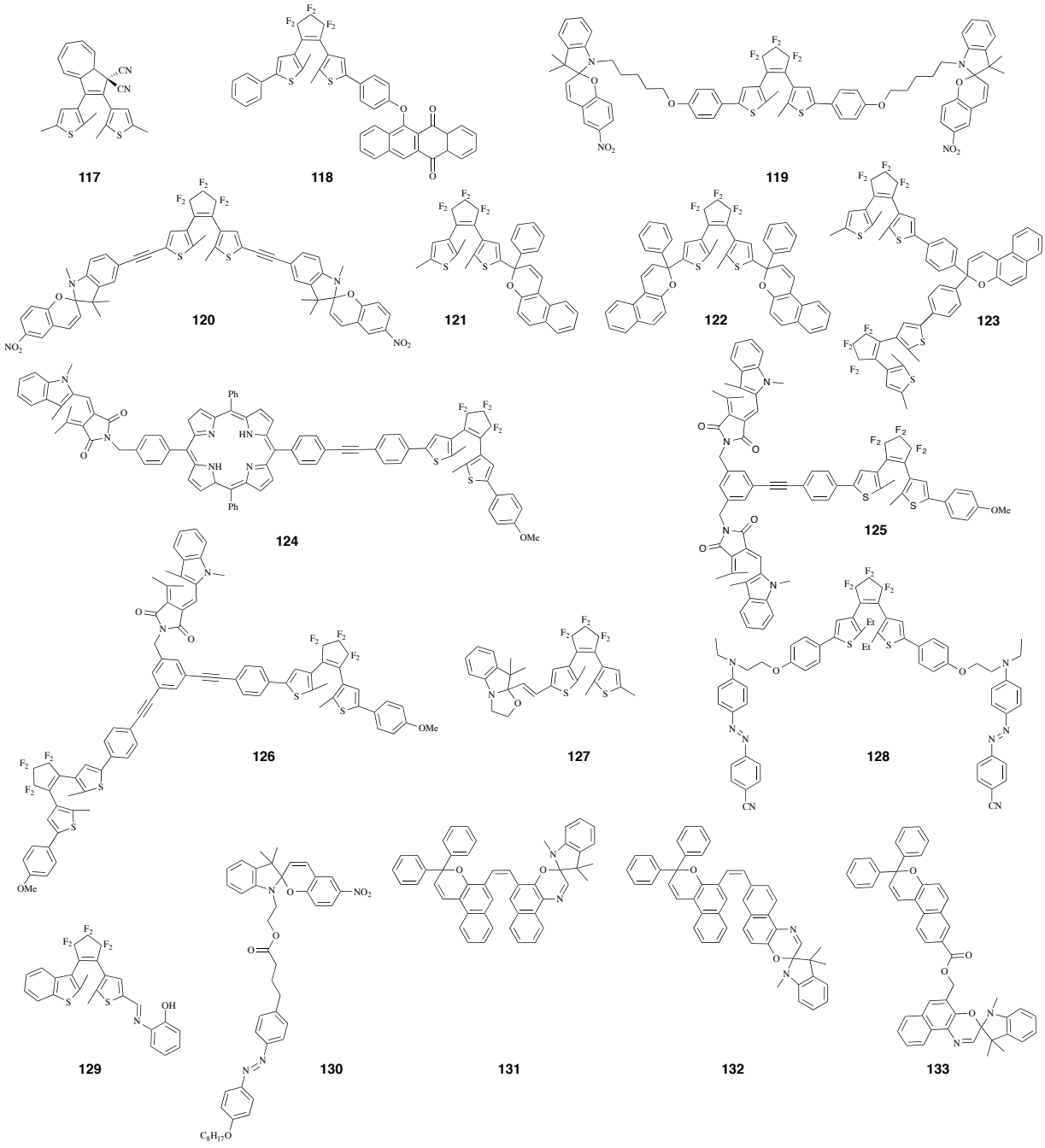

Fig. 31 Multiphotochromic compounds composed of different classes of photochromes.

weakly coupled structure, four isomers exist (combining the open/closed form of the DTE and the *trans*/*ana* isomers of the PNQ) and are accessed by light stimuli. A key feature in the design of this hybrid switch is that the irradiation wavelengths inducing the isomerisation of the PNQ (365 and 434 nm) lie between those required for the conversion of the DTE (313 and 557 nm). Both isomerisation processes are consequently almost independent and PNQ is isomerised to a significant extent when switching the DTE (and *vice-versa*). The most stable open-*trans* isomer presents an absorption that is the sum of the absorption of the two sub-units, confirming that the ground-state electronic interactions are weak. While the

DTE photoactivity is as high as in the monomer, the quantum yield of the slower PNQ isomerisation is lower than in the isolated unit. In Ref. 222, the proportion of the different forms at the different photostationary states induced, by irradiation at different wavelengths was investigated also.

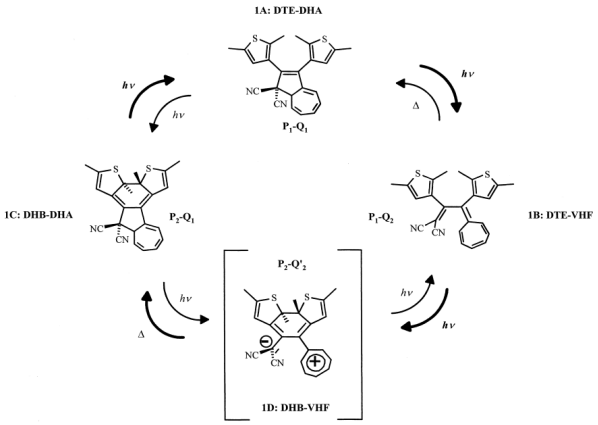

Fig. 32 Isomerisation pathways in **117**. Reprinted with permission from Ref. 221, Copyright 2001 Wiley-VCH Verlag GmbH & Co. KGaA, Weinheim.

In **119**, a DTE has been substituted with two SPs through a phenoxy bridge bearing a C_5 chain, limiting the direct communication between the three units.[223] In toluene, irradiation at 365 nm only induces the ring closure of the DTE (92% in the photostationary state) whereas the return to the open DTE is triggered by irradiation at 600 nm. Interestingly, irradiation in EtOH activates both the DTE and the SP. The open DTE/MC form is not obtained as the DTE closure is a fast process compared to the opening of the SP. The attachement of the SP to the DTE enhances the thermal stability of the MC isomer, a fact already observed in bidentate SP complexes (see Section 4). Lee and coworkers also obtained a hybrid compound constituted of a central DTE and two SP units.[147] This hybrid system, **120**, was synthesised as a member of a bis-SP series, the DTE being considered as a chromophore, and only two states are reported.

In a series of studies by Delbaere and coworkers, one or two NPs were attached directly to a DTE.[224–227] All four possible states of **121** arising from the respective open and closed isomers of both the DTE and the NP units were reached, and their absorption spectra differed significantly (the resulting colours are shown in Figure 33). As expected, only the two isomers presenting closed NP are thermally stable, and the structures with the open NP need to be studied under continuous irradiation. The closed DTE/open NP system is found to slow down the thermal relaxation of the NP, but this does not hold for the open DTE/open NP isomer, hinting at an extension of the π delocalisation length is a key factor. Irradiation at 313 nm activates both photochromes and leads to the formation of both the closed DTE/closed NP and the open DTE/open NP structures, the latter thermally reverts to the open DTE/closed NP isomer. Further irradiation produces the doubly switched (closed DTE/ open NP) isomer. NMR kinetic studies were also performed, and they indicated that the two photochromes are not independent: the DTE being only active when the NP is closed while the NP isomerises irrespective of the state of the DTE.[226] Further study of **121** shed light on the presence of several open NP (*trans*/*cis*) isomers, which allowed one to obtain seven possible isomers and five different colours. In **122**, two NPs are linked to the central DTE. In addition to the six possible photochromic states, *cis*/*trans* isomerisation of the open NP is again active, as well as diastereoisomers, making **122** an 18-state system.[227] As in **121**, the open NP is found to be stabilised when the DTE is closed and the central DTE is active only when both NPs are closed. The extended π delocalisation in the **oco** isomer induces a near IR absorption (ca. 800 nm). Finally, in a very recent report,[228] another DTE/NP combination has been achieved by linking two DTEs to a central NP (**123**). In this case the photocyclisation of the DTEs can be achieved in a stepwise fashion by irradiation at 313 nm and thus the **oo**, **co**, and **cc** isomers of the DTEs can be combined with the open and closed states of the NP to yield 6 isomers characterised by ^{1}H NMR spectroscopy. In contrast to **122**, only the *cis* configuration is found for the open NP, "limiting" the number of potential isomers. Again not all pathways between those states are efficient as there is no possibility to close the DTEs once the NP is opened, and further developments are proposed to bypass this gated-photochromism by increasing the length of the DTE-NP linker.[228]

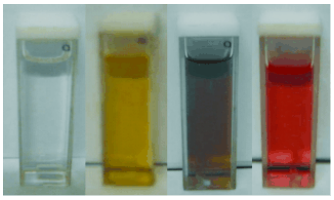

Fig. 33 Coloration of a solution of **121**: colourless (open DTE/closed NP), yellow (open DTE/open NP), brown (closed DTE/open NP) and red (closed DTE/closed NP). Reprinted with permission from Ref. 224, Copyright 2005 Wiley-VCH Verlag GmbH & Co. KGaA, Weinheim.

A hybrid system combining a DTE and FG separated by a porphyrin (**124**) has been synthesised by Gust *et al.*[229] Four thermally stable states can be obtained and the fluorescence of the porphyrin can be used as a readout signal as it is greatly modified depending on the state of the two switches, due to energy transfer quenching. **124** is an example in which the communication between the individual components does not impede the photochromism systematically. Indeed, **124** showed valuable multi-addressability: at 310 nm the DTE cyclisa-

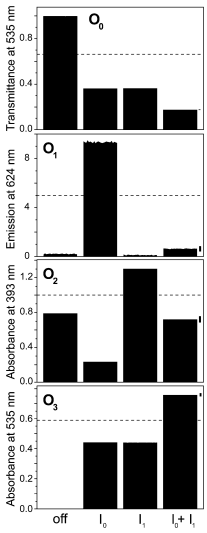

Fig. 34 Illustration of the 2-to-4 decoder functions obtained with **125**: four outputs (wavelengths), O_0 to O_3 are modulated using I_0 (397 nm) and I_1 (302 nm) inputs. The dashed lines indicate thresholds for separating on and off responses. Reprinted with permission from Ref. 230, Copyright 2008 American Chemical Society.

tion is triggered primarily, at 410 nm the FG closure is predominant and irradiation at 366 nm produces the fully closed system. Selective opening of the DTE can be induced by irradiation at $>$ 630 nm whereas irradiation in the 450–650 nm range restores the fully open structure. Another DTE/FG hybrid, **125**, where a DTE and two identical FGs are connected via a bis-phenyl ethynylene bridge, has been reported by Gust *et al.*, thus potentially leading to six photochromic compounds.[230,231] As with **124**, it is possible to selectively close the DTE or the (two) FGs by irradiation at 302 and 397 nm, respectively. The two FGs close efficiently under prolonged irradiation and the isomer with a singly closed FG was expected to be present but was not isolated. Photostationary states enriched in each of the four types of thermally-stable isomers could be obtained and the spectra of those states corresponded to a linear combination of their components due to the limited electronic interaction. **125** is an effective multi-addressable switch, that can be used in the design of logic gates.[231] Indeed, the use of several wavelength inputs allows one to perform "AND" and "XOR" logical operations as well as arithmetic operations. As illustrated in Figure 34, both the absorbance at a specific wavelength or the emission can be used as readout signals. The reverse design, **126**, that combines two DTEs with a central FG has also been investigated and turned out to be an efficient multi-switch derivative as well.[232]

In 2010, Sevez *et al.* reported a DTE and a IA connected through an ethenylene bridge to form **127**.[233] The system possesses four accessible states, with distinct absorption spectra. Some pathways between the isomers are however inefficient as side-products are formed, *e.g.*, the most conjugated closed DTE/open IA showed a low fatigue resistance. The photoreactivity of **127** has been studied in detail recently.[234] It was shown that, in addition to the oxazolidine and the DTE opening or closing with, respectively, chemical (acid/base) and light stimuli, the double bond linking these two switches can undergo a light-induced *E*/*Z* isomerisation. Therefore, **127** possesses a total of 2^3 isomers, all of which have been characterised by ^{1}H NMR spectroscopy. Some pathways between the eight different forms are however found to be inefficient (see Figure 35). A significant electronic coupling between the IA and the DTE is found, and the absorption spectrum of **127** is not the simple superposition of the spectra of its components. The state of a function can control or lock the possibility to switch the others, so to reach "gated" photochromism. For instance, the efficiency of the ring closure of the DTE is decreased from 90% to 50% while opening the IA, whereas the photochromism (in both directions) is shutdown when the double bond is in the *E* form.

In the hybrid **128**, two AZBs have been linked to a DTE through an alkyl chain.[235] After irradiation at 300 nm, the orange solution (absorption in the visible due to the azo groups) turns green with a new hallmark DTE absorption band at 623 nm. Irradiation at 620 or a 550 nm induces ring opening of the DTE and the solution goes back to orange with the AZB units unaffected. Irradiating at 450 nm to induce the *cis-trans* AZB isomerisation also unexpectedly and efficiently (95%) triggers the ring opening of the DTE even if the absorbance of the DTE is weak in that region (see spectra in Figure 36). This phenomenon was rationalised as due to ET from the AZB to the DTE, even if the actual mechanism was not elucidated.

A phenolic Schiff base has been covalently attached to a DTE in **129**.[236] Under the action of a base (NaOH) the deprotonated system can photocyclize into a benzoxazole unit, and this reaction can be combined with photoreactivity of the DTE. A six state system is thus obtained by using a combination of light and chemical stimuli. The ring closure of the DTE is still efficient irrespective of the form of the side group and the thermal stability of the closed DTE is enhanced by the presence of the benzoxazole.

5.2 Other derivatives

A smaller number of hybrid multiphotochromes are available that are DTE-free (**130**–**133**) and they are typically based on SP or SO. In **130** a SP and a AZB moieties are connected through a long non-conjugated alkyl chain.[237,238] As expected, the absorption spectrum of this compound resembles a combination of its two parts. Nevertheless, the absorp-

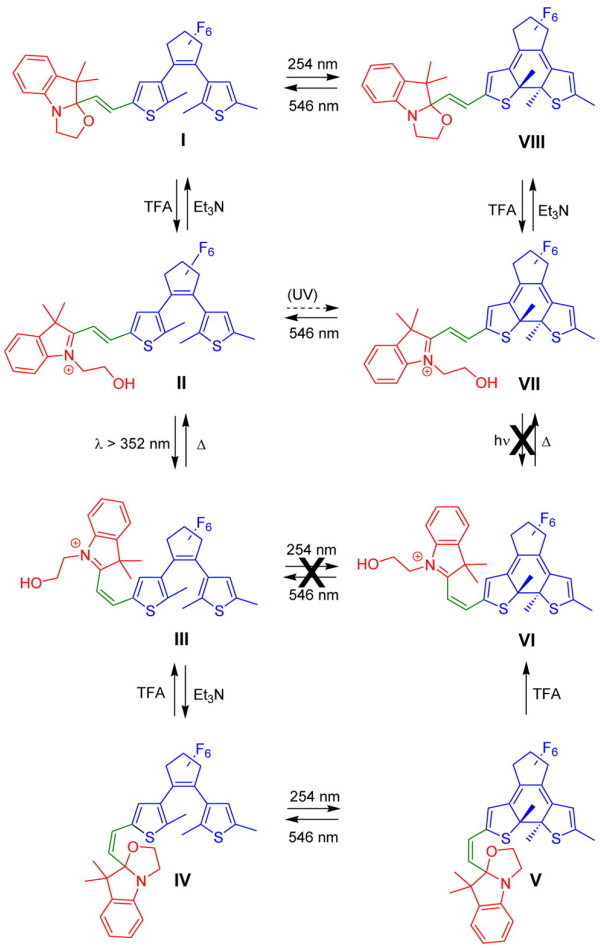

Fig. 35 Isomerisation pathways in **127** under chemical and light stimuli. Reprinted with permission from Ref. 234, Copyright 2014 American Chemical Society.

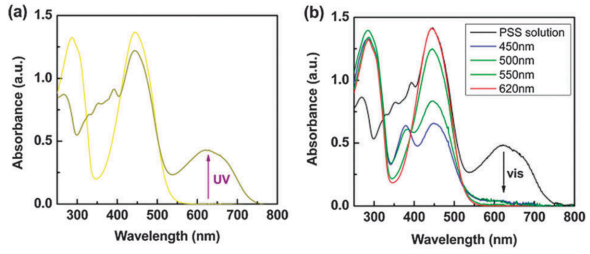

Fig. 36 Changes in the absorption spectrum of a solution of **128** (a) under a 300 nm irradiation and (b) after irradiation of the photostationary state with 450–620 nm visible light. Reproduced from Ref. 235 with permission from The Royal Society of Chemistry.

tion maximum of the MC isomer is redshifted by 90 nm (to 590 nm) compared to the isolated MC structure, as the AZB is supposed to act as an electron donor towards the cationic indoline moiety. In solution, the four possible isomers are detectable and can be addressed selectively by irradiating at specific wavelengths: (i) *Z* to *E* switching is obtained by irradiation at 390–400 nm; (ii) the reverse reaction can be induced by irradiation at 443 nm and can be achieved thermally in 5 min. at room temperature also; (iii) the thermally reversible SP to MC isomerisation is induced by irradiation at 270–290 nm; (iv) irradiation at 290–390 nm switches both photochromes. Incorporation of **130** in a PMMA film results however in the loss of its photochromic properties.

The otherwise similar **131** and **132**, where a SO and a NP are linked with an ethylene bridge, exhibit different photochromic behaviour.[152] Indeed, in **131** only the SO unit is photoactive, whereas both parts can be switched in the latter. In **132**, the optical properties of the dimer is the sum of its components, both colouration and thermal fading taking place in a few seconds, a typical time scale for such photochromes.[239] Interestingly, the open SO is thermally stable in **131**, due to the extension of the π-conjugation offered by the NP moiety. Samat and co-workers also highlight that the central hexatriene pattern that can potentially electrocyclize does not offer an additional photoactive route in **131** nor in **132**. The related system **133**, where the two photochromes are bridged through an ester group, behaves like **132**, though the absorption of the coloured isomers are redshifted by 30 nm compared to their isolated counterparts. In another compound a DHA was appended to a tetraethynylethene derivative, and the DHA-VHF isomerisation could be combined with the *cis-trans* switching of the tetraethynylethene.[240]

5.3 Summary

Hybrid multiphotochromic compounds show highly promising properties, as frequently the response of the subunits to light stimuli are intrinsically different, allowing for more facile control of the different states. Therefore, even if the resulting multimer does not present emerging optical properties, the addition of the absorption spectra of the components is enough to reach a molecule that can react distinctively to different stimuli. In this regard the DTE/bis-FG derivative (**125**) has proven to be a particularly efficient system to obtain an all-photopic-multiencoder,[230,231] whereas DTE/spiro hybrids (**121**, **122**, **123** and **127**) offer a very large number of addressable states thanks to the existence of a wide variety of spiro conformers. As above, we stress here that beyond the molecular picture "hybrid" photochromic copolymers can also be reached, *e.g.*, copolymers of AZB and FG have been proposed by Chinnusamy *et al.*[241]

6 Theoretical studies

6.1 Overview

As discussed in the previous sections, the photoactivity and optical properties of multiphotochromic compounds are non-trivial and often not predictable on the basis of intuitive chemical concepts. The rationalisation and the prediction of the interaction between the different components of complex molecular switches with theoretical tools has consequently stimulated efforts to understand the properties of systems developed with the ultimate aim of designing more efficient multiphotochromes.

The optical properties of isolated photochromic systems have been thoroughly explored with a range of quantum chemical methods.[242–245] It is necessary to locate conical intersections[246] when probing photochromic reaction pathways and hence methods able to simultaneously treat multiple electronic states should be employed. However, multiphotochromic compounds represent extended conjugated systems and contain too many "active" electrons to be treated with multiconfigurational methods, such as the Complete Active Space Self-Consistent Field (CASSCF) method. As a consequence, the exploration of the potential energy surfaces of the excited states involved in photoreactivity[247–252] remains beyond our present reach for multiphotochromes, and one has to resort to cruder methods. The theoretical studies of coupled photochromes has employed Density Functional Theory primarily, and its Time-Dependent counterpart (TD-DFT),[253,254] first to predict the optical properties of all isomers, next to unravel the electronic structure of the excited states and finally to quantify the coupling between the various photochromes. Besides purely theoretical studies, there are of course joint theory-experimental efforts.[112,197,203].

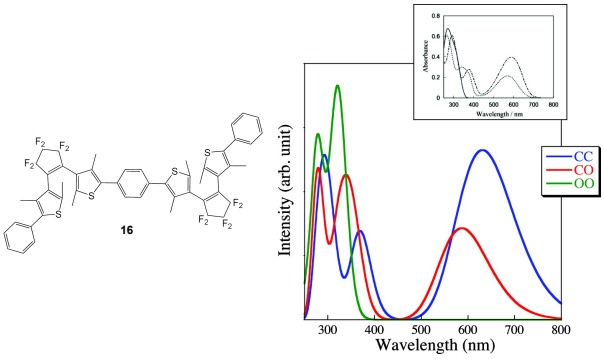

Fig. 37 Comparison between experimental (upper panel) and calculated [PCM-CAM-B3LYP/6-311+G(2d,p)] UV/vis absorption spectra of the different isomers of **16**. Reprinted with permission from Ref. 71, Copyright 2010 American Chemical Society.

A computational scheme relying on DFT and TD-DFT to access both the conformational and optical properties of those photoactive compounds has been proposed to estimate the photoswitching properties of coupled photochromes.[255] The resulting theoretical UV-Visible spectra are generally in very good agreement with experimental data (as shown in Figure 37 for **16**). In a second step, the photochromism of the system can be inferred by undertaking a close analysis of the topology of the virtual orbitals involved at the key absorption bands. This approach can be illustrated by considering the cyclisation of a single DTE, in which the first virtual orbital involves a bonding interaction between the carbon atoms that take part in the bond formation process (see Figure 38). The occurence of this bonding contribution and the ability to populate by irradiation this virtual orbital within the electronic states is therefore a first criterion to evaluate the feasibility of the ring closure of each DTE in a multiphotochromic compound (and the same reasoning can be applied for other types of photochromes that undergo an electrocyclisation process). However, even for dimers, this analysis of the TD-DFT results is not always straightforward as the simplistic approach of studying only the shape of the two frontier orbitals, that are the HOMO and LUMO, is inadequate.[90] It is indeed necessary to go beyond this frontier orbital model and to investigate the topology of the several low lying virtual orbitals.

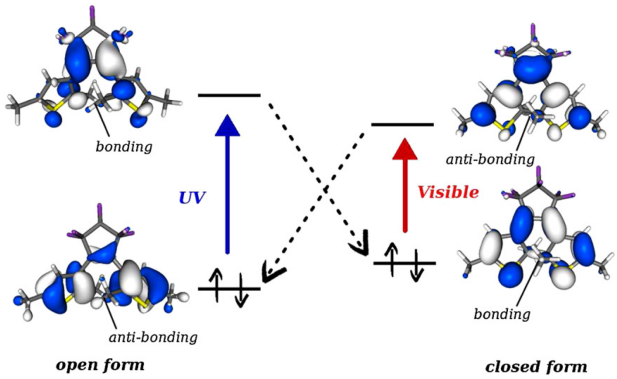

Fig. 38 HOMO and LUMO molecular orbitals in an open (left) and closed (right) model DTE obtained at the B1B95/6-311G(d,p) level. Reprinted from Ref. 256, Copyright 2012, with permission from Elsevier.

6.2 DTE dyads

The DTE dimer **24** with a sexithiophene linker synthesised by Areephong *et al.*[112] has been studied theoretically.[115,116] In initial studies, the DFT geometries (TD-DFT transition energies) were found to match the experimental X-ray structures (measured absorption spectra).[116] Later Staykov *et al.* rationalized the photochromic, the optical and electrochemical

properties.[115] The topology and the relative energies of the frontier orbitals were used as a guide to explain experimental findings. Our group also investigated the behaviour of the dimers of DTEs linked through a phenyl unit in both *para* (**16**) and *meta* positions[257] or a fluorene (**18**),[258] as well as the dimer **5**,[258] and showed that rationalisation of the experimental observations (partial or full photochromism) can be successfully carried out with the protocol described above.

The impact of the spatial arrangement and the nature of the linker separating the two DTEs has been investigated in a systematic study considering **2**, **63** (with *n=0*), **16** and **19**.[71] In most cases, the analysis of the virtual orbitals involved in the electronic transitions accurately predicts the feasibility of the ring closure. In other words, despite the lack of direct quantification of the energy transfer processes between the DTEs that are often incriminated for the loss of the full closing, the study of the perturbation of the electronic structure induced by extensive communication between the different photochromes reveals the loss of the typical virtual orbital shape associated with ring-closure. In Ref. 71, only the behaviour of the covalently bonded dimer (**2**) could not be predicted, as the experimentally-observed formation of the non-photochromic byproduct was not investigated. In a subsequent study, it was also demonstrated that, beyond electronic aspects, geometrical (the distance between the two reactive carbon atoms) and energetic (the relative stabilities of the different isomers) can also play a role, especially in compact DTE dyads, *e.g.*, **3** and **4**.[90]

The optical properties of the metallic complex **97** encompassing two DTEs were investigated with theoretical tools.[211] In this case, consistent with experimental findings,[202] a pathway via a triplet state was identified as the sole possible process for the second isomerisation, because virtual orbitals with a "photochromic topology" were not observed for the singlet states.

6.3 DTE multimers

The DFT/TD-DFT approach has been applied to understand the optical properties of DTE multimers.[172,173,179] For the linear trimer of DTE **63** (with *n=1*) reported by Kaieda *et al.*, the efficiency of the different closure pathways was probed and the experimental conclusions were successfully validated, except for the ring closure of the central unit in the **coo** isomer that was incorrectly predicted as efficient, probably due to the lack of explicit modelling of ET in the computational protocol.[165,172] This computational methodology also helped to determine why only two out of three DTEs are active in **66**.[166,173] The large hexamer **75**[170] has been investigated as well.[179] The behaviour (simultaneous full-closure) of the system was explained. In addition, while in the original compound the six DTEs are found to behave similarly (they possess the same electronic structure, see the symmetry of the frontier orbitals in Figure 39), incorporating differently substituted DTEs was shown to yield a potentially multi-addressable photoactive supramolecule, displaying distinct absorption profiles for mixed closed/open structures.

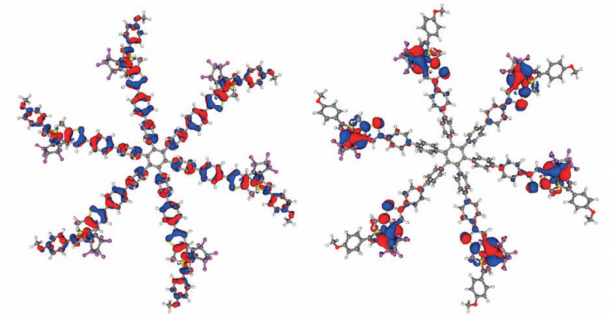

Fig. 39 Frontier molecular orbitals (HOMO and LUMO+2) of the hexamer of DTE **75** obtained at the PCM-CAM-B3LYP/6-31G(d) level. From Ref. 179 – Reproduced by permission of The Royal Society of Chemistry.

6.4 Dimers and multimers of other photochromes

AZB multimers have also been subject of theoretical investigations.[259,260] Durgun *et al.* probed the isomerisation pathway in several azonbenzenophanes,[259] up to a ring possessing six units (see Figure 40 for the tetramer). The effects of substitution by -OH groups on the α position of the benzene and the impact of the connector between consecutive AZBs (with a shared phenyl ring or with intermediate methyl groups) were studied, with the aim of designing inventive energy devices that could store light energy and release heat thanks to the thermal back isomerisation.

Additionally, Jaunet-Lahary *et al.* investigated at the DFT level the NLO properties of AZB dimers presenting a push-pull structure.[260] As with DTEs,[261] they showed that the NLO contrast between the *Z* and *E* forms is supralinearly enhanced in multimers (compared to the corresponding monomers).

Chindam *et al.* have rationalised the optical properties of the di-fulgimides series reported by Luyksaar *et al.* (compound **42**),[142] and they investigated the effect of chemical substitution on the optical properties of new dissymmetric compounds, designed to access multi-addressable systems.[262] From the calculations on the experimentally available compounds, the mixed **co** form was predicted to exist though it was not detected experimentally, an apparent discrepancy that might be ascribed to the symmetric nature of the compounds, yielding hardly distinguishable optical signatures for the **co** and **cc** isomers.

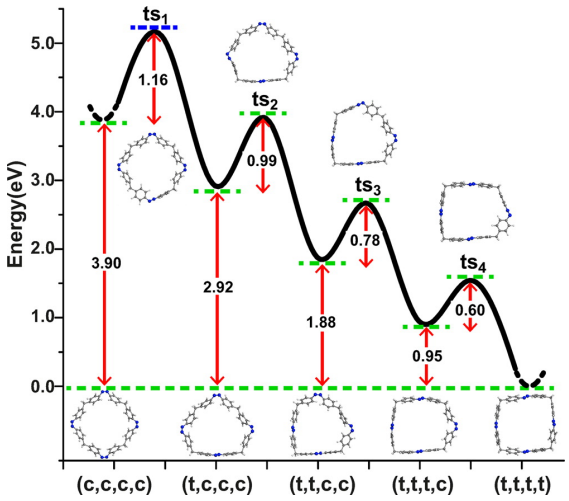

Fig. 40 Computed back isomerisation pathway from the full *Z* to the full *E* forms. The values shown are the ΔH and the activation energies for each step, and represent respectively the amount of energy stored and the stability of the device. Reprinted with permission from Ref. 259, Copyright 2013 American Chemical Society.

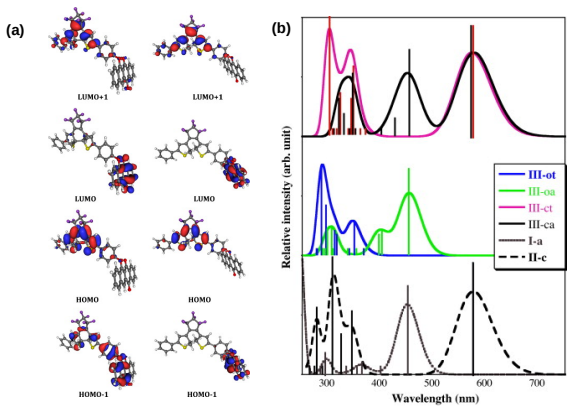

Fig. 41 (a) Frontier molecular orbitals of **118** in the closed/*trans* (left) and closed/*ana* forms. (b) Theoretical absorption spectra of the different isomers of **118** [I (*trans*, (t), and *ana*, (a)) and II (**o** and **c**) are respectively the PNQ and DTE fragments, and III is the hybrid]. Reprinted from Ref. 267, Copyright 2011, with permission from Elsevier.

6.5 Hybrid systems

The optical properties and photoreactivities of hybrid photochromic systems composed of a DTE and another photochrome have been investigated. A difficulty encountered here is the choice of an exchange-correlation functional able to accurately describe the optical properties of the different units in the hybrid system.[263]

In **127**, the virtual orbitals involved in the closure of the DTE and the opening of the IA were identified.[264] For the most conjugated closed DTE/open IA structure, the significant modification of the virtual orbitals of the DTE may explain the lower efficiency of the ring-closing compared to the isolated system. In a subsequent study, the influence of the conformation of the system on the optical properties and the ^{1}H NMR chemical shifts in **121** was studied.[265] The conformation has been found to have little impact on the position of the absorption bands but the computed chemical shifts obtained can be used as fingerprints to help identifying the possible conformers found experimentally. The impossibility to go directly from the open DTE/open NP to the closed DTE/open NP isomer, that has been noted in the several studies by Delbaere and coworkers[226–228] could also be explained by investigating the shape of the key orbitals. The DTE-PNQ hybrid **118** synthesized by Myles *et al.*[266] was also modeled with TD-DFT.[267] The relative lack of communication between the two units and the experimentally observed superimposition of their spectra in the hybrid compound are reproduced (see Figure 41).

For compound **117**, theory was used to explore the energy profiles corresponding to the photochromic reactions of both the DTE and DHA moieties.[268] The thermal and photochemical reactions in the dimer have been identified, together with the height of the energetic barriers. In the same vein, Belfon *et al.* used TD-DFT to determine the geometry and the optical properties of **125**, and to rationalize the photoactivity of the different isomers.[269] Recently, Li and coworkers have conducted a DFT study on the hybrid trimer **128**,[270] containing a DTE substituted by two AZBs.[235] They could explain why excitation of the AZBs at 450 nm induced ring-opening of the DTE. Indeed, by performing a close analysis of the computed electronic transitions and the involved molecular orbitals (see Figure 42), they proposed a rapid internal conversion process that would allow, from this abnormally energetic excitation, population of the DTE's LUMO after a "fall" of the electron from the higher states centered on the AZBs.

6.6 Concluding remarks

There have been numerous DFT and TD-DFT investigations of multiphotochromic compounds and these studies have shown that, despite the intrinsic weaknesses of the theory (TD-DFT is a static approach relying on a single determinant), relevant insights on the interaction between the constituent parts of a system can be obtained and the photoreactivity can often – but not always – be predicted by a careful analysis of the virtual molecular orbitals involved. From a technical point of view, the use of a range-separated hybrid functional, combined to the description of the environment with a dielectric continuum, appears to be the most accurate theoretical tool with an affordable computational cost:

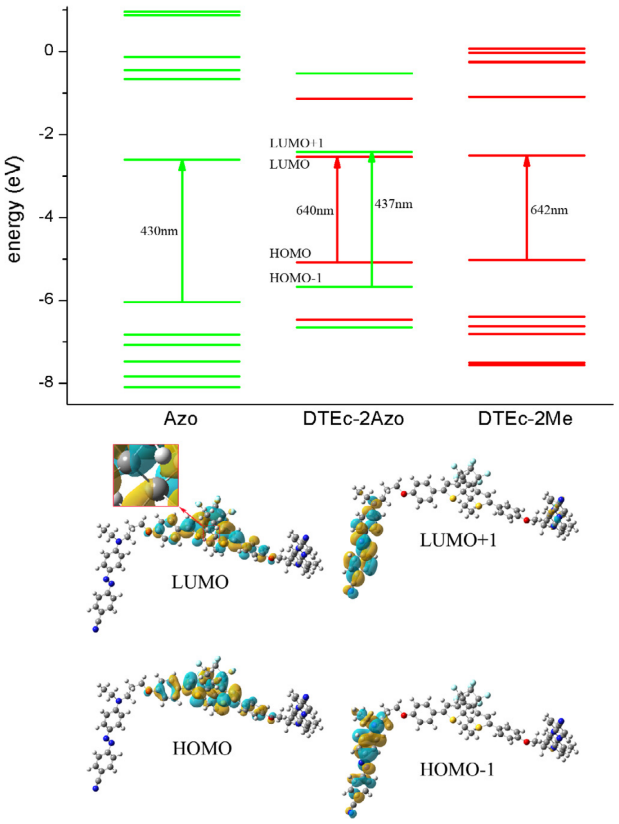

Fig. 42 Electronic energy diagram, with key transitions and corresponding molecular orbitals for **128** considering a closed DTE. Reprinted from Ref. 270, Copyright 2015, with permission from Elsevier.

the computed UV-visible electronic transitions are in good agreement with those measured. Nevertheless, the behaviour of some multiphotochromes remains unexplained with this crude approach,[71,172] and further development is needed to take into account dynamic processes,[248] and more importantly to describe potential intramolecular ET mechanisms that have been implicated as limiting factors. Quantification of ET in large multichromophoric molecules is indeed possible nowadays.[271,272]

7 General conclusions

In this review, we have presented molecular multiphotochromic molecules that are available to date. There is a large diversity of structures, using between two to six switches connected through a variety of organic and inorganic structures. As a summary, Table 1 provides a list of the available dimers together with their optical and photochemical properties, which illustrates clearly the variety of multiphotochromes available already. Nevertheless, effective multi-addressable and multi-active compounds remain a minority. For multimers constituted from a single family of compounds, one can distinguish two main categories:

1. when the individual switches do not interact significantly with each other, one can expect random stepwise isomerisation with a resulting signal that presents "only" an enhanced intensity compared to the individual photochrome and a statistical mixture of compounds. In other words, such independent architecture improves the contrast between the two forms, but does not grant access to more states nor advantages for storage processes;

2. when the subunits interact significantly, the intermediate mixed isomers (*e.g.*, open-closed) can possibly be isolated before the other switches become active (stepwise photochromism) and if the coupling is sufficient, the optical response of all isomers can become different. However, using a conjugated organic linker between the photochromes often inhibits the photoactivity of all but one switch, especially for DTEs. In simple terms, there is a modification of the electronic structure and the first isomerisation creates a low-lying excited state on the switched photochrome. This new state traps the energy gained by other units upon irradiation.

This illustrates the difficulty to hold the balance between photoactivity and multiple responses. There are several successful strategies to reach such a goal:

1. the incorporation of the photochromes in a metallic coordination complex that generally helps in maintaining photoactivity;

2. the introduction of asymmetry, *e.g.*, by using a normal and an inverse DTE that are activated at different wavelengths;

3. the use of subunits belonging to different families of photochromes to directly implement contrasted optical responses.

Compounds such as **61**, **122**, **125** or **127** have indeed been shown to yield at least four distinguishable isomers that can be obtained with irradiation at different wavelengths, though typically some transformation paths cannot be accessed directly. In this quite active and challenging field, the most effective systems probably remained to be discovered, a task for which quantum mechanical tools are expected to be increasingly helpful in reducing the trial and error approach necessary in intuitive designs.

Acknowledgements

A.F. thanks the European Research Council (ERC) for his post-doctoral. grant (Marches no°278845). D.J. acknowledges both the European Research Council for the starting grant (Marches no°278845) and the Région des Pays de la Loire for the *recrutement sur poste stratégique*.

References

1 B. L. Feringa, *Molecular Switches*, Wiley-VCH, Weinheim, 2001.
2 M. Irie, Y. Yokoyama and T. Seki, *New Frontiers in Photochromism*, Springer Japan, 2013.
3 H. Dürr and H. Bouas-Laurent, *Photochromism: Molecules and Systems*, Elsevier, New York, 2003.
4 Z. F. Liu, K. Hashimoto and A. Fujishima, *Nature*, 1990, **347**, 658–660.
5 H. Mustroph, M. Stollenwerk and V. Bressau, *Angew. Chem., Int. Ed.*, 2006, **45**, 2016–2035.
6 G. W. Buning, *Organic Materials for Photonics*, Elsevier, Oxford, 1993, pp. 367 – 397.
7 B. L. Feringa, W. F. Jager and B. de Lange, *Tetrahedron*, 1993, **49**, 8267 – 8310.
8 M. Irie, *Chem. Rev.*, 2000, **100**, 1685–1716.
9 H. Tian and S. Yang, *Chem. Soc. Rev.*, 2004, **33**, 85–97.
10 K. Matsuda and M. Irie, *J. Photochem. Photobiol. C.*, 2004, **5**, 169–182.
11 M. Irie, T. Fukaminato, K. Matsuda and S. Kobatake, *Chem. Rev.*, 2014, **114**, 12174–12277.
12 S. Aloise, M. Sliwa, G. Buntinx, S. Delbaere, A. Perrier, F. Maurel, D. Jacquemin and M. Takeshita, *Phys. Chem. Chem. Phys.*, 2013, **15**, 6226–6234.
13 S. Aloise, R. Yibin, I. Hamdi, G. Buntinx, A. Perrier, F. Maurel, D. Jacquemin and M. Takeshita, *Phys. Chem. Chem. Phys.*, 2014, **16**, 26762–26768.
14 A. Perrier, S. Aloise, M. Olivucci and D. Jacquemin, *J. Phys. Chem. Lett.*, 2013, **4**, 2190–2196.
15 S. Kawata and Y. Kawata, *Chem. Rev.*, 2000, **100**, 1777–1788.
16 S. Pu, H. Tang, B. Chen, J. Xu and W. Huang, *Mater. Lett.*, 2006, **60**, 3553–3557.
17 M.-Q. Zhu, G.-F. Zhang, C. Li, M. P. Aldred, E. Chang, R. A. Drezek and A. D. Q. Li, *J. Am. Chem. Soc.*, 2011, **133**, 365–372.
18 O. Ivashenko, J. T. van Herpt, B. L. Feringa, P. Rudolf and W. R. Browne, *Langmuir*, 2013, **29**, 4290–4297.
19 E. Berman, *J. Phys. Chem.*, 1962, **66**, 2275–2275.
20 G. Berkovic, V. Krongauz and V. Weiss, *Chem. Rev.*, 2000, **100**, 1741–1754.
21 B. V. Gemert, *Mol. Cryst. Liq. Cryst. Sci. Technol., Sect. A*, 2000, **344**, 57–62.
22 A. Santiago and R. S. Becker, *J. Am. Chem. Soc.*, 1968, **90**, 3654–3658.
23 Y. Yokoyama, *Chem. Rev.*, 2000, **100**, 1717–1740.
24 V. Deblauwe and G. Smets, *Makromol. Chem.*, 1988, **189**, 2503–2512.
25 Y. Yoshioka and M. Irie, *Electron. J. Theor. Chem.*, 1996, **1**, 183–190.
26 H. Rau, *Photoreactive Organic Thin Films*, Academic Press, San Diego, 2002, pp. 3 – 47.
27 H. M. D. Bandara and S. C. Burdette, *Chem. Soc. Rev.*, 2012, **41**, 1809–1825.
28 D. Bléger, J. Schwarz, A. M. Brouwer and S. Hecht, *J. Am. Chem. Soc.*, 2012, **134**, 20597–20600.
29 C. E. Weston, R. D. Richardson, P. R. Haycock, A. J. P. White and M. J. Fuchter, *J. Am. Chem. Soc.*, 2014, **136**, 11878–11881.
30 T. Hugel, N. B. Holland, A. Cattani, L. Moroder, M. Seitz and H. E. Gaub, *Science*, 2002, **296**, 1103–1106.
31 N. B. Holland, T. Hugel, G. Neuert, A. Cattani-Scholz, C. Renner, D. Oesterhelt, L. Moroder, M. Seitz and H. E. Gaub, *Macromolecules*, 2003, **36**, 2015–2023.
32 S. Lamsaard, S. J. Asshoff, B. Matt, T. Kudernac, C. J. L. M., S. P. Fletcher and N. Katsonis, *Nat. Chem.*, 2014, **6**, 229–235.
33 X. Liang, H. Asanuma and M. Komiyama, *J. Am. Chem. Soc.*, 2002, **124**, 1877–1883.
34 O. Pieroni, A. Fissi, N. Angelini and F. Lenci, *Acc. Chem. Res*, 2001, **34**, 9–17.
35 S. L. Broman and M. B. Nielsen, *Phys. Chem. Chem. Phys.*, 2014, **16**, 21172–21182.
36 F. Mançois, L. Sanguinet, J.-L. Pozzo, M. Guillaume, B. Champagne, V. Rodriguez, F. Adamietz, L. Ducasse and F. Castet, *J. Phys. Chem. B*, 2007, **111**, 9795–9802.
37 S. Delbaere, B. Luccioni-Houze, C. Bochu, Y. Teral, M. Campredon and G. Vermeersch, *J. Chem. Soc., Perkin Trans. 2*, 1998, 1153–1158.
38 R. H. Mitchell, *Eur. J. Org. Chem.*, 1999, 2695–2703.
39 F. Buchholtz, A. Zelichenok and V. Krongauz, *Macromolecules*, 1993, **26**, 906–910.
40 C.-C. Ko and V. Wing-Wah Yam, *J. Mater. Chem.*, 2010, **20**, 2063–2070.
41 V. Guerchais, L. Ordronneau and H. L. Bozec, *Coord. Chem. Rev.*, 2010, **254**, 2533–2545.
42 E. C. Harvey, B. L. Feringa, J. G. Vos, W. R. Browne and M. T. Pryce, *Coord. Chem. Rev.*, 2014, **282–283**, 77–86.
43 O. Ivashenko, J. T. van Herpt, B. L. Feringa, P. Rudolf and W. R. Browne, *Langmuir*, 2013, **29**, 4290–4297.
44 W. R. Browne and B. L. Feringa, *Annu. Rev. Phys. Chem.*, 2009, **60**, 407–428.
45 R. Klajn, J. F. Stoddart and B. A. Grzybowski, *Chem. Soc. Rev.*, 2010, **39**, 2203–2237.
46 Q. Luo, H. Cheng and H. Tian, *Polym. Chem.*, 2011, **2**, 2435–2443.
47 W. Szymański, J. M. Beierle, H. A. V. Kistemaker, W. A. Velema and B. L. Feringa, *Chem. Rev.*, 2013, **113**, 6114–6178.
48 J. T. van Herpt, M. C. A. Stuart, W. R. Browne and B. L. Feringa, *Chem. - Eur. J.*, 2014, **20**, 3077–3083.
49 A.-R. Jang, E. K. Jeon, D. Kang, G. Kim, B.-S. Kim, D. J. Kang and H. S. Shin, *ACS Nano*, 2012, **6**, 9207–9213.
50 A. J. Kronemeijer, H. B. Akkerman, T. Kudernac, B. J. van Wees, B. L. Feringa, P. W. M. Blom and B. de Boer, *Adv. Mater.*, 2008, **20**, 1467–1473.
51 F. Castet, V. Rodriguez, J.-L. Pozzo, L. Ducasse, A. Plaquet and B. Champagne, *Acc. Chem. Res.*, 2013, **46**, 2656–2665.
52 L. Ordronneau, H. Nitadori, I. Ledoux, A. Singh, J. A. G. Williams, M. Akita, V. Guerchais and H. Le Bozec, *Inorg. Chem.*, 2012, **51**, 5627–5636.
53 I. Asselberghs, K. Clays, A. Persoons, M. D. Ward and J. McCleverty, *J. Mater. Chem.*, 2004, **14**, 2831–2839.
54 B. Champagne, A. Plaquet, J.-L. Pozzo, V. Rodriguez and F. Castet, *J. Am. Chem. Soc.*, 2012, **134**, 8101–8103.
55 F. Mançois, J.-L. Pozzo, J. Pan, F. Adamietz, V. Rodriguez, L. Ducasse, F. Castet, A. Plaquet and B. Champagne, *Chem. - Eur. J.*, 2009, **15**, 2560–2571.
56 M. Natali and S. Giordani, *Chem. Soc. Rev.*, 2012, **41**, 4010–4029.
57 C. Yun, J. You, J. Kim, J. Huh and E. Kim, *J. Photochem. Photobiol. C.*, 2009, **10**, 111–129.
58 T. Fukaminato, T. Doi, N. Tamaoki, K. Okuno, Y. Ishibashi, H. Miyasaka and M. Irie, *J. Am. Chem. Soc.*, 2011, **133**, 4984–4990.
59 S.-C. Pang, H. Hyun, S. Lee, D. Jang, M. J. Lee, S. H. Kang and K.-H. Ahn, *Chem. Commun.*, 2012, **48**, 3745–3747.
60 W. R. Browne, T. Kudernac, N. Katsonis, J. Areephong, J. Hjelm and B. L. Feringa, *J. Phys. Chem. C*, 2008, **112**, 1183–1190.
61 H. Logtenberg and W. R. Browne, *Org. Biomol. Chem.*, 2013, **11**, 233–

243.
62 E. C. Harvey, J. Areephong, A. A. Cafolla, C. Long, W. R. Browne, B. L. Feringa and M. T. Pryce, *Organometallics*, 2014, **33**, 3309–3319.
63 H. Logtenberg, J. H. M. van der Velde, P. de Mendoza, J. Areephong, J. Hjelm, B. L. Feringa and W. R. Browne, *J. Phys. Chem. C*, 2012, **116**, 24136–24142.
64 T. Nakashima, K. Miyamura, T. Sakai and T. Kawai, *Chem. - Eur. J.*, 2009, **15**, 1977–1984.
65 H.-h. Liu and Y. Chen, *J. Mater. Chem.*, 2011, **21**, 1246–1249.
66 F. M. Raymo, S. Giordani, A. J. P. White and D. J. Williams, *J. Org. Chem.*, 2003, **68**, 4158–4169.
67 G. Sevez, J. Gan, J. Pan, X. Sallenave, A. Colin, H. Saadoui, A. Saleh, F. Vögtle and J.-L. Pozzo, *J. Phys. Org. Chem.*, 2007, **20**, 888–893.
68 L. Sanguinet, J.-L. Pozzo, V. Rodriguez, F. Adamietz, F. Castet, L. Ducasse and B. Champagne, *J. Phys. Chem. B*, 2005, **109**, 11139–11150.
69 F. Mançois, V. Rodriguez, J.-L. Pozzo, B. Champagne and F. Castet, *Chem. Phys. Lett.*, 2006, **427**, 153–158.
70 A. Perrier, F. Maurel and D. Jacquemin, *Acc. Chem. Res.*, 2012, **45**, 1173–1182.
71 D. Jacquemin, E. A. Perpète, F. Maurel and A. Perrier, *J. Phys. Chem. C*, 2010, **114**, 9489–9497.
72 E. Runge and E. Gross, *Phys. Rev. Lett.*, 1984, **52**, 997–1000.
73 R. Bauernschmitt and R. Ahlrichs, *Chem. Phys. Lett.*, 1996, **256**, 454–464.
74 D. Jacquemin, E. A. Perpète, I. Ciofini and C. Adamo, *Acc. Chem. Res.*, 2009, **42**, 326–334.
75 H. Tian and S. Wang, *Chem. Commun.*, 2007, 781–792.
76 J. Zhang, Q. Zou and H. Tian, *Adv. Mater.*, 2013, **25**, 378–399.
77 G. Copley, T. A. Moore, A. L. Moore and D. Gust, *Adv. Mater.*, 2013, **25**, 456–461.
78 H. Tian and Y. Feng, *J. Mater. Chem.*, 2008, **18**, 1617–1622.
79 D. Gust, J. Andreasson, U. Pischel, T. A. Moore and A. L. Moore, *Chem. Commun.*, 2012, **48**, 1947–1957.
80 U. Pischel, J. Andréasson, D. Gust and V. F. Pais, *ChemPhysChem*, 2013, **14**, 28–46.
81 J. Biteau, F. Chaput, K. Lahlil, J.-P. Boilot, G. M. Tsivgoulis, J.-M. Lehn, B. Darracq, C. Marois and Y. Lévy, *Chem. Mater*, 1998, **10**, 1945–1950.
82 H. Nishi and S. Kobatake, *Macromolecules*, 2008, **41**, 3995–4002.
83 S. A. Díaz, G. O. Menéndez, M. H. Etchehon, L. Giordano, T. M. Jovin and E. A. Jares-Erijman, *ACS Nano*, 2011, **5**, 2795–2805.
84 K. Uchida, G. Masuda, Y. Aoi, K. Nakayama and M. Irie, *Chem. Lett.*, 1999, **28**, 1071–1072.
85 A. Peters and N. R. Branda, *Adv. Mater. Opt. Electron.*, 2000, **10**, 245–249.
86 M. Irie, T. Lifka, K. Uchida, S. Kobatake and Y. Shindo, *Chem. Commun.*, 1999, 747–750.
87 D. Mendive-Tapia, A. Perrier, M. J. Bearpark, M. A. Robb, B. Lasorne and D. Jacquemin, *Phys. Chem. Chem. Phys.*, 2014, **16**, 18463–18471.
88 F. Stellacci, C. Bertarelli, F. Toscano, M. C.Gallazzi, G. Zotti and G. Zerbi, *Adv. Mater.*, 1999, **11**, 292–295.
89 K. Higashiguchi, K. Matsuda, M. Matsuo, T. Yamada and M. Irie, *J. Photochem. Photobiol. A*, 2002, **152**, 141–146.
90 A. Perrier, F. Maurel and D. Jacquemin, *J. Phys. Chem. C*, 2011, **115**, 9193–9203.
91 F. Maurel, A. Perrier, E. A. Perpète and D. Jacquemin, *J. Photochem. Photobiol A*, 2008, **199**, 211–223.
92 K. Higashiguchi, K. Matsuda and M. Irie, *Angew. Chem., Int. Ed.*, 2003, **42**, 3537–3540.
93 K. Yagi and M. Irie, *Chem. Lett.*, 2003, **32**, 848–849.
94 B. Li, Y.-H. Wu, H.-M. Wen, L.-X. Shi and Z.-N. Chen, *Inorg. Chem.*, 2012, **51**, 1933–1942.
95 T. Kawai, T. Sasaki and M. Irie, *Chem. Commun.*, 2001, 711–712.
96 H.-L. Wong, C.-C. Ko, W. H. Lam, N. Zhu and V. W.-W. Yam, *Chem. - Eur. J.*, 2009, **15**, 10005–10009.
97 S. Saita, T. Yamaguchi, T. Kawai and M. Irie, *ChemPhysChem*, 2005, **6**, 2300–2306.
98 I. Jung, H. Choi, E. Kim, C.-H. Lee, S. O. Kang and J. Ko, *Tetrahedron*, 2005, **61**, 12256 – 12263.
99 C.-C. Ko, W. H. Lam and V. Wing-Wah Yam, *Chem. Commun.*, 2008, 5203–5205.
100 H. Wang, W. Xu and D. Zhu, *Tetrahedron*, 2012, **68**, 8719–8723.
101 V. Aubert, E. Ishow, F. Ibersiene, A. Boucekkine, J. A. G. Williams, L. Toupet, R. Metivier, K. Nakatani, V. Guerchais and H. Le Bozec, *New J. Chem.*, 2009, **33**, 1320–1323.
102 L. Ordronneau, J. Boixel, V. Aubert, M. S. Vidal, S. Moya, P. Aguirre, L. Toupet, J. A. G. Williams, H. Le Bozec and V. Guerchais, *Org. Biomol. Chem.*, 2014, **12**, 979–992.
103 S. Kobatake and M. Irie, *Tetrahedron*, 2003, **59**, 8359–8364.
104 K. Matsuda and M. Irie, *J. Am. Chem. Soc.*, 2001, **123**, 9896–9897.
105 S. Kobatake, S. Kuma and M. Irie, *Bull. Chem. Soc. Jpn.*, 2004, **77**, 945–951.
106 J. Areephong, W. R. Browne and B. L. Feringa, *Org. Biomol. Chem.*, 2007, **5**, 1170–1174.
107 S. Kobatake, S. Kuma and M. Irie, *J. Phys. Org. Chem.*, 2007, **20**, 960–967.
108 E. A. Shilova, A. Heynderickx and O. Siri, *J. Org. Chem.*, 2010, **75**, 1855–1861.
109 M. Cipolloni, A. Heynderickx, F. Maurel, A. Perrier, D. Jacquemin, O. Siri, F. Ortica and G. Favaro, *J. Phys. Chem. C*, 2011, **115**, 23096–23106.
110 H. J. Kim, J. H. Jang, H. Choi, T. Lee, J. Ko, M. Yoon and H.-J. Kim, *Inorg. Chem.*, 2008, **47**, 2411–2415.
111 W. Tan, X. Li, J. Zhang and H. Tian, *Dyes and Pigments*, 2011, **89**, 260–265.
112 J. Areephong, J. H. Hurenkamp, M. T. W. Milder, A. Meetsma, J. L. Herek, W. R. Browne and B. L. Feringa, *Org. Lett.*, 2009, **11**, 721–724.
113 M. T. Milder, J. Areephong, B. L. Feringa, W. R. Browne and J. L. Herek, *Chem. Phys. Lett.*, 2009, **479**, 137–139.
114 M. T. W. Milder, J. L. Herek, J. Areephong, B. L. Feringa and W. R. Browne, *J. Phys Chem. A*, 2009, **113**, 7717–7724.
115 A. Staykov, J. Areephong, W. R. Browne, B. L. Feringa and K. Yoshizawa, *ACS Nano*, 2011, **5**, 1165–1178.
116 D. Jacquemin, C. Michaux, E. A. Perpète, F. Maurel and A. Perrier, *Chem. Phys. Lett.*, 2010, **488**, 193 – 197.
117 S. Kuehn, S. Friede, M. Zastrow, K. Schiebler, K. Rueck-Braun and T. Elsaesser, *Chem. Phys. Lett.*, 2013, **555**, 206–211.
118 S. Yamamoto, K. Matsuda and M. Irie, *Chem. - Eur. J.*, 2003, **9**, 4878–4886.
119 R. H. Mitchell and S. Bandyopadhyay, *Org. Lett.*, 2004, **6**, 1729–1732.
120 F. Cisnetti, R. Ballardini, A. Credi, M. T. Gandolfi, S. Masiero, F. Negri, S. Pieraccini and G. P. Spada, *Chem. - Eur. J.*, 2004, **10**, 2011–2021.
121 J. Robertus, S. F. Reker, T. C. Pijper, A. Deuzeman, W. R. Browne and B. L. Feringa, *Phys. Chem. Chem. Phys.*, 2012, **14**, 4374–4382.
122 M. V. Peters, R. Goddard and S. Hecht, *J. Org. Chem*, 2006, **71**, 7846–7849.
123 A. Mohammadi and M. Safarnejad, *Spectrochim. Acta, Part A*, 2014, **126**, 105–111.
124 J. Vapaavuori, A. Goulet-Hanssens, I. T. Heikkinen, C. J. Barrett and A. Priimagi, *Chem. Mater.*, 2014, **26**, 5089–5096.
125 D. Bléger, J. Dokić, M. V. Peters, L. Grubert, P. Saalfrank and S. Hecht, *J. Phys. Chem. B*, 2011, **115**, 9930–9940.
126 L. Viau, S. Bidault, O. Maury, S. Brasselet, I. Ledoux, J. Zyss, E. Ishow, K. Nakatani and H. Le Bozec, *J. Am. Chem. Soc*, 2004, **126**, 8386–8387.

127 S. Bidault, L. Viau, O. Maury, S. Brasselet, J. Zyss, E. Ishow, K. Nakatani and H. LeBozec, *Adv. Funct. Mater.*, 2006, **16**, 2252–2262.

128 L. Viau, I. Malkowsky, K. Costuas, S. Boulin, L. Toupet, E. Ishow, K. Nakatani, O. Maury and H. Le Bozec, *ChemPhysChem*, 2006, **7**, 644–657.

129 Z. Yu and S. Hecht, *Chem. - Eur. J.*, 2012, **18**, 10519–10524.

130 R. Breukers, S. Janssens, S. Raymond, M. Bhuiyan and A. Kay, *Dyes Pigm.*, 2015, **112**, 17–23.

131 H.-M. Kang, , J.-W. Jung and C.-G. Cho, *J. Org. Chem.*, 2007, **72**, 679–682.

132 H. Rau and E. Lueddecke, *J. Am. Chem. Soc.*, 1982, **104**, 1616–1620.

133 E. Wei-Guang Diau, *J. Phys. Chem. A*, 2004, **108**, 950–956.

134 Y.-W. Hao, H.-Y. Wang, Y.-J. Huang, B.-R. Gao, Q.-D. Chen, L.-B. Li and H.-B. Sun, *J. Mater. Chem. C*, 2013, **1**, 5244–5249.

135 Y. Norikane, K. Kitamoto and N. Tamaoki, *J. Org. Chem.*, 2003, **68**, 8291–8304.

136 E. Bassotti, P. Carbone, A. Credi, M. Di Stefano, S. Masiero, F. Negri, G. Orlandi and G. P. Spada, *J. Phys. Chem. A*, 2006, **110**, 12385–12394.

137 Y. Norikane and N. Tamaoki, *Eur. J. Org. Chem.*, 2006, 1296–1302.

138 Y. Norikane, R. Katoh and N. Tamaoki, *Chem. Commun.*, 2008, 1898–1900.

139 M. Müri, K. C. Schuermann, L. De Cola and M. Mayor, *Eur. J. Org. Chem.*, 2009, 2562–2575.

140 Y. Norikane and N. Tamaoki, *Org. Lett.*, 2004, **6**, 2595–2598.

141 S. A. Nagamani, Y. Norikane and N. Tamaoki, *J. Org. Chem.*, 2005, **70**, 9304–9313.

142 S. Luyksaar, M. Krayushkin, Y. Pyankov and V. Barachevsky, *Chem. Heterocycl. Compound*, 2010, **46**, 822–828.

143 K. Fukushima, A. J. Vandenbos and T. Fujiwara, *Chem. Mater.*, 2007, **19**, 644–646.

144 O. Ivashenko, J. T. van Herpt, P. Rudolf, B. L. Feringa and W. R. Browne, *Chem. Commun.*, 2013, **49**, 6737–6739.

145 O. Ivashenko, J. T. van Herpt, B. L. Feringa, P. Rudolf and W. R. Browne, *J. Phys. Chem. C*, 2013, **117**, 18567–18577.

146 M. Natali and S. Giordani, *Org. Biomol. Chem.*, 2012, **10**, 1162–1171.

147 S. Lee, S. Ji and Y. Kang, *Bull. Korean Chem. Soc.*, 2012, **33**, 3740–3744.

148 N. Shao, J. Jin, H. Wang, J. Zheng, R. Yang, W. Chan and Z. Abliz, *J. Am. Chem. Soc.*, 2010, **132**, 725–736.

149 B. F. Zhang, M. Frigoli, F. Angiuli, F. Vetrone and J. A. Capobianco, *Chem. Commun.*, 2012, **48**, 7244–7246.

150 D. L. Watkins and T. Fujiwara, *J. Mater. Chem. C*, 2013, **1**, 506–514.

151 D. L. Watkins and T. Fujiwara, *J. Photochem. Photobiol. A*, 2012, **228**, 51–59.

152 A. Samat, V. Lokshin, K. Chamontin, D. Levi, G. Pepe and R. Guglielmetti, *Tetrahedron*, 2001, **57**, 7349–7359.

153 J. D. Hepworth and B. M. Heron, *Functional Dyes*, Elsevier Science, Amsterdam, 2006, pp. 85 – 135.

154 W. Zhao and E. M. Carreira, *J. Am. Chem. Soc.*, 2002, **124**, 1582–1583.

155 C. D. Gabbutt, B. M. Heron, A. C. Instone, S. B. Kolla, K. Mahajan, P. J. Coelho and L. M. Carvalho, *Dyes Pigm.*, 2008, **76**, 24 – 34.

156 C. D. Gabbutt, T. Gelbrich, J. D. Hepworth, B. Heron, M. B. Hursthouse and S. M. Partington, *Dyes Pigm.*, 2002, **54**, 79 – 93.

157 S. Aiken, C. D. Gabbutt, B. M. Heron and S. B. Kolla, *Dyes Pigm.*, 2015, **113**, 239–250.

158 M. Frigoli, C. Moustrou, A. Samat and R. Guglielmetti, *Helv. Chim. Acta*, 2000, **83**, 3043–3052.

159 A. E. Navarro, E. Moggia, C. Moustrou, A. Heynderickx, F. Fages, P. Leriche and H. Brisset, *Tetrahedron*, 2005, **61**, 423 – 428.

160 W. Zhao and E. M. Carreira, *Org. Lett.*, 2006, **8**, 99–102.

161 P. J. Coelho, M. A. Salvador, B. Heron and L. M. Carvalho, *Tetrahedron*, 2005, **61**, 11730–11743.

162 R. H. Mitchell, T. R. Ward, Y. Chen, Y. Wang, S. A. Weerawarna, P. W. Dibble, M. J. Marsella, A. Almutairi and Z.-Q. Wang, *J. Am. Chem. Soc.*, 2003, **125**, 2974–2988.

163 A. U. Petersen, S. L. Broman, S. T. Olsen, A. S. Hansen, L. Du, A. Kadziola, T. Hansen, H. G. Kjaergaard, K. V. Mikkelsen and M. Brondsted;Nielsen, *Chem. - Eur. J.*, 2015, **21**, 3968–3977.

164 K. Higashiguchi, K. Matsuda, N. Tanifuji and M. Irie, *J. Am. Chem. Soc.*, 2005, **127**, 8922–8923.

165 T. Kaieda, S. Kobatake, H. Miyasaka, M. Murakami, N. Iwai, Y. Nagata, A. Itaya and M. Irie, *J. Am. Chem. Soc*, 2002, **124**, 2015–2024.

166 H. Choi, I. Jung, K. H. Song, K. Song, D.-S. Shin, S. O. Kang and J. Ko, *Tetrahedron*, 2006, **62**, 9059–9065.

167 A. Tomari, T. Yamaguchi, N. Sakamoto, Y. Fujita and M. Irie, *Chem. Lett.*, 2004, **33**, 1380–1381.

168 D.-X. Zeng and Y. Chen, *Chin. J. Chem.*, 2006, **24**, 264–268.

169 H. Tian, B. Chen and P.-H. Liu, *Chem. Lett.*, 2001, **30**, 990–991.

170 J. Areephong, H. Logtenberg, W. R. Browne and B. L. Feringa, *Org. Lett.*, 2010, **12**, 2132–2135.

171 Q. Luo, S. Cheng and H. Tian, *Tetrahedron Lett.*, 2004, **45**, 7737–7740.

172 D. Jacquemin, E. A. Perpète, F. Maurel and A. Perrier, *J. Phys. Chem. Lett.*, 2010, **1**, 2104–2108.

173 D. Jacquemin, E. A. Perpete, F. Maurel and A. Perrier, *Phys. Chem. Chem. Phys.*, 2010, **12**, 7994–8000.

174 J. Yin, Y. Lin, X. Cao, G.-A. Yu and S. H. Liu, *Tetrahedron Lett*, 2008, **49**, 1582 – 1585.

175 H. Tian, B. Chen, H.-Y. Tu and K. Müllen, *Adv. Mater.*, 2002, **14**, 918–923.

176 Q. Luo, B. Chen, M. Wang and H. Tian, *Adv. Funct. Mater.*, 2003, **13**, 233–239.

177 J. Yi, Z. Chen, J. Xiang and F. Zhang, *Langmuir*, 2011, **27**, 8061–8066.

178 Z. Chen, Z. Li, Y. Bin, L. Huang and F. Zhang, *Sci. China, Ser. B: Chem.*, 2008, **51**, 263–268.

179 A. Perrier, F. Maurel, W. R. Browne and D. Jacquemin, *Chem. Commun.*, 2013, **49**, 4247–4249.

180 H. Cho and E. Kim, *Macromolecules*, 2002, **35**, 8684–8687.

181 S. Wang, X. Li, B. Chen, Q. Luo and H. Tian, *Macromol. Chem. Phys.*, 2004, **205**, 1497–1507.

182 T. J. Wigglesworth and N. R. Branda, *Chem. Mater.*, 2005, **17**, 5473–5480.

183 H. Nishi, T. Namari and S. Kobatake, *J. Mater. Chem.*, 2011, **21**, 17249–17258.

184 J. L. Humphrey, K. M. Lott, M. E. Wright and D. Kuciauskas, *J. Phys. Chem. B*, 2005, **109**, 21496–21498.

185 S. Bellotto, R. Reuter, C. Heinis and H. A. Wegner, *J. Org. Chem.*, 2011, **76**, 9826–9834.

186 Á. Moneo, G. C. Justino, M. F. N. N. Carvalho, M. C. Oliveira, A. M. M. Antunes, D. Bléger, S. Hecht and J. P. Telo, *J. Phys. Chem. A*, 2013, **117**, 14056–14064.

187 M. D. Segarra-Maset, P. W. N. M. van Leeuwen and Z. Freixa, *Eur. J. Inorg. Chem.*, 2010, **2010**, 2075–2078.

188 D. Bleger, Z. Yu and S. Hecht, *Chem. Commun.*, 2011, **47**, 12260–12266.

189 J. Bahrenburg, C. M. Sievers, J. B. Schonborn, B. Hartke, F. Renth, F. Temps, C. Nather and F. D. Sonnichsen, *Photochem. Photobiol. Sci.*, 2013, **12**, 511–518.

190 R. Reuter, N. Hostettler, M. Neuburger and H. A. Wegner, *Eur. J. Org. Chem.*, 2009, 5647–5652.

191 Y.-T. Shen, L. Guan, X.-Y. Zhu, Q.-D. Zeng and C. Wang, *J. Am. Chem. Soc.*, 2009, **131**, 6174–6180.

192 L. Schweighauser, D. Haussinger, M. Neuburger and H. A. Wegner, *Org. Biomol. Chem.*, 2014, **12**, 3371–3379.

193 M. J. Cho, G. W. Kim, W. G. Jun, S. K. Lee, J.-I. Jin and D. H. Choi,

Thin Solid Films, 2006, **500**, 52–60.
194 Q. Zhang, Z. Ning, Y. Yan, S. Qian and H. Tian, *Macromol. Rapid Commun.*, 2008, **29**, 193–201.
195 H. Nitadori, L. Ordronneau, J. Boixel, D. Jacquemin, A. Boucekkine, A. Singh, M. Akita, I. Ledoux, V. Guerchais and H. L. Bozec, *Chem. Commun.*, 2012, **48**, 10395–10397.
196 L. Ordronneau, V. Aubert, R. Metivier, E. Ishow, J. Boixel, K. Nakatani, F. Ibersiene, D. Hammoutene, A. Boucekkine, H. Le Bozec and V. Guerchais, *Phys. Chem. Chem. Phys.*, 2012, **14**, 2599–2605.
197 L. Ordronneau, V. Aubert, V. Guerchais, A. Boucekkine, H. Le Bozec, A. Singh, I. Ledoux and D. Jacquemin, *Chem. - Eur. J.*, 2013, **19**, 5845–5849.
198 Y.-W. Zhong, N. Vila, J. C. Henderson and H. D. Abruña, *Inorg. Chem.*, 2009, **48**, 991–999.
199 Y.-W. Zhong, N. Vilà, J. C. Henderson and H. D. Abruña, *Inorg. Chem.*, 2009, **48**, 7080–7085.
200 B. Qin, R. Yao, X. Zhao and H. Tian, *Org. Biomol. Chem.*, 2003, **1**, 2187–2191.
201 K. Senechal-David, N. Zaman, M. Walko, E. Halza, E. Riviere, R. Guillot, B. L. Feringa and M.-L. Boillot, *Dalton Trans.*, 2008, 1932–1936.
202 M. N. Roberts, C.-J. Carling, J. K. Nagle, N. R. Branda and M. O. Wolf, *J. Am. Chem. Soc.*, 2009, **131**, 16644–16645.
203 B. Li, H.-M. Wen, J.-Y. Wang, L.-X. Shi and Z.-N. Chen, *Inorg. Chem.*, 2013, **52**, 12511–12520.
204 Y.-M. Hervault, C. M. Ndiaye, L. Norel, C. Lagrost and S. Rigaut, *Org. Lett.*, 2012, **14**, 4454–4457.
205 B. Li, J.-Y. Wang, H.-M. Wen, L.-X. Shi and Z.-N. Chen, *J. Am. Chem. Soc.*, 2012, **134**, 16059–16067.
206 E. Murguly, T. B. Norsten and N. R. Branda, *Angew. Chem., Int. Ed.*, 2001, **40**, 1752–1755.
207 M. Han, R. Michel, B. He, Y.-S. Chen, D. Stalke, M. John and G. H. Clever, *Angew. Chem., Int. Ed.*, 2013, **52**, 1319–1323.
208 V. W.-W. Yam, J. K.-W. Lee, C.-C. Ko and N. Zhu, *J. Am. Chem. Soc.*, 2009, **131**, 912–913.
209 S. Chen, L.-J. Chen, H.-B. Yang, H. Tian and W. Zhu, *J. Am. Chem. Soc.*, 2012, **134**, 13596–13599.
210 H. L. Bozec and V. Guerchais, *C. R. Chim.*, 2013, **16**, 1172–1182.
211 A. Perrier, F. Maurel, I. Ciofini and D. Jacquemin, *Chem. Phys. Lett.*, 2011, **502**, 77–81.
212 G.-T. Xu, B. Li, J.-Y. Wang, D.-B. Zhang and Z.-N. Chen, *Chem. - Eur. J.*, 2015, **21**, 3318–3326.
213 R. Sakamoto, M. Murata, S. Kume, H. Sampei, M. Sugimoto and H. Nishihara, *Chem. Commun.*, 2005, 1215–1217.
214 M. Han, T. Hirade and M. Hara, *New J. Chem.*, 2010, **34**, 2887–2891.
215 S. Park, O. N. Kadkin, J.-G. Tae and M.-G. Choi, *Inorg. Chim. Acta*, 2008, **361**, 3063–3068.
216 S. V. Paramonov, V. Lokshin and O. A. Fedorova, *J. Photochem. Photobiol. C*, 2011, **12**, 209 – 236.
217 R. A. Kopelman, S. M. Snyder and N. L. Frank, *J. Am. Chem. Soc.*, 2003, **125**, 13684–13685.
218 C.-C. Ko, L.-X. Wu, K. M.-C. Wong, N. Zhu and V. W.-W. Yam, *Chem. - Eur. J.*, 2004, **10**, 766–776.
219 S. Yagi, S. Nakamura, D. Watanabe and H. Nakazumi, *Dyes Pigm.*, 2009, **80**, 98–105.
220 T. Mrozek, J. Daub and H. Gorner, *Chem. Commun.*, 1999, 1487–1488.
221 T. Mrozek, H. Görner and J. Daub, *Chem. - Eur. J.*, 2001, **7**, 1028–1040.
222 A. Myles, T. Wigglesworth and N. Branda, *Adv. Mater.*, 2003, **15**, 745–748.
223 H. Choi, B.-S. Ku, S.-R. Keum, S. O. Kang and J. Ko, *Tetrahedron*, 2005, **61**, 3719–3723.
224 M. Frigoli and G. H. Mehl, *Angew. Chem., Int. Ed.*, 2005, **44**, 5048–5052.
225 S. Delbaere, G. Vermeersch, M. Frigoli and G. H. Mehl, *Org. Lett.*, 2006, **8**, 4931–4934.
226 S. Delbaere, J.-C. Micheau, M. Frigoli, G. H. Mehl and G. Vermeersch, *J. Phys. Org. Chem.*, 2007, **20**, 929–935.
227 S. Delbaere, G. Vermeersch, M. Frigoli and G. H. Mehl, *Org. Lett.*, 2010, **12**, 4090–4093.
228 F. G. Erko, L. Cseh, J. Berthet, G. H. Mehl and S. Delbaere, *Dyes Pigm.*, 2015, **115**, 102–109.
229 S. D. Straight, P. A. Liddell, Y. Terazono, T. A. Moore, A. L. Moore and D. Gust, *Adv. Funct. Mater.*, 2007, **17**, 777–785.
230 J. Andréasson, S. D. Straight, T. A. Moore, A. L. Moore and D. Gust, *J. Am. Chem. Soc.*, 2008, **130**, 11122–11128.
231 J. Andréasson, U. Pischel, S. D. Straight, T. A. Moore, A. L. Moore and D. Gust, *J. Am. Chem. Soc.*, 2011, **133**, 11641–11648.
232 M. Bälter, S. Li, J. R. Nilsson, J. Andréasson and U. Pischel, *J. Am. Chem. Soc.*, 2013, **135**, 10230–10233.
233 G. Sevez, J. Gan, S. Delbaere, G. Vermeersch, L. Sanguinet, E. Levillain and J.-L. Pozzo, *Photochem. Photobiol. Sci.*, 2010, **9**, 131–135.
234 G. Szalóki, G. Sevez, J. Berthet, J.-L. Pozzo and S. Delbaere, *J. Am. Chem. Soc.*, 2014, **136**, 13510–13513.
235 Y. He, Y. Zhu, Z. Chen, W. He and X. Wang, *Chem. Commun.*, 2013, **49**, 5556–5558.
236 W. Geng, C. Zheng, S. Cui, G. Liu and S. Pu, *J. Photochem. Photobiol. A*, 2014, **282**, 47 – 52.
237 K. Kinashi and Y. Ueda, *Mol. Cryst. Liq. Cryst.*, 2006, **445**, 223–230.
238 K. Kinashi, Y. Ono, Y. Naitoh, A. Otomo and Y. Ueda, *J. Photochem. Photobiol. A.*, 2011, **217**, 35–39.
239 E. Pottier, R. Dubest, R. Guglielmetti, P. Tardieu, A. Kellmann, F. Tfibel, P. Levoir and J. Aubard, *Helv. Chim. Acta*, 1990, **73**, 303–315.
240 L. Gobbi, P. Seiler, F. Diederich, V. Gramlich, C. Boudon, J.-P. Gisselbrecht and M. Gross, *Helv. Chim. Acta*, 2001, **84**, 743–777.
241 S. Chinnusamy and K. Palaninathan, *J. Polym. Sci., Part A: Polym. Chem.*, 2010, **48**, 1565–1578.
242 S. Nakamura and M. Irie, *J. Org. Chem.*, 1988, **53**, 6136–6138.
243 I. Mikhailov and A. Masunov, *Computational Science – ICCS 2009*, Springer Berlin Heidelberg, 2009, vol. 5545, pp. 169–178.
244 R. J. Maurer and K. Reuter, *Chem. Phys.*, 2011, **135**, 224303.
245 C. Wiebeler and S. Schumacher, *J. Phys. Chem. A*, 2014, **118**, 7816–7823.
246 Y. Asano, A. Murakami, T. Kobayashi, A. Goldberg, D. Guillaumont, S. Yabushita, M. Irie and S. Nakamura, *J. Am. Chem. Soc.*, 2004, **126**, 12112–12120.
247 M. Boggio-Pasqua, M. Ravaglia, M. J. Bearpark, M. Garavelli and M. A. Robb, *J. Phys. Chem. A*, 2003, **107**, 11139–11152.
248 D. Mendive-Tapia, A. Perrier, M. J. Bearpark, M. A. Robb, B. Lasorne and D. Jacquemin, *Phys. Chem. Chem. Phys.*, 2014, **16**, 18463–18471.
249 A. Perrier, S. Aloise, M. Olivucci and D. Jacquemin, *J. Phys. Chem. Lett.*, 2013, **4**, 2190–2196.
250 T. Ishikawa, T. Noro and T. Shoda, *The Journal of Chemical Physics*, 2001, **115**, 7503–7512.
251 L. Liu, S. Yuan, W.-H. Fang and Y. Zhang, *J. Phys. Chem. A*, 2011, **115**, 10027–10034.
252 F. Liu and K. Morokuma, *J. Am. Chem. Soc.*, 2013, **135**, 10693–10702.
253 A. Dreuw and M. Head-Gordon, *Chem. Rev.*, 2005, **105**, 4009–4037.
254 M. E. Casida, *J. Mol. Struct.: THEOCHEM*, 2009, **914**, 3 – 18.
255 An hybrid exchange-correlation functional, typically PBE0[273] is used to optimise the geometry of the systems, whereas a range-separated hybrid functional (e.g., CAM-B3LYP,[274] ωB97x[275] or ωB97x-D[276]), that is adequate for charge transfer states, is applied to compute the vertical excitations with TD-DFT.[70] Both steps are conducted in a dielectric continuum to reproduce the bulk environment arising from solvation (e.g., with the Polarizable Continuum Model)[277].

256 A. Fihey, A. Perrier and F. Maurel, *J. Photochem. Photobiol. A.*, 2012, **247**, 30 – 41.
257 D. Jacquemin, E. A. Perpète, F. Maurel and A. Perrier, *J. Phys. Chem. Lett.*, 2010, **1**, 434–438.
258 A. Perrier, F. Maurel and D. Jacquemin, *Chem. Phys. Lett.*, 2011, **509**, 129–133.
259 E. Durgun and J. C. Grossman, *J. Phys. Chem. Lett.*, 2013, **4**, 854–860.
260 T. Jaunet-Lahary, A. Chantzis, K. J. Chen, A. D. Laurent and D. Jacquemin, *J. Phys. Chem. C*, 2014, **114**, 28831–28841.
261 K. J. Chen, A. D. Laurent and D. Jacquemin, *J. Phys. Chem. C*, 2014, **118**, 4334–4345.
262 R. Chindam, H. M. Hoque, A. S. Ali, F. Z. Rafique and J. D. Gough, *J. Photochem. Photobiol. A*, 2014, **279**, 38–46.
263 For example, the optical properties of **122** were determined with PBE0, CAM-B3LYP, ωB97X and ωB97X-D.[264] ωB97X-D is found to provide the best overall agreement for the two photochromes, even if ωB97X performs better on the indolinooxazolidine moiety. Likewise in **113** PBE0 (CAM-B3LYP) is more suited for the PNQ (DTE) moiety.
264 D. Jacquemin, E. A. Perpète, F. Maurel and A. Perrier, *Comput. Theor. Chem.*, 2011, **963**, 63 – 70.
265 D. Jacquemin, E. A. Perpete, F. Maurel and A. Perrier, *Phys. Chem. Chem. Phys.*, 2010, **12**, 13144–13152.
266 S. Chen, Y. Yang, Y. Wu, H. Tian and W. Zhu, *J. Mater. Chem.*, 2012, **22**, 5486–5494.
267 F. Maurel, A. Perrier and D. Jacquemin, *J. Photochem. Photobiol. A*, 2011, **218**, 33–40.
268 A. Perrier, F. Maurel and D. Jacquemin, *Phys. Chem. Chem. Phys.*, 2011, **13**, 13791–13799.
269 K. A. Belfon and J. D. Gough, *Chem. Phys. Lett.*, 2013, **585**, 63–68.
270 L. Li, F.-Q. Bai and H.-X. Zhang, *Spectrochim. Acta, Part A*, 2015, **137**, 987–994.
271 M. Di Donato, A. Iagatti, A. Lapini, P. Foggi, S. Cicchi, L. Lascialfari, S. Fedeli, S. Caprasecca and B. Mennucci, *J. Phys. Chem. C*, 2014, **118**, 23476–23486.
272 A. Angioni, S. Corni and B. Mennucci, *Phys. Chem. Chem. Phys.*, 2013, **15**, 3294–3303.
273 C. Adamo and V. Barone, *J. Chem. Phys.*, 1999, **110**, 6158–6170.
274 T. Yanai, D. P. Tew and N. C. Handy, *Chem. Phys. Lett.*, 2004, **393**, 51 – 57.
275 J.-D. Chai and M. Head-Gordon, *J. Chem. Phys*, 2008, **128**, 084106.
276 J.-D. Chai and M. Head-Gordon, *Phys. Chem. Chem. Phys.*, 2008, **10**, 6615–6620.
277 J. Tomasi, B. Mennucci and R. Cammi, *Chem. Rev.*, 2005, **105**, 2999–3094.

Table 1 Summary of the optical properties of photochromic dimers. The **a** and **b** subscripts referring to the states of the photochromes respectively stand for open and closed for DTEs and FGs, *E* and *Z* for AZBs, and closed and open for SPs and NPs. *n* is the number of states in the dimer, ϕ is the isomerisation quantum yield (the conversion percentage in the PSS – abbreviated *% conv.* –is also given when available) and λ_{max} is the wavelength of maximal absorption of the different isomers. The "-" sign indicates non-existing data (partial photochromism), whereas "*NA*" indicates data that are not given in the publication.

System	Ref	*n*	solvent[a]	$\phi_{\mathbf{aa}\rightarrow\mathbf{ba}}(\phi_{\mathbf{ba}\rightarrow\mathbf{aa}})$	$\phi_{\mathbf{ba}\rightarrow\mathbf{bb}}(\phi_{\mathbf{bb}\rightarrow\mathbf{ba}})$	$\lambda_{max(\mathbf{aa})}$ (nm)	$\lambda_{max(\mathbf{ba})}$ (nm)	$\lambda_{max(\mathbf{bb})}$ (nm)
1	84	2	hexane	*NA*	-	<350	445	-
2	85	2	cyc.	*NA*	-	324	505	-
3 (inverse)	89	3	hexane	0.20(0.54)	-	ca. 330	45	-
(hybrid)	89	3	hexane	0.034 (0.52)	-	ca. 330	475	-
4 (inverse)	92	3	hexane	0.14 (0.57)	-	ca. 340	ca. 430	-
(normal)	92	3	hexane	0.032 (0.013)	-	ca. 340	ca. 590	-
5	93	2	hexane	0.36	-	*NA*	574	-
6	94	2	CH_2Cl_2	0.44	-	ca. 380 (sh)	620	-
7	95	2	THF	*NA*	-	340 (450 : linker)	ca. 550	-
8 (a-e)	96	2	benzene	0.35-0.38	-	348-350	556-558	-
9	97	2	THF	*NA* (76% conv.)	-	ca. 340	543	-
10 R = H, thiophene	97	2	THF	*NA*	-	ca. 360	552	-
R=O-alkyl, thiophene	97	2	THF	0.17	-	407	568	-
R=O-alkyl, thiazole	97	2	THF	0.32	-	406	649	-
R=O-alkyl, oxazole	97	2	THF	0.12	-	404	604	-
11	223	2	chl.	*NA*	-	ca. 330	600	-
12	99	2	benzene	0.36 (0.06)	-	ca. 330	ca. 560	-
13	99	2	benzene	0.24 (0.04)	-	ca. 350	ca. 560	-
14 R=Me	100	2	hexane	*NA* (49% conv.)	-	386	468	-
R=CH_6H_5	100	2	hexane	*NA* (88% conv.)	-	ca. 400	ca. 510	-
15 D=NMe_2, R=TMS	101	2	cyc.	0.081 (0.016)	-	435	584	-
D=NBu_2, R=Me	102	3	cyc.	(70% conv.)	-	449	569	-
D=MeO, R=Me	102	3	CH_2Cl_2	58% conv.	31% conv.	404	553	553
16	103	3	hexane	0.50(0.0094) (56% conv.)	*NA*(0.0026) (41% conv.)	271	569	588
17	104	3	eth. ac.	23% conv.	77% conv.	ca. 305	560	576
18	105	3	hexane	0.46(0.0058)	0.29(0.0058)	309	595	595
19 R=OMe, H_6	106	3	heptane	37% conv.	56% conv.	274	506	506
R=OMe, F_6	106	3	heptane	-	99% (**ba** + **bb**)	294	578	578
R=H, H_6	106	3	heptane	36% conv.	56% conv.			
R=H, F_6	106	3	heptane	-	99% (**ba** + **bb**)			
20 R=Me	107	3	hexane	*NA*	*NA*	ca. 300	452	452
R=Br	107	3	hexane	16% conv.	0.6% conv.	ca. 300	465	465
21 non-protonated	108	2	acetone	-	10%	381	-	511
protonated	108	2	acetone	-	*NA*	394	-	573
22	110	2	toluene	-	63% conv.	303	-	590
23	111	2	THF	-	0.18(0.26)	290 (DTE), 533 (PDI)	-	585
24 R=Ph	112	2	hexane	-	90% conv.	435	-	634
R=Cl	112	2	hexane	-	*NA*	389 (sh)	-	567
25	117	2	CCl_4	-	0.38	ca. 295	-	607
26	120	2	CH_3CN	-	$\pi\pi^*$: 0.12 $n\pi^*$: 0.30	$\pi\pi^*$: 326 $n\pi^*$: 436	-	ca. 430
27	120	2	CH_3CN	$\pi\pi^*$: 0.017 $n\pi^*$: 0.03	-	$\pi\pi^*$: 361 $n\pi^*$: ca. 450	ca. 450	-
28	121	4	CH_2Cl_2	28% conv.	33% conv.	331	ca. 450	ca. 450
29	122	1	CH_3CN	ca. 330 nm				
30	123	1	various	-	-	330-334 nm	-	-

Table 1 – continued from previous page

System	Ref	*n*	solvent[a]	$\phi_{aa\rightarrow ba}(\phi_{ba\rightarrow aa})$	$\phi_{ba\rightarrow bb}(\phi_{bb\rightarrow ba})$	$\lambda_{max(aa)}$ (nm)	$\lambda_{max(ba)}$ (nm)	$\lambda_{max(bb)}$ (nm)
31 R_1=R_2=R_3=R_4=H	125	3	cyc.	22% conv.	25% conv.	ca. 370	ca. 460	ca. 460
R_1=R_4=H, R_2=R_3=Me	125	3	cyc.	10% conv.	88% conv.	ca. 350	ca. 440	ca. 440
R_1=R_2=R_3=R_4=Me	125	3	cyc.	4% conv.	95% conv.	ca. 350	ca. 440	ca. 440
32 *term*	129	3	CH_3CN	7.8(2.5) (46% conv.)	8.1(15.9) (43% conv.)	ca. 310	ca. 430	ca. 430
int	129	3	CH_3CN	2.0(1.3) (30% conv.)	2.5(6.5) (55% conv.)	ca. 310	ca. 430	ca. 430
core	129	3	CH_3CN	1.6(0.8) (37% conv.)	3.7(4.9) (49% conv.)	ca. 310	ca. 430	ca. 430
33	130	2	DMSO	*NA*	*NA*	515	-	*NA*
34	137	3	CH_3CN	$\pi\pi^*$: 0.19(0.06) (32%), $n\pi^*$: 0.29(0.31) (36%)	$\pi\pi^*$: 0.15(0.30) (63%), $n\pi^*$: 0.10(0.43) (5%)	322, 443	ca. 320, ca. 430	ca. 280, ca. 430
35	132	2	benzene	$\pi\pi^*$: 0.21, $n\pi^*$: 0.24	-	340, 436	ca. 300, ca. 430	-
36	132	2	benzene	-	-	ca. 330, ca. 460	ca. 330, ca. 460	-
37	137	3	CH_3CN	$\pi\pi^*$: 0.25(0.26) (29%), $n\pi^*$:0.34(0.35) (50%)	$\pi\pi^*$: 0.09(0.18) (57%), $n\pi^*$:0.15(0.51) (6%)	313, 451	ca. 320, ca. 440	ca. 290, ca. 425
38	136	2	CH_3CN	0.11 (50%)	-	392	347, 466	-
39	138	2	CH_3CN	-	9% *EE* to *ZZ* photochemical conv.	314	-	416
40	139	2	THF	-	0.28(0.45) (85% conv.)	ca. 320, ca. 450		ca. 320, ca. 450
41 R=H	140	3	chl.	0.01	*NA* (32% total conv.)	320, 365	320, 365	320, 365
R=tBu	140	3	toluene	*NA*	*NA*	323, 383	323, 383	323, 383
42 a	142	2	toluene	*NA*	*NA*	330	-	528
b	142	2	toluene	*NA*	*NA*	335	-	530
c	142	2	toluene	*NA*	*NA*	335	-	530
d	142	2	toluene	*NA*	*NA*	310	-	530
43	143	2	toluene	-	*NA*	ca. 300, ca 400	-	590
44 R=CH_2CH_2OH	146	2	CH_3CN	*NA*	*NA*	303	-	579
R=$(CH_2)_3C(O)OCH_2CH_3$	146	2	CH_3CN	*NA*	*NA*	308	-	586
R=$C_2H_4OC(O)C_7H_{15}$	144	2	CH_3CN	-	-	306	-	589
R=linker to gold nanoparticle	145	2	CH_2Cl_2	*NA*	*NA*	*NA*	*NA*	*NA*
45	147	2	et. ac.	*NA*	*NA*	ca. 325	-	600
46	147	2	et. ac.	*NA*	*NA*	ca. 375	-	628
47 piperazine l., complexing GSH	148	2	Et-wat.	*NA*	*NA*	334	-	446
binaphtol l., complexing GSH	148	2	Et-wat.	*NA*	*NA*	*NA*	-	ca. 450
48	149	2	THF	*NA*	*NA*	ca. 340	-	ca. 575
49	151	2	THF	*NA*	*NA*	ca. 350	-	606
50	151	2	THF	*NA*	*NA*	*NA*	-	*NA*
51	151	2	THF	*NA*	*NA*	ca. 350	-	609
52	152	2	toluene	*NA*	*NA*	*NA*	-	447, 610
53 symetric	152	2	toluene	*NA*	*NA*	*NA*	-	ca. 475
53 non-symetric	152	2	toluene	*NA*	*NA*	*NA*	-	446
54 R=benzene, Ar=Ph, *para*	160	3	toluene	*NA*	*NA*	361	434 (RT)	494(-20°)
R=benzene, Ar=Ph, *meta*	160	3	toluene	*NA*	*NA*	ca. 360	432 (RT)	*NA* (-20°)
55 link=phenyl	161	2	toluene	-	*NA*	*NA*	-	533, 600
56	157	2	toluene	*NA*	*NA*	*NA* (shoulder)	-	450-550
57	154	3	$CHCl_3$	*NA*	*NA*	334	517	580
58	159	2	THF	*NA*	*NA*	333	*NA*	511
59	119	2	cyc.	-	*NA*	below 300	-	415, 525
59' link=benzene	162	2	cyc.	*NA*	*NA*	486 (not stable)	406	268
59' link=chrysene	162	2	cyc.	-		427	-	313
60 *para*	163	2	CH_3CN	*NA*	*NA*	408	-	466
60 *meta*	163	3	CH_3CN	0.65	*NA*	365	476	466
89 D=H, X=OAc	196	3	CH_2Cl_2	0.70(0.006)	0.065(0.006)	*NA*	*NA*	628

Table 1 – continued from previous page

System	Ref	*n*	solvent[a]	$\phi_{aa\rightarrow ba}(\phi_{ba\rightarrow aa})$	$\phi_{ba\rightarrow bb}(\phi_{bb\rightarrow ba})$	$\lambda_{max(aa)}$ (nm)	$\lambda_{max(ba)}$ (nm)	$\lambda_{max(bb)}$ (nm)
D=OMe, X=OAc	196	3	CH_2Cl_2	0.52(0.004)	0.055(0.004)	*NA*	*NA*	646
D=NMe_2, X=OAc	196	3	CH_2Cl_2	0.23(0.0009)	0.048(0.0009)	*NA*		687
D=NBu_2, X=Cl	196	3	CH_2Cl_2	0.0024(0.00013)	0.0005(0.00013)	*NA*	*NA*	714
91 X=$Zn(OAc)_2$	102	3	cyc.	*NA*	*NA*	349, 485 (ICT)	*NA*	570
X=$Re(CO)_3Br$	102	1	cyc.	-	-	353, 530 (ICT)	*NA*	-
93 R=Bn	206	2	$EtCl_2$	-	*S,S*: 94% conv., *R,R*: 92% conv.	321	-	636
R=*i*Pr	206	2	$EtCl_2$	-	*S,S*: 70% conv., *R,R*: 79% conv.	*NA*	-	*NA*
94	200	2	THF	-	0.42	295	-	558
95 M=Fe, R=Cl	198	2	CH_3CN	-	-	374, 575 (MLCT)	-	-
M=Co, R=Cl	198	2	CH_3CN	-	40% conv.	388	-	534
M=Fe, R=Ph	198	2	CH_3CN	-	*NA*	375, 574 (MLCT)	-	375, 574 (MLCT)
M=Co, R=Ph	198	2	CH_3CN	-	100% conv.	391	-	580
97	202	3	CH_2Cl_2	20% PSS	80% PSS	280 (DTE), 350 (linker)	280 (DTE), 350 (linker), ca. 650	ca. 650
98 inverse	203	2	CH_2Cl_2	5% conv.	-	332	ca. 450	-
inverse/normal	203	3	CH_2Cl_2	80% conv.	*NA*	355	525	525
normal	203	3	CH_2Cl_2	60% conv.	67% conv.	355	567	585
normal, Pyridine	203	3	CH_2Cl_2	49% conv.	100% conv.	ca. 350	628	642
100 R=pyridine	205	3	CH_2Cl_2	0.76(0.065) (¿95% conv.)	0.16 (75% conv.)	347	684	698
R=ferrocene	212	3	toluene	0.32(0.005) (100% conv.)	0.02 (80% conv.)	353	666	691
101	204	3	toluene	*NA*	quantitative	352	717	736
102	94	3	CH_2Cl_2		0.54(>95% conv.)	306	608	622
104	208	2	CH_3CN	0.34(0.14 at 340 nm, 0.014 at 510 nm)	-	274	562	-
105	208	2	CH_3CN	*NA*	-	344	540	-
109	213	3	CH_2Cl_2	λ-dependent: 4-45% conv. to EZ, 7-44% conv. to ZE	-	ca.300, ca. 400, 578 (MLCT)	ca. 300, ca. 400, 578 (MLCT)	-
110	214	2	CH_2Cl_2	-	60% conv.	356, 450	-	356,450
111	215	3	CH_2Cl_2	*NA*	*NA*	355, 440	355, 440	355, 440
115	218	2	CH_2Cl_2	-	0.15	350, 440(MLCT)	-	604
116	219	2	CH_3CN	-	*NA*	ca. 300 (sh)	-	555 (with Ca)

[a]Abbreviations for solvent: cyc: cyclohexane, et. ac.: ethyl acetate, chl: chloroform, et.-wat: ethanol-water

Graphical TOC

We review molecular compounds encompassing several photochromic units with a focus on their functionalities.

Bio sketch

Dr. Arnaud Fihey

Dr. Arnaud Fihey was born in Chteau-Gontier (France) in 1988. He obtained his Ph.D in the field of computational chemistry in 2014 from the Université Paris Diderot (France), modeling the interaction between photoactive molecules and metallic aggregates with quantum and classical methods. He is currently a post-doctoral associate at the Université de Nantes (France), and his work mainly devoted to the theoretical description of the optical properties of electronically coupled organic photochromes.

Dr. Aurélie Perrier

Aurélie Perrier was born in France in 1978; she received her Ph.D. in Physical Chemistry from the University of Bordeaux in 2005 with Prof. J. C. Rayez. After one year as a postdoctoral fellow at the University of Siena (Italy) with Prof. M. Olivucci, she joined the University of Paris Diderot as associate professor in 2007 and works in the group of Prof. C. Adamo at Chimie ParisTech Institute. Her interests include the modeling of the electronic and optical properties of photoactive organic molecules and metallic nanoparticles.

Prof. Wesley R. Browne

Wesley R. Browne completed his PhD with Prof. J. G. Vos, in 2002, at Dublin City University (Ireland) followed by a postdoctoral period at Queens University Belfast, with Prof J. J. McGarvey and from 2003 to 2007 at the University of Groningen with Prof. B. L. Feringa. In 2007, he was awarded a VIDI independent research grant and, in 2008, appointed as Assistant Professor at the University of Groningen. In 2013, he was appointed to his present position of Associate Professor and in 2015 as Chair of Molecular Inorganic Chemistry. His current research interests include transition metal based oxidation catalysis, photo and electro responsive molecular based surfaces.

Prof. Denis Jacquemin

Denis Jacquemin was born in Dinant (Belgium) in 1974 and received his Ph.D. in Chemistry from the University of Namur in 1998, before moving to the University of Florida for his postdoctoral stay. In 2003, he was appointed as Research Associate of the FNRS in Belgium. He is currently full Professor at the University of Nantes (France), junior member of the Institut Universitaire de France and principal investigator of the ERC Marches project devoted to improving multiphotochromes. His researches are focused on modeling electronically excited-state processes in organic compounds using a panel of *ab initio* approaches.